Global Perspectives on Observing Ocean Boundary Current Systems

Robert E. Todd[1*], Francisco P. Chavez[2], Sophie Clayton[3], Sophie Cravatte[4], Marlos Goes[5,6], Michelle Graco[7], Xiaopei Lin[8], Janet Sprintall[9], Nathalie V. Zilberman[9], Matthew Archer[10], Javier Arístegui[11], Magdalena Balmaseda[12], John M. Bane[13], Molly O. Baringer[5], John A. Barth[14], Lisa M. Beal[6], Peter Brandt[15,16], Paulo H.R. Calil[17], Edmo Campos[18], Luca R. Centurioni[9], Maria Paz Chidichimo[19], Mauro Cirano[20], Meghan F. Cronin[21], Enrique N. Curchitser[22], Russ E. Davis[9], Marcus Dengler[15], Brad deYoung[23], Shenfu Dong[5], Ruben Escribano[24], Andrea J. Fassbender[2], Sarah E. Fawcett[25], Ming Feng[26], Gustavo J. Goni[5], Alison R. Gray[27], Dimitri Gutiérrez[7], Dave Hebert[28], Rebecca Hummels[15], Shin-ichi Ito[29], Marjorlaine Krug[30], François Lacan[31,4], Lucas Laurindo[6], Alban Lazar[32], Craig M. Lee[33], Matthieu Lengaigne[32], Naomi M. Levine[34], John Middleton[35], Ivonne Montes[36], Mike Muglia[13,37], Takeyoshi Nagai[38], Hilary I. Palevsky[39], Jaime B. Palter[40], Helen E. Phillips[41], Alberto Piola[42], Albert J. Plueddemann[1], Bo Qiu[43], Regina R. Rodrigues[44], Moninya Roughan[45], Daniel L. Rudnick[9], Ryan R. Rykaczewski[46], Martin Saraceno[42,47], Harvey Seim[13], Alex Sen Gupta[45], Lynne Shannon[48], Bernadette M. Sloyan[49], Adrienne J. Sutton[21], LuAnne Thompson[27], Anja K. van der Plas[50], Denis Volkov[5,6], John Wilkin[22], Dongxiao Zhang[51,21], Linlin Zhang[52]

[1]Woods Hole Oceanographic Institution, Woods Hole, MA, USA

[2]Monterey Bay Aquarium Research Institute, Moss Landing, CA, USA

[3]Old Dominion University, Norfolk, VA, USA

[4] LEGOS, Universite de Toulouse, IRD, CNES, CNRS, UPS, Toulouse, France

[5]NOAA Atlantic Oceanographic and Meteorological Laboratory, Miami, FL, USA

[6]Rosenstiel School of Marine and Atmospheric Science, University of Miami, Miami, FL, USA

[7]Instituto del Mar del Peru, Lima, Peru

[8]Ocean University of China and Qingdao National Laboratory for Marine Science and Technology, Qingdao, China

[9]Scripps Institution of Oceanography, UC San Diego, La Jolla, CA, USA

[10]Jet Propulsion Laboratory, California Institute of Technology, Pasadena, CA, USA

[11]Instituto de Oceanografía y Cambio Global, Universidad de Las Palmas de Gran Canaria, Las Palmas, Spain

[12]European Centre for Medium-range Weather Forecasts, Reading, UK

[13]University of North Carolina at Chapel Hill, Chapel Hill, NC, USA

[14]Oregon State University, Corvallis, OR, USA

[15]GEOMAR Helmholtz Center for Ocean Research, Kiel, Germany

[16]Kiel University, Kiel, Germany

[17]Institute of Coastal Research, Helmholtz-Zentrum Geesthacht, Geesthacht, Germany

[18]University of São Paulo, São Paulo, Brazil

[19]Consejo Nacional de Investigaciones Científicas y Téchnicas / Servicio de Hidrografía Naval, Buenos Aires, Argentina

[20]Universidade Federal do Rio de Janeiro, Rio de Janeiro, Brazil

[21]NOAA Pacific Marine Environmental Laboratory, Seattle, WA, USA

[22]Rutgers University, New Brunswick, NJ, USA

[23]Memorial University, St. John's, Newfoundland, Canada

[24]Instituto Milenio de Oceanografía, Universidad de Concepción, Concepción, Chile

[25]Department of Oceanography, University of Cape Town, Cape Town, South Africa

[26]CSIRO Oceans and Atmosphere, Crawley, Western Australia, Australia

[27]School of Oceanography, University of Washington, Seattle, WA, USA

[28]Fisheries and Oceans Canada, Dartmouth, Nova Scotia, Canada

[29]Atmosphere and Ocean Research Institute, University of Tokyo, Kashiwa, Japan

[30]Council for Scientific and Industrial Research, Cape Town, South Africa

[31]LEGOS, University of Toulouse, CNRS, CNES, UPS, Toulouse, France

[32]LOCEAN-IPSL, Sorbonne Université, Paris, France

[33]Applied Physics Laboratory, University of Washington, Seattle, WA, USA

[34]University of Southern California, Los Angeles, CA, USA

[35]South Australian Research and Development Institute (Aquatic Sciences), West Beach, South Australia, Australia

[36]Instituto Geofísico del Perú, Lima, Peru

[37]UNC Coastal Studies Institute, Wanchese, NC, USA

[38]Tokyo University of Marine Science and Technology, Tokyo, Japan

[39]Wellesley College, Wellesley, MA, USA

[40]University of Rhode Island, Narragansett, RI, USA

[41]University of Tasmania, Hobart, Tasmania, Australia

[42]University of Buenos Aires, Buenos Aires, Argentina

[43]University of Hawaii at Manoa, Honolulu, HI, USA

[44]Universidade Federal de Santa Catarina, Florianópolis, Brazil

[45]University of New South Wales, Sydney, NSW, Australia

[46]University of South Carolina, Columbia, SC, USA

[47]Consejo Nacional de Investigaciones Científicas y Técnicas, Buenos Aires, Argentina

[48]Department of Biological Sciences, University of Cape Town, Cape Town, South Africa

[49]CSIRO Oceans and Atmosphere, Hobart, Tasmania

[50]Ministry of Fisheries and Marine Resources, Swakopmund, Namibia

[51]Joint Institute for the Study of the Atmosphere and Ocean, University of Washington, Seattle, WA, USA

[52]Institute of Oceanology, Chinese Academy of Sciences, Qingdao, China

*** Correspondence:**
Robert E. Todd
rtodd@whoi.edu

Keywords: western boundary current systems, eastern boundary current systems, ocean observing systems, time series, autonomous underwater gliders, drifters, remote sensing, moorings

Abstract

Ocean boundary current systems are key components of the climate system, are home to highly productive ecosystems, and have numerous societal impacts. Establishment of a global network of boundary current observing systems is a critical part of ongoing development of the Global Ocean Observing System. The characteristics of boundary current systems are reviewed, focusing on scientific and societal motivations for sustained observing. Techniques currently used to observe boundary current systems are reviewed, followed by a census of the current state of boundary current observing systems globally. Next steps in the development of boundary current observing systems are considered, leading to several specific recommendations.

1. Introduction

Ocean boundary current systems are where society most frequently interacts with the ocean through fisheries, maritime transportation, oil and gas extraction, and recreation. These systems are home to intense and highly variable oceanic currents that redistribute mass, heat, salt, biogeochemical constituents, plankton, and pollution. Circulation patterns also influence the life history, foraging behavior, and abundance of many marine species (e.g., Mansfield et al., 2017). The coastal and open ocean are linked through boundary current systems where events such as coastal upwelling, sea level anomalies, primary productivity, fisheries, and weather are propagated between domains via various processes (e.g., eddies, Rossby waves, advection). Boundary currents may be broadly categorized as either western boundary currents (WBCs; Imawaki et al., 2013) or eastern boundary currents (EBCs) based on their governing dynamics. In each ocean basin, WBCs play a prominent role in the climate system by redistributing heat from the equator towards the poles, while EBCs are some of the most biologically productive regions in the world and respond dramatically to climate variability (Chavez et al., 2008; Chavez and Messié, 2009).

In our changing climate, shifting hydrological cycles and weather patterns are expected to strongly impact oceanic boundary current processes. Observational evidence for such shifts is beginning to appear. Wu et al. (2012) noted enhanced warming of subtropical WBCs and their extensions during the twentieth century, possibly linked to their poleward shift or intensification. Changes in the stability of WBCs have also been noted, with instabilities in the Gulf Stream shifting westward (Andres, 2016), increasing influence of warm core rings on shelf circulation (Gawarkiewicz et al., 2018), and a trend towards greater instability in the East Australian and Agulhas Currents (Sloyan and O'Kane, 2015; Beal and Elipot, 2016).

Oceanic ecosystems are being exposed to increasing pressure from major stressors including warming, deoxygenation, fishing, and acidification. EBCs in particular are projected to be strongly impacted by these stressors (Bakun et al., 2015). For instance, the Peru-Chile (Humboldt) Current system (Section 4.1.2), a highly productive EBC and a regional source of greenhouse gases, is naturally affected by upwelling of offshore waters with low oxygen and pH onto the continental shelf (Helly and Levin, 2004) and by periodic El Niño Southern Oscillation (ENSO) events that change the water masses distributions, oxygenation, and productivity (Chavez et al., 2008; Gutiérrez, 2016; Graco et al., 2017); further stress could have significant consequences for the regional ecosystem. Similarly, changes in the Gulf Stream under global warming are predicted to negatively impact fisheries in the Gulf of Maine and on the New England Shelf (Saba et al., 2016; Claret et al., 2018).

Sustained, interdisciplinary observations in boundary current regions are required for a global ocean observing system. For OceanObs'09, Send et al. (2010) proposed a global network of sustained monitoring arrays as part of the Global Ocean Observing System (GOOS). Send et al. (2010) broadly defined the properties to be observed as 1) the transports of mass, heat, and freshwater needed for monitoring the global climate in conjunction with basin-scale measurements and 2) local boundary-specific properties including eddy activity, changes in potential vorticity, air-sea interactions (Cronin et al., 2019), ecosystem dynamics, and biogeochemistry. More recently, the 2017 GOOS workshop on 'Implementation of Multi-Disciplinary Sustained Ocean Observations' (IMSOO; Palacz et al., 2017) focused, in part, on how to proceed with the development of a truly multidisciplinary boundary current observing system, building upon the more physical and climate-focused plans of Send et al. (2010). In particular, it was noted that observations that resolve along-boundary variability are needed in order to understand climate impacts on various societally relevant uses of boundary current systems (e.g., fisheries). The need to maintain a global perspective that targets all boundary current systems has been repeatedly recognized (Send et al., 2010; Palacz et al., 2017), particularly in developing nations where fisheries can be centrally important (Palacz et al., 2017). To that end, IMSOO planned to review established observing systems in the California Current System and East Australian Current in order to develop a blueprint for an adaptive, multidisciplinary observing system with relocatable subsystems to capture finer scales (Palacz et al., 2017).

Oceanic boundaries present a variety of challenges for sustained observing systems (Send et al., 2010). With strong flows in relatively shallow areas, spatial scales of O(1)-O(10) km, and temporal scales often shorter than a few days (e.g., He et al., 2010; Todd et al., 2013; Rudnick et al, 2017), the broad-scale (i.e., Argo and gridded satellite altimetry), long-duration (e.g., HOTS, BATS, Station P, CARIACO) measurements that constitute the observing system for the ocean interior are insufficient for boundary current systems. Multiple observing strategies are needed to measure the Essential Ocean Variables (EOVs) that can be used to understand and track the physical and biogeochemical processes of interest within boundary currents (Lindstrom et al., 2012). The optimal combination of observing methods will depend upon characteristics unique to each region. Send et al. (2010) noted that an additional challenge in observing boundary current systems is that there is no well-defined offshore 'end' of a boundary current, but rather a temporally and spatially variable transition to the interior. At the same time, oceanic boundaries generally lie within exclusive economic zones (EEZs), so the implementation of observing platforms requires significant international cooperation.

The overarching purpose of this review is to examine the current state of the boundary current system component of GOOS, updating and building upon the OceanObs'09 review of Send et al. (2010). Section 2 considers the scientific and societal needs that comprehensive boundary current observing systems must fulfill. Section 3 reviews how various observing techniques are employed in boundary currents, highlighting key scientific advances from each platform. Section 4 surveys the current state

of boundary current observing systems globally. Table 2 provides a comprehensive collection of publications and datasets from the past decade, organized by region and platform. Section 5 then considers the future development of boundary current observing systems. Section 6 concludes with specific recommendations to promote development of a comprehensive global network of boundary current observing systems.

2. Scientific and Societal Needs

The Framework for Ocean Observing (Lindstrom et al., 2012), developed after OceanObs'09, recommended that ocean observing systems be 1) 'fit for purpose' and driven by 'scientific inquiry and societal needs'; 2) include physical, biogeochemical, and biological observations; 3) operate collaboratively based on established best practices; 4) balance innovation with stability; 5) promote alignment of independent user groups; 6) build on existing infrastructure as much as possible; and 7) provide maximum benefit to all users from each observation. Here we present the scientific and societal needs that that should be met by comprehensive observing of oceanic boundary current systems, focusing on three broad categories: ecosystems and biogeochemistry (Section 2.1), weather and climate (Section 2.2), and connections between the shelves and deep ocean (Section 2.3).

2.1 Ecosystems and Biogeochemistry

Boundary current systems play an important role in carbon cycling through the physical and biological carbon pumps. WBCs are major sites of air-sea CO_2 exchange (e.g., Rodgers et al., 2008; Gorgues et al., 2010; Nakano et al., 2011) and have been shown to exhibit enhanced contemporary carbon uptake from the atmosphere (Takahashi et al., 2009; Landschützer et al., 2014). WBC CO_2 uptake is driven by a large pCO_2 disequilibrium with the overlying mid-latitude atmosphere, which is due to the rapid cooling of low Revelle factor waters advected from the tropics to midlatitudes. Since thick subtropical mode waters form during wintertime convection on the equatorward edges of the WBC extensions, the mode waters are key carbon sinks (e.g., Bates et al., 2002; Gruber et al., 2002; Ito and Follows, 2003; Levine et al., 2011; DeVries, 2014; Iudicone et al., 2016) and have been the target of detailed observational carbon studies (Andersson et al., 2013; Palevsky and Quay, 2017). However, it is still unclear how variability in the rate of mode water formation might impact ocean carbon uptake in these regions and what impacts these changes might have on the biological pump and higher trophic levels (e.g., fisheries). In the Kuroshio Extension region, there is evidence that the majority of carbon exported from the surface ocean during the spring and summer productive season is subsequently respired in the seasonal thermocline and ventilated back to the atmosphere during wintertime mode water formation (Palevsky et al., 2016; Fassbender et al., 2017a; Palevsky and Quay, 2017; Bushinsky and Emerson, 2018). The Southern Hemisphere WBCs are chronically undersampled, particularly during winter, leading to significant uncertainty in their contribution to the global ocean carbon sink.

Boundary current systems are highly productive regions (Chavez et al., 2008). The mechanisms of nutrient supply to surface waters that drive increased primary productivity differ among EBC and WBC systems, but their global contributions are similar (Chavez and Toggweiller, 1995). In EBC systems, the dominant source of nutrients is coastal upwelling (Chavez and Messie, 2009), while in WBC systems, geostrophic and eddy driven upwelling predominate (Pelegri and Csanady, 1991). Nutrient streams are important in the Gulf Stream (Pelegrí and Csanady, 1991; Pelegrí et al., 1996; Palter and Lozier, 2008; Williams et al., 2006, 2011) and the Kuroshio (Guo et al., 2012, 2013), transporting subsurface positive nitrate anomalies which are delivered to the photic zone primarily by mesoscale and submesoscale processes (Nagai and Clayton, 2017; Zhang et al., 2018; Yamamoto et

al., 2018; Honda et al., 2018). Nutrient cycles and drivers have not yet been studied in WBC systems of the Southern Hemisphere.

WBCs are also enriched in micro-nutrients (e.g., Fe, Zn, Cd, Co, and Ni) from land-sea exchanges. They ultimately feed open ocean surface waters and, at lower latitudes, the equatorial undercurrent, where these micro-nutrients are critical in maintaining high levels of productivity. For instance, iron transported by boundary currents in the western Pacific feeds into the Pacific Equatorial Undercurrent, which then supplies iron to the Equatorial East Pacific (e.g., Mackey et al., 2002; Ryan et al., 2006). In the North Atlantic, Gulf Stream rings supply iron to the subtropical gyre (e.g., Conway et al., 2018). Subpolar WBCs such as the Oyashio and Malvinas Current are also likely to transport waters enriched in nutrients; wind-driven and shelfbreak upwelling then supply nutrients to the euphotic layers, enhancing biological productivity (Matano and Palma, 2008; Ito et al., 2010; Valla and Piola, 2015). Locations at which subtropical and subpolar WBCs meet provide ideal environments for biological production as warm subtropical waters converge with nutrient-rich subpolar waters (Brandini et al., 2000).

The upwelling of deep, poorly ventilated water masses rich in inorganic nutrients and CO_2 and low in O_2 make EBCs areas of high air-sea fluxes, and the sensitivity of the upwelling process to climate variability contributes to large interannual and decadal scale changes in the magnitude of these fluxes (Friederich et al., 2002; Brady et al., 2018). EBCs also exhibit strong cross-shore gradients in fluxes; narrow strips of the nearshore ocean act as intense sources of CO_2 to the atmosphere, while the abundance of nutrients in these upwelled waters facilitates primary production that results in net uptake of CO_2 (Hales et al., 2005). The supply of poorly ventilated waters combined with high levels of organic-matter remineralization resulting from intense primary production in surface waters can trigger periods of anoxia and low pH in shelf waters (Feely et al., 2008; Zhang et al., 2010) with severe consequences for demersal and pelagic ecosystems (Chan et al., 2008; Monteiro et al., 2008; Bertrand at al., 2011).

Boundary currents play an important role in ocean ecosystems across all trophic levels. The intense levels of primary production associated with EBCs support rich ecosystems with relatively short food chains, and these systems provide at least 20% of the world's wild-caught fish despite covering less than 1% of the global ocean (Chavez and Messié, 2009). WBCs and EBCs are also oceanic regions where coastal and open ocean ecosystems are brought together and interact. Modeling studies have suggested that boundary currents are hotspots of microbial biodiversity (Barton et al., 2010; Clayton et al., 2013). This has been supported in the Kuroshio Extension by some in situ surveys (Clayton et al., 2014, 2017). At the other end of the trophic spectrum, recent work combining tag data and satellite altimetry data has shown that white sharks (*Carcharodon carcharias*) actively occupy warm-core anticyclonic eddies in the Gulf Stream (Gaube et al., 2018). The warmer waters in these mesoscale features allow the sharks to reduce the physiological costs of thermoregulation in cold water, thereby making prey more accessible and energetically more profitable. Similarly, the location of the Kuroshio axis and associated changes in water temperature have been shown to influence the behavior of juvenile Pacific bluefin tuna (*Thunnus orientalis*; Fujioka et al., 2018). In the Southern Benguela EBC upwelling system, the coastal, wind-driven upwelling along the southwest African coast supports planktonic food supplies for young pelagic fish, while the temperate Agulhas Bank shelf region provides suitable spawning habitat for large communities of fish including in particular anchovy and sardine (Hutchings et al., 2009c). Likewise, southern elephant seals feed along the intense fronts and eddies in the Brazil/Malvinas Confluence (Campagna et al., 2006). WBCs are also known to play an important role in the migration of other coastal and pelagic organisms, such as eels (Shinoda et al., 2011; Rypina et al., 2014) and salmon (Wagawa et al., 2016).

Marine heat waves (MHWs) are strongly linked with boundary current systems. For instance, the exceptional and devastating MHW event off Western Australia during summer of 2010/2011 was caused by a strengthening of the Leeuwin Current associated with La Niña conditions (Pearce and Feng, 2013; Feng et al., 2015), a 2014-2015 MHW had unprecedented impacts on the California Current System (Di Lorenzo and Mantua 2016; Zaba and Rudnick 2016), and a MHW in 2015-2016 impacted the Tasman Sea (Oliver et al., 2017). These discrete, prolonged periods of anomalously warm waters at particular locations (Hobday et al., 2016) can stress ecosystems, leading to increased mortality of marine species, closing of commercial and recreational fisheries, and coral bleaching (Cavole et al., 2016; Stuart-Smith et al., 2018). The addition of other stressors such as ocean acidification and deoxygenation, which are projected to increase in future warming scenarios, could amplify the ecosystem impacts of MHWs. Sustained physical and biogeochemical observations are necessary to improve forecasts of the frequency and magnitude of MHWs, as well as to assess the risk and vulnerability of marine ecosystems to extreme climate events (Frölicher and Laufkötter, 2018).

2.2 Climate and Weather

Boundary currents are an integral part of the global climate system as they redistribute heat and facilitate carbon uptake from the atmosphere (Section 2.1). In the Atlantic, boundary currents are key components of the Atlantic Meridional Overturning Circulation (AMOC; Frajka-Williams et al., 2019). Low-latitude WBCs that connect the subtropics to the equator at thermocline and intermediate levels are important contributors to the mass and heat budgets of the equatorial oceans, which influence climate modes such as ENSO (Lengaigne et al., 2012). Low-latitude WBCs are also suspected to contribute to the decadal modulation of the equatorial thermocline background state (e.g., Lee and Fukumori, 2003). Sustained monitoring of WBC transports would be particularly useful for climate and seasonal-to-decadal forecast centers (see Smith et al., 2019).

As climate change progresses, boundary current systems are likely to undergo further significant changes. Subtropical WBCs and their extensions are the fastest warming regions of the world ocean (Wu et al., 2012; Yang et al., 2016). Climate model simulations have suggested that western boundary current extensions may move poleward under climate change (Saba et al., 2016). This poleward expansion of energetic WBCs may impact extreme temperatures and marine species migration (Johnson et al., 2011), as well as enhance eddy activity regionally (e.g., Oliver et al., 2015). While low-resolution climate models suggest strengthening and poleward migration of several of these currents under climate change, particularly in the Southern Hemisphere (Sen Gupta et al., 2012; Hu et al., 2015; Pontes et al., 2016), studies leveraging in situ velocity and satellite data suggest no significant increase in their transports since the early 1990s (Rossby et al., 2014; Beal and Elipot, 2016). This discrepancy motivates the collection of long-term measurements of baroclinic changes in boundary currents (i.e., subsurface temperature and salinity properties), as well as the vertical structure of the velocity, in order to understand and predict future changes.

In addition, ocean warming and a magnified hydrological cycle could drive significant changes in shelf ocean stratification, while changes to wind forcing will directly alter rates of upwelling. These ocean circulation processes, and meteorological forcing at the scales that impact upwelling, are poorly represented in climate models (Richter, 2015; Zuidema et al., 2016). Thus, we have little capability to predict how upwelling, winds and other physical drivers of ocean property exchanges at the coastal/open ocean boundary will change in the future. The impact these changes will have on coastal ecosystems is simply unknown.

Detection and attribution of global sea level variability has improved considerably in the last decade (Cazenave et al., 2014; Marzeion et al., 2014). The location and strength of WBCs considerably influence the mean local sea level (Domingues et al., 2016; Archer et al., 2017a) possibly accounting for part of the mismatch between forecasts and observations of sea level at the coast (Ezer, 2015). Relationships between large scale wind anomalies, basin-wide sea surface height (SSH), and WBCs (e.g., Boening et al., 2012; Volkov et al., 2019) suggest that observations of current strength and oceanic teleconnections can be used to improve seasonal to decadal coastal sea level forecasts, leading to improved assessments of impacts on infrastructure and groundwater quality (Slangen et al., 2014; Park and Sweet, 2015).

Boundary current systems influence synoptic and longer scale weather patterns. Large upper ocean heat content within WBCs can fuel development and intensification of tropical cyclones (Bright et al., 2002; Wu et al., 2008; Nguyen and Molinari, 2012; Galarneau et al., 2013). Strong sea surface temperature (SST) gradients across WBCs, particularly during winter months, destabilize the atmospheric boundary layer, fueling the mid-latitude storm tracks and atmospheric blocking frequency, which in turn impact regional climate (Kelly et al., 2010; Nakamura, 2012; O'Reilly and Czaja, 2015; O'Reilly et al., 2016; Révelard et al., 2016; Ma et al., 2017). For instance, a weaker Gulf Stream SST front leads to a decrease in cold and dry spells over Europe (O'Reilly et al., 2016), while a sharper SST front in the Kuroshio Extension increases cyclogenesis and shifts the storm track northward, causing warming over eastern Asia and the western United States that can reduce snow cover by 4-6% (O'Reilly and Czaja, 2015; Révelard et al., 2016). Variability in the warm waters of the Agulhas influences summer rainfall over parts of South Africa (Jury et al., 1993; Nkwinkwa Njouodo et al., 2018). In EBC systems, SST minima are collocated with maxima in sea level pressure that are in turn associated with alongshore wind stress, wind stress curl, and cloud cover along the boundary (Sun et al., 2018), suggesting coupling with the full Hadley-Walker tropical atmospheric circulation, though the details of such coupling remain an open question.

Accurate weather and climate forecasting thus requires accurate representation of boundary current systems. However, most of the current ocean reanalyses used to initialize the monthly, seasonal, and decadal forecasts exhibit large errors in the boundary currents (Rouault et al., 2003; Valdivieso et al., 2017), hampering forecast performance. Coupled climate models, such as those used in the Intergovernmental Panel on Climate Change reports, also exhibit large deficiencies in boundary current regions (e.g., Zuidema et al., 2016; Siqueira and Kirtman, 2016), including warm SST biases in EBCs (e.g., Large and Danabasoglu, 2006). Current modelling and data assimilation capabilities are insufficient to fully represent boundary currents at the small spatial scales needed for forecasting. Subramanian et al. (2019) further consider how observing efforts, including within boundary currents, can contribute to improved subseasonal-to-seasonal forecasting.

2.3 Shelf-Deep Ocean Connections

The coastal ocean and nearshore zones support a broad range of human activities in maritime industries and resource extraction, and the environmental health and productivity of these regions deliver important ecosystem services. As already noted, the proximity of energetic boundary currents in deep water adjacent to continental shelves mediates shelf-sea/deep-ocean exchange of properties. Along many coasts, this forcing can match or exceed local drivers of circulation such as tides, wind, and river inflows. Coastal ocean and shelf edge dynamics have immediate impacts on ecosystem function and productivity on weekly to seasonal time scales, but can also drive multi-decadal changes in ecosystem structure through effects on habitat ranges and biodiversity, not only in coastal zones but also at basin scales.

While we have a broad understanding of the dynamics of upwelling in both WBC and EBC regimes, quantitative estimates of net shelf-sea/deep-ocean exchanges of freshwater and tracers integrated over extended along-shelf distances are few. Quantifying these exchanges is challenging where shelf-edge flow-bathymetry interactions foster variability at short length and time scales. Similarly, exchange flows are not always readily observable at the sea surface from satellite or shore-based remote sensing technologies (Section 3.6) because they are associated with bottom boundary layer flow driven by the boundary current encountering the sea-floor or subduction at the sea surface due to boundary current detachment and mixing. Two efforts along the U.S. East Coast are striving to make such measurements using multi-platform observing arrays: the Processes driving Exchange At Cape Hatteras (PEACH) program and the Ocean Observatories Initiative (OOI; Smith et al., 2018; Trowbridge et al., 2019) Pioneer Array (see Section 4.2.1). Similarly, in situ and satellite remote sensing observations combined with high-resolution numerical simulations have provided insights into the shelf-sea/deep-ocean exchanges near the confluence of the Brazil and Malvinas Currents (Guerrero et al., 2014; Matano et al., 2014; Strub et al., 2015).

On narrow continental shelves adjacent to intense boundary currents, the impact of deep-ocean circulation on the shelf system is immediate, driving significant fluxes across the continental shelf edge through mesoscale and boundary layer dynamics. For example, mesoscale and submesoscale meandering of the Agulhas jet leads to strong episodic exchanges with shelf waters (Leber et al., 2017; Krug et al., 2017) that support high productivity over the eastern Agulhas Bank (Probyn et al., 1994) and may influence the well-known sardine run (Fréon et al., 2010). On broad continental shelves, bathymetric constraints on cross-isobath flow can hamper exchange at the shelf edge, trapping terrestrial inflows and establishing appreciable cross-shelf buoyancy gradients that in turn sustain shelf-edge fronts (Fratantoni and Pickart 2007; Howatt et al., 2018).

With changing climate, ocean warming and changes to the hydrological cycle could drive changes in vertical thermal stratification and across-shelf salinity stratification, altering ocean conditions at the inshore edge of boundary current systems (e.g., Gawarkiewicz et al., 2018) and potentially impacting across-shelf fluxes of nutrients and micro-nutrients that are important to sustaining coastal productivity (Fennel et al., 2006). Changes in watershed land use and global weather will alter the volume and characteristics of river flows discharged into the coastal zone. At continental shelf scales, key areas of uncertainty in the oceanographic response to climate variability and change include sub-mesoscale processes and open ocean-shelf exchange. Sustained observing efforts are needed that more fully capture the influence of boundary currents on exchanges with the coastal zone. Designing and deploying boundary current observing systems capable of operating across shelf and deep ocean regimes to deliver coherent views of the shelf-edge exchange is challenging.

3. Observing Techniques

The highly variable and multi-scale characteristics of boundary currents necessitate an integrated observing system approach, in which high-resolution observations are nested within a backbone of observations over a broad area. Under the Framework for Ocean Observing (Lindstrom et al., 2012), design and implementation of ocean observing systems is focused around a set of EOVs that include physical, biogeochemical, and ecosystem parameters (Table 1 and http://www.goosocean.org/eov). Design of an observing system for a particular region (e.g., a specific boundary current system) should proceed through a series of 'readiness levels'. In the concept phase, initial feasibility studies and peer review of proposed plans take place. Then, in the pilot phase, small-scale deployments are used to test and validate the proposed approach. Once the observing system reaches the mature phase, it is part of the sustained global ocean observing system. No single observing platform can provide

all of the necessary measurements (Table 1), so an optimal mix of observing platforms is needed. Determination of this mix of platforms will be specific to a particular boundary current system, taking into consideration the unique processes and scales at play in that system. Here we briefly review how various observing platforms are currently being used in boundary current systems; Table 2 refers to many other examples of these observing techniques being applied to boundary current systems.

3.1 Time Series

Time series measured from platforms fixed to the seafloor have long been and continue to be central to observing system design and implementation since they uniquely enable collection of long-term measurements at high temporal resolution (minutes to hours) at key locations. Traditional tall moorings (e.g., Johns et al., 2005) typically carry instruments on the mooring wire, within subsurface floats, and on surface buoys, if present; instruments are available to measure most physical EOVs and a growing number of biogeochemical and ecosystem EOVs (Table 1). Moored surface buoys additionally carry suites of meteorological sensors on the buoy tower and sensors for biogeochemical and physical EOVs on the buoy bridle and mooring line just below the sea surface; these air- and sea-surface measurements can be combined to estimate the air-sea exchanges of heat, moisture, CO_2, and momentum (Cronin et al., 2019). Inverted echo sounders (IESs) measure the time for sound pulses to travel from the bottom-mounted IES to the surface and back, which, in regions with good databases of hydrographic measurements, can provide full water column estimates of temperature, salinity, and density using the gravest empirical mode technique (Meinen and Watts, 2000). In the Florida Strait, a unique time series of volume transport has resulted from measuring the voltage induced in a submarine cable by seawater moving through the Earth's magnetic field (Larsen and Stanford, 1985; Baringer and Larsen, 2001; Meinen et al., 2010).

Dense, moored arrays of instruments remain the most effective way to return volume and property transport measurements with high temporal resolution. Subsurface moorings are more typical in WBCs due to the strong surface currents, although surface moorings have also been successfully deployed in the Gulf Stream (Weller et al., 2012) and Kuroshio Extension (Cronin et al., 2013). Arrays of IESs can be used to infer geostrophic shear profiles, and, with the addition of bottom pressure sensors (PIES) and near-bottom current measurements (CPIES), can provide estimates of the absolute geostrophic current (Donohue et al., 2010; Meinen et al., 2018). However, the high costs of building, deploying, and turning around such arrays makes them feasible only at a few key locations. Other observing assets are needed to provide spatially broad measurements.

3.2 Ship-Based Measurements

Measurements from both dedicated research vessels and ships of opportunity have been central to observing boundary current systems for decades. Research vessels can measure nearly every EOV (Table 1) through the full depth of the water column and are uniquely capable of collecting many types of samples (e.g., net tows, large-volume water samples). Ongoing sustained research vessel surveys of ocean boundary currents include the global GO-SHIP transects at 25-50 km resolution (Talley et al., 2016) and the California Cooperative Oceanic Fisheries Investigations (CalCOFI) surveys (McClatchie, 2014) in the California Current System (see Section 4.1.1). The servicing of boundary current mooring arrays, generally undertaken from research vessels, provides unique opportunities to undertake intensive process studies targeting key scientific questions. The primary limitations on research vessels' contribution to sustained boundary current observing are their high

costs of operation (typically tens of thousands of dollars per day, excluding science personnel) and the infrequency of cruises.

The World Meteorological Organization (WMO) Voluntary Observing Ship (VOS) Program and Ship Of Opportunity Program (SOOP) both make use of non-research vessels to collect observations globally, substantially augmenting the amount of ship-based observing. Both programs collect meteorological measurements with real-time observations benefiting weather forecasting, while SOOP additionally uses commercial ships to collect oceanographic measurements along frequently occupied trade routes in the global ocean. Oceanic measurements from SOOP include temperature profiles from expendable bathythermographs (XBTs) at 10-25 km resolution in boundary currents (Goni et al., 2019), surface temperature, salinity, plankton, and pCO_2 from flow-through systems, and, on specially-equipped vessels, velocity profiles from hull-mounted ADCPs (e.g., M/V *Oleander*; Rossby et al., 2010). Several repeat transects across boundary currents have been maintained for multiple decades and so represent some of the longer data sets available (see Section 4). Fast-moving ships are often able to occupy transects directly across strong boundary currents in short periods of time, a feat not yet possible with other sampling platforms. However, subsurface measurements of variables other than temperature and velocity have remained elusive from ships of opportunity, and recovery of instruments deployed over the side is not practical on cargo vessels.

3.3 Autonomous Underwater Gliders

Autonomous underwater gliders (Rudnick, 2016b; Testor et al., 2019) routinely collect long-duration, high-resolution observations in a variety of boundary current systems globally (Todd et al., 2018a; Table 2). Gliders typically profile from the surface to 500-1000 m, taking 3-6 h to complete a cycle from the surface to depth and back while covering 3-6 km horizontally through the water at a speed of about 0.25 m s^{-1}. During a mission lasting 3-6 months, a glider's survey track extends well over 2000 km. Owing to the relatively slow speed of gliders, care must be taken when interpreting the observations, which contain both spatial and temporal variability (Rudnick and Cole, 2011). Sustained deployment of networks of gliders can provide observations with both high spatial resolution and year-round coverage (e.g., Fig. 1a,b).

Realizable glider-based sampling plans in boundary currents vary primarily due to the strength of currents relative to a glider's speed. In EBCs and other boundary currents with relatively weak depth-average currents, gliders can occupy repeat survey lines. The California Underwater Glider Network (CUGN; Fig. 1, left), which consists of three cross-shore transects off southern and central California that have been continuously occupied for more than a decade (Rudnick et al., 2017), exemplifies sustained glider observations in an EBC. In WBCs and other boundary currents where depth-average currents are significantly faster than a glider's speed through the water, gliders can be navigated so as to cross the observed flow as they are advected downstream, returning oblique transects. For example, multi-year surveys of the Gulf Stream (Fig. 1, right; Todd et al., 2016, 2018b; Todd 2017; Todd and Locke-Wynn 2017) have now returned over 150 high-resolution transects across the WBC of the North Atlantic. Testor et al. (2019) further discuss efforts associated with the OceanGliders Boundary Ocean Observing Network (BOON).

Gliders can carry a variety of sensors (e.g., Fig. 1c-f). Measurements of pressure, temperature (Fig. 1d), conductivity, and depth-average currents are standard, enabling estimates of absolute geostrophic transport and other physical parameters at relevant scales in boundary currents. Measurements of bio-optical (e.g., Niewiadomska et al., 2008; Henderikx Freitas et al., 2016) and bio-acoustic properties (e.g., Baumgartner and Fratantoni, 2008; Van Uffelen et al., 2017), dissolved

oxygen (e.g., Fig. 1e; Perry et al., 2008), nitrate, turbulent microstructure (St. Laurent and Merrifield, 2017), and velocity profiles (Fig. 1f; Todd et al., 2017) are becoming increasingly common. The main constraints on sensors for gliders are the requirements for small size, low power consumption, and multi-month stability. As sensor technology continues to mature, gliders will be well suited to carry sensors for additional EOVs, such as pH, in boundary currents.

3.4 Drifters

Surface Velocity Program (SVP) drifters drogued at 15 m depth (Niiler et. al. 1995; Niiler, 2001; Centurioni, 2018) deployed as part of the Global Drifter Program (GDP) and of the Global Surface Drifter Array (GSDA) are also important for understanding the structure and variability of boundary current systems. The GSDA archive dates back to February 1979 and includes over 32 million records of geographical location, 15-m depth velocity, and SST at 6-hour resolution (e.g., Hansen and Poulain, 1996; Lumpkin and Pazos, 2007).

Drifter observations have been widely used in both EBCs and WBCs (see Table 2). Recently improved analysis techniques (e.g., Lumpkin, 2003; LaCasce, 2008; Koszalka and LaCasce, 2010; Laurindo et al., 2017) and expansion of the Lagrangian drifter array have allowed gridded, Eulerian statistics of near-surface velocity to be produced at higher resolution, resulting in improved estimates of near-surface flow in boundary currents (e.g., Fig. 2) at seasonal to interannual time scales (e.g., Niiler et. al, 2003; Lumpkin and Johnson, 2013). Drifter observations in boundary currents offer opportunities for new analyses of long-term variability and trends (e.g., Johnson, 2001; Lumpkin and Johnson, 2013) and the dispersion of tracers and marine debris in the upper ocean (Lumpkin et al., 2012; Van Sebille et al., 2015), which is driven by turbulence at scales from surface waves through the submesoscale to large-scale geostrophic eddies (Lumpkin et al., 2017; Lund et al., 2018).

3.5 Argo Floats

Over the past two decades, autonomous profiling Argo floats have become cost-effective and robust platforms. Over 3700 active Argo floats provide global measurements of temperature, salinity, and pressure in the upper 2000 m of the ocean, and some are also equipped with sensors measuring biogeochemical properties (Riser et al., 2016; Jayne et al., 2017; Roemmich et al., 2019). Though the Argo network was not designed to capture the details of boundary currents and lacks the resolution necessary to resolve narrow boundary currents, Argo data have nevertheless been used extensively in both WBCs and EBCs (see Table 2). Argo complements other boundary current observing efforts by: providing collocated temperature and salinity measurements that are used to infer geostrophic shear from XBT temperature profiles, extending geostrophic shear from XBT and ocean glider data to 2000 m, measuring reference velocities at parking depth (typically 1000 m), and linking transport measurements of boundary currents to the ocean interior through basin-wide integration (e.g., Zilberman et al., 2018). Following recommendations at OceanObs'09 (Roemmich et al., 2010), the Argo program is currently moving to double float density in WBC regions (Jayne et al., 2017). The Kuroshio (Fig. 3a) and Gulf Stream have historically been among the more densely-populated sectors in the Argo array, while other boundary current regions (e.g., the Peru-Chile system, Fig. 3b) lack the desired coverage.

3.6 Remote Sensing

Among the many oceanic variables that are routinely measured from satellites (Table 1), SSH, SST, and ocean color have been most used to study boundary current systems. Satellite measurements typically have resolutions of O(1)-O(10) km along the satellite track, with repeated measurements on

daily to ten-day time scales at a given location. Boundary currents often have strong signatures in both SSH and SST, so satellite-derived gradients in these properties can approximate the strength and/or position of these currents (e.g., Imawaki, 2001), including variability on longer time scales (e.g., Qiu and Chen, 2005; Qiu et al., 2014; Andres 2016). Synergy between dynamic height derived from temperature and salinity profiles and SSH can be exploited to produce synthetic reconstructions of boundary currents (van Sebille et al., 2010; Beal and Elipot, 2016; Majumder and Schmid, 2018; Zilberman et al., 2018), although these reconstructions crucially depend on assumptions about the non-steric (barotropic and mass) variability. Weaknesses of SSH for observing boundary currents include reduced measurement quality within 40 km of the coast due to large uncertainties in the wet-tropospheric correction, unfiltered tides, and a lack of sufficient temporal and spatial resolution to capture the full spectrum of near-surface current variability observed by drifters (Poulain and Niiler, 1989; Centurioni and Niiler, 2003; Fratantoni and Richardson, 2006; Centurioni et al., 2008, 2009; Maximenko et al., 2009). Products that combine SSH and drifter measurements have improved eddy kinetic energy and dynamic topography estimates (Maximenko et al., 2009; Lumpkin and Garzoli, 2011; Rio et al., 2014, 2018). Estimates of chlorophyll derived from satellite ocean color measurements provide information on biological productivity in boundary current systems worldwide (e.g., Messié and Chavez, 2015; Gómez-Letona et al., 2017). Because ocean color observations have higher resolution (O(1) km) than satellite altimetry, they potentially provide insight into the rich fields of submesoscale instabilities that exist within boundary current systems (Fig. 4; Everett et al., 2014; Lee and Kim, 2018).

High-frequency (HF) radars (Paduan and Washburn, 2013) have been used effectively to monitor surface current variability of boundary currents (e.g., Kim et al., 2011; Archer et al., 2018). They directly map the total surface current within O(100) km of the coast at high resolution in time (~1 hour) and space (~1 km) during long-term deployments (~10 years). HF radar observations have proven useful for investigating both the mean surface velocity structure of boundary currents and associated submesoscale features that develop as boundary currents meander and shed eddies (Soh and Kim, 2018; Archer et al., 2018). Combining HF radar velocity estimates with satellite-based measurements of SST and ocean color (e.g., Fig. 4) can provide a multidisciplinary view of surface circulation features at O(1)-km scales (e.g., Schaeffer et al., 2017). Some radar sites have been in continuous operation for more than a decade, offering opportunities to examine interannual to decadal variability of surface circulation. New radar sites can be installed and daisy-chained with existing sites, providing measurements of the alongshore evolution of boundary currents, as has been achieved along the west coast of the U.S. (Kim et al., 2011).

4 Current Status of Regional Boundary Current Observing Systems

Existing observing systems for particular boundary currents are in various stages of development. Here we review the current status of the observing systems currently operating in several EBCs and WBCs globally. The California Current System (Section 4.1.1) is arguably the most well sampled boundary current in the world, offering hope that a fully integrated physical and biogeochemical system is achievable. Other boundary current systems, particularly in the southern hemisphere, are much less sampled. As was the case a decade ago (Send et al., 2010) biogeochemical and ecosystem EOVs (Table 1) remain much less well sampled than physical EOVs. Table 2 provides a more comprehensive collection of recent scientific results for each boundary current system as well as sources of publicly available observations.

4.1 Eastern Boundary Current Systems

4.1.1 California Current System

The California Current System is the EBC system of the subtropical North Pacific (Checkley and Barth, 2009). The equatorward flowing California Current carries relatively cool and fresh waters of subpolar origin, while the poleward California Undercurrent (Gay and Chereskin, 2009; Todd et al., 2011b) transports warmer saltier waters from the tropics along the continental margin. The California Current System is strongly influenced by the predominantly upwelling-favorable winds along the west coast of North America.

Owing to the need to understand the collapse of the regional sardine fishery in the 1940s, there is a well-developed multidisciplinary observing system in the California Current System with a decades-long history of routine observations by the CalCOFI program (McClatchie, 2014, and references therein). Since 1949, CalCOFI has made regular (currently quarterly) measurements of physical, biological, and chemical properties at fixed stations along survey lines oriented perpendicular to the coast from research vessels (Fig. 5). The establishment of the California Current Ecosystem Long Term Ecological Research program in 2004 brought further ship-based surveys and long-term moorings (Fig. 5) focused on nonlinear transitions in the pelagic ecosystem in response to ENSO, the Pacific Decadal Oscillation, and secular trends. In the Northern California Current, the Newport Hydrographic Line (44° 39.1’ N) has been continuously occupied since 1961 (Huyer et al., 2007). Since 2005, autonomous underwater gliders have continuously surveyed along three of the CalCOFI lines as part of the CUGN (Section 3.3; Figs. 1 and 5) as well as along cross-shore transects as far north as the Washington coast (Fig. 5), returning measurements of physical properties and some biological proxies; the gliders complement the ship-based surveys by providing observations at higher spatial and temporal resolution (e.g., Rudnick et al., 2017), albeit of a more limited set of properties. An array of PIES with end-point moorings off of southern California monitors full-depth geostrophic transport; gliders routinely retrieve data from the PIES and transmit them to shore (Send et al., 2013). Since 2007, NOAA has led large-scale coastal surveys along the U.S. West Coast every 2-4 years to determine the spatial distributions of carbon, oxygen, nutrient, biological, and hydrographic parameters (Feely et al., 2008, 2018). Starting in 2010, moored platforms throughout the California Current System established high-frequency time series of physical and biogeochemical parameters (Nam et al., 2011; Harris et al., 2013; Sutton et al., 2016). More recently, the OOI Endurance Array (Smith et al., 2018; Trowbridge et al., 2019) has been deployed in the northern California Current System (Fig. 5); moorings on the shelf and continental slope provide high-resolution time series while gliders provide high-spatial-resolution observations between the mooring sites. A network of shore-based HF-radars provides real-time surface currents within about 150 km of the coast along nearly the entire U.S. West Coast (Kim et al., 2011).

4.1.2 Peru-Chile Current System

The Peru-Chile Current System (or Humboldt Current System) is the EBC system of the subtropical south Pacific, extending from the equator to southern Chile (~45°S). It is characterized by a persistent stratus cloud deck, equatorward surface currents, strong wind-driven coastal upwelling, poleward undercurrents, and filaments and eddies that develop along the coasts of Peru and Chile (see Colas et al., 2012 and references therein). A subsurface oxygen minimum zone (e.g., Paulmier and Ruiz-Pino, 2009) results in upwelled waters being nutrient rich but low in oxygen (e.g., Silva et al., 2009; Pizarro et al., 2016). Due to its proximity to the equator, the Peru-Chile Current System is strongly influenced by equatorial variability through propagation of Kelvin and coastal trapped waves (Dewitte et al., 2012; Mosquera-Vasquez et al., 2013) and anomalous advection during strong El Niños (e.g., Colas et al., 2008).

The dramatic impacts of El Niño events on both weather and fisheries have driven monitoring of oceanographic properties and fish stock assessments along the Peruvian coast since the 1960s (Fig. 6; Grados et al., 2018). Over the past decade, these surveys have taken place monthly along the northern Peruvian coast and at least twice per year along the entire Peruvian coast; shipboard ADCP surveys are conducted at least seasonally. Biweekly time series along the 100-m isobath between Paita (5°S) and Ilo (17°S), coastal tide-gauge stations, daily SST measurements at coastal laboratories, and a nearshore thermistor chain and bottom-mounted ADCP at 4°30' S (Fig. 6) allow monitoring of temperature and sea level anomalies and associated fluctuations in thermocline, oxycline, and nutricline depths. Measurements from the TAO/TRITON moored array and the Argo program (Fig. 3b) provide key broad-scale context to these coastal observations. Efforts are underway to improve monitoring of the Peru-Chile Current System. For instance, sustained glider surveys across the frontal region off northern Peru, where El Niño impacts are large, are planned to begin by 2020.

4.1.3 Leeuwin Current System and South Australian Current System

The boundary currents along the western and southern coasts of Australia have some unique features. The Leeuwin Current, which is the subtropical EBC of the southeastern Indian Ocean, is unusual in that it flows poleward along an eastern boundary, transporting warm, fresh tropical waters southward due to forcing by the Indonesian Throughflow and ocean atmosphere interactions in the Indian Ocean (Godfrey and Weaver, 1991); it is important for the upper ocean heat balance in the southeast Indian Ocean (Domingues et al., 2006). The Leeuwin Current hosts broad-scale downwelling (Furue et al., 2017; Liang et al., 2017) where eastward surface currents merge with the Leeuwin Current and then downwell into the Leeuwin Undercurrent at depths of 200-1000 m. The equatorward Leeuwin Undercurrent carries waters of subantarctic origin along the western Australian coast (Woo and Pattiaratchi 2008), leaving the coast near 22°S to contribute to the lower limb of a zonal overturning (Furue et al., 2017) and the subtropical gyre (Schott et al., 2009). In winter, the Leeuwin Current merges with the southwestward-flowing Holloway Current off the northwest coast of Australia, the eastward-flowing South Australian Current off the south coast and the southward-flowing Zeehan Current off the west coast of Tasmania to form the longest shelf-break boundary current system in the world (Ridgway and Condie, 2004; D'Adamo et al., 2009; Ridgway and Godfrey, 2015). Along the continental slope south of Australia, the westward flowing Flinders Current results from the collision of the equatorward deep ocean Sverdrup transport with the deep shelf slope of the Great Australian Bight (Middleton and Cirano, 2002; Middleton and Bye, 2007) and is a unique northern boundary current.

Coastal sea level observations at Fremantle have long been used as a proxy for the strength of the Leeuwin Current (Feng et al., 2003). Since 2008, the Australian Integrated Marine Observing System (IMOS; Hill et al., 2010) has been monitoring the shelf component of the Leeuwin Current near 32°S using shelf moorings (Feng et al., 2013), gliders, and HF radars (Fig. 7). Short-term deployments (2012-2014) have also been carried out off the northwest coast of Australia (Ridgway and Godfrey, 2015). XBT surveys from Ships of Opportunity in and out of Fremantle, though not targeted for the Leeuwin Current, have taken place since the mid-1980s (Wijffels et al., 2008). IMOS makes ongoing observations of the South Australian Current system with dedicated moorings and glider missions monitoring the Flinders Current (Fig. 7).

4.1.4 Benguela Current System

The Benguela Current Large Marine Ecosystem is the eastern boundary upwelling system of the South Atlantic. The equatorward Benguela Current is unique in that it is bounded by warm currents

644 at its northern and southern edges, the Angola Current to the north and the Agulhas Current (Section
645 4.2.4) to the south. Coastal upwelling is linked to the seasonal position of the South Atlantic high
646 pressure system, resulting in a number of upwelling cells along the southern African coast with
647 divergent seasonality; the strongest year-round upwelling occurs off Lüderitz (~26°S), effectively
648 dividing the Benguela Current System into northern and southern sub-systems. The northern
649 Benguela upwelling system is highly productive (e.g., Louw et al, 2016), but also prone to hypoxia
650 over the continental shelf that is modulated by a seasonal poleward undercurrent bringing low-
651 oxygen waters to the shelf in summer and fall and an equatorward undercurrent that brings
652 oxygenated water in winter and spring (Duncombe Rae, 2005; Mohrholz et al., 2008; Monteiro et al.,
653 2008). The southern Benguela upwelling system experiences intense, pulsed upwelling in summer
654 and quiescence in winter (Shannon and Nelson, 1996; Weeks et al., 2006; Hutchings et al., 2009a),
655 although the direction of net Ekman transport appears to be offshore year-round (Carr and Kearns
656 2003). This region also experiences hypoxia (and occasionally, anoxia) in inshore waters, particularly
657 in the region of St. Helena Bay (Pitcher and Probyn, 2011; Pitcher et al., 2014), but low-oxygen
658 events are driven solely by bacterial respiration of organic matter from surface waters (Monteiro and
659 van der Plas, 2006) and can result in mass mortalities of commercial fish stocks and rock lobster
660 (e.g., Van der Lingen et al., 2006; Cockcroft et al., 2000, 2008).

661 In the southern Benguela current system, monthly ship-based sampling of fisheries-relevant
662 parameters took place through the 1950s and 1960s, then intermittently until 1988, after which
663 surveys of fisheries, hydrographic, and chemical properties have been conducted 2-3 times per year
664 (Fig. 8; Moloney et al., 2004). Since 2012, quarterly surveys as part of the Integrated Ecosystem
665 Programme have additionally monitored the carbonate system. Various multifunctional moorings
666 have been deployed over the years, including a buoy for oxygen and temperature and a harmful algal
667 bloom detection system in the vicinity of St. Helena Bay (see Hutchings et al., 2009b).The Namibian
668 Ministry of Fisheries and Marine Resources conducts regular monitoring of hydrographic conditions
669 and commercial fish resources in Namibian waters of the northern Benguela (Fig. 8); regular
670 shipboard oceanographic monitoring began in 1999 with sampling frequency varying from two to
671 eight occupations annually along most lines and up to twice per month off Lüderitz during the lobster
672 fishing season. Long-term, though intermittent, moored observations have been collected at 23°S,
673 14’03°E, and coastal stations are maintained along the Namibian coast (Fig. 8).

674 **4.1.5 Canary Current System**

675 The Canary Current large marine ecosystem extends from the northern tip of the Iberian Peninsula
676 (43°N) to south of Senegal (12°N), corresponding to the extent of the northeasterly trade winds in the
677 northeastern Atlantic. Upwelling occurs year-round with meridional shifts in the trade winds leading
678 to seasonality in the latitudinal range of upwelling, particularly in the south (Benazzouz et al. 2014;
679 Faye et al., 2015), where strong intraseasonal to longer time-scale variability is driven by internal or
680 remotely forced pulsations of the trade winds, passages of African easterly waves, and oceanic
681 coastally trapped waves (Polo et al. 2008; Diakhaté et al. 2016; Oettli et al. 2016). The ecosystem is
682 broadly divided by the Strait of Gibraltar into the Iberian and the Northwest African areas, though
683 strong subregional differences are observed due to variability in factors including coastal
684 configuration, oxygen concentration, nutrient fertilization, and productivity (Arístegui et al., 2009).
685 The continental shelf in the Canary Current System is the most extensive of any EBC, and persistent
686 circulation features are associated with the topography of the shelf. Large filaments of coastal
687 upwelled water stretch offshore from the numerous capes and promontories (e.g., Cape Guir and
688 Cape Blanc), transporting waters rich in organic matter into the oligotrophic subtropical gyre
689 (Álvarez-Salgado et al. 2007; Lovechio et al., 2018). The Canary Archipelago interrupts the

equatorward flow of the Canary Current, leading to strong mesoscale variability downstream of the islands (Arístegui et al., 1994). Island eddies and upwelling filaments interact to exchange water properties, resulting in an efficient route for transporting organic matter to the open ocean (Arístegui et al., 1997; Barton et al., 1998). As a major upwelling area, the Canary Current System is a highly productive and the focus of intensive fisheries. Interannual and decadal variability in fisheries landings and distributions of small pelagic fishes has been related to environmental changes associated with the North Atlantic Oscillation and, to a lesser extent, ENSO in the southern part of the region (see reviews in Arístegui et al., 2006, 2009).

There have been numerous process-oriented field programs in Canary Current System in the past 20 years, including the Coastal Transition Zone (CTZ; Barton and Arístegui, 2004) and Canary Islands Azores Gibraltar Observations (CANIGO; Parrilla et al., 2002) programs. However, physical, biogeochemical, and ecosystem monitoring efforts have been less routine compared to other EBCs (Fig. 9). The European Station for Time series in the Ocean Canary Islands (ESTOC) has completed over 20 years of continuous meteorological and surface and mid-water physical and biogeochemical monitoring. The Cape Verde Ocean and Atmospheric Observatories (CVOO/CVAO) are a deep water mooring and an atmospheric station that have been deployed since 2006 in a region critical for climate and greenhouse gas studies and for investigating dust impacts on marine ecosystems. Both ESTOC and CVOO/CVAO are part of the European open ocean fixed point observatories (FixO3). An additional mooring has been recording oceanographic properties and particle fluxes with sediment traps off Cape Blanc continuously since 2003 (Nowald et al., 2015). Long-term measurements of coastal oceanic and atmospheric properties from buoys off Morocco and Senegal have begun during the last four years. Ship-based hydrographic and biogeochemical sampling has taken place twice per year since 2006 at the latitude of the Canary Archipelago as part of the RAPROCAN program (Fig. 9), which aims to monitor the Canary Current and maintain the ESTOC mooring. Gliders have periodically surveyed between the African coast and the Cape Verde Islands (Fig. 9; Karstensen et al., 2017; Kolodziejczyk et al., 2018).

4.2 Western Boundary Current Systems

4.2.1 Northwestern Atlantic

The Gulf Stream comprises the upper limb of the AMOC in the North Atlantic subtropical gyre, carrying warm, saline waters from the tropics to higher latitudes. It flows along the eastern seaboard of the U.S. before separating from the continental margin near Cape Hatteras. The Labrador Current is the WBC of the subpolar gyre. The North Atlantic Deep Western Boundary Current is a deep limb of the AMOC that carries cold water masses from the tail of the Grand Banks of Newfoundland equatorward (Pickart and Watts, 1990). It encounters the Gulf Stream at the tail of the Grand Banks and again at Cape Hatteras, where a portion is entrained into the abyssal interior (Bower and Hunt, 2000a,b; Pickart and Smethie, 1993) while the rest continues to flow equatorward along the western boundary and into the southern hemisphere (Section 4.2.6). The strength of the Deep Western Boundary Current may influence the latitude at which the Gulf Stream detaches from the continental margin (Thompson and Schmitz, 1989). Along the edge of the adjacent Middle Atlantic Bight shelf, a persistent shelfbreak front and associated shelfbreak jet (Linder and Gawarkiewicz, 1998) transport waters equatorward with secondary frontal circulation leading to upwelling and elevated primary productivity (Marra et al., 1990). The shelfbreak jet continues southward until just north of Cape Hatteras, where it turns offshore as it encounters the much stronger Gulf Stream (Gawarkiewicz and Linder, 2006).

The boundary current observing system for the subtropical northwest Atlantic (Fig. 10) is anchored by decades-long measurements at several fixed locations along the boundary. In the Florida Strait near 27°N, cable-based measurements of Gulf Stream transport and quarterly to bi-monthly ship-based sampling have been ongoing since 1982 as part of the Western Boundary Time Series (WBTS; Baringer and Larsen, 2001; Meinen et al., 2010). Far to the northeast, where the Gulf Stream has separated from the continental margin, XBT, shipboard ADCP, and surface temperature and salinity measurements are obtained twice weekly from M/V *Oleander*, a cargo ship running between New Jersey and Bermuda (Rossby et al., 2010, 2014; Wang et al., 2010). The AX10 XBT line between New York and Puerto Rico crosses the Gulf Stream just upstream of the Oleander line and conducts high-resolution sampling within the boundary current (e.g., Domingues et al., 2018). Since 2015, gliders have been used to routinely survey across the Gulf Stream between Florida and Massachusetts (Todd 2017; Todd and Locke-Wynn, 2017; Todd et al., 2018b), providing subsurface observations that fill the gap between the WBTS and *Oleander* and AX10 lines. Two moored arrays with complementary repeat hydrographic sampling have focused on the Deep Western Boundary Current for a decade or more. The RAPID-MOCHA array of subsurface moorings and PIES near 26.5°N has been in place since 2004 with hydrographic stations reoccupied about every nine months (Meinen et al., 2013). Farther north, the Line W array of subsurface moorings was in place from 2004-2014 with repeat ship-based sampling every 6-12 months (Toole et al., 2017). The OOI Pioneer Array south of New England (Smith et al., 2018; Trowbridge et al., 2019) and the PEACH array near Cape Hatteras use a mixture of moorings, gliders (e.g., Gawarkiewicz et al., 2018), and land-based remote sensing (e.g., Haines et al., 2017) to characterize the dynamics of the shelfbreak jet and exchange between the shelf and deep ocean in the vicinity of the Gulf Stream and its eddies. In the subpolar northwestern Atlantic at 53°N, transport of the Labrador Current has been monitored since 1997 using a combination of moored and shipboard observations (Zantopp et al., 2017).

4.2.2 Northwestern Pacific

In the northwest Pacific, bifurcation of the westward North Equatorial current between 11° and 13°N along the Philippine coast (Qiu and Chen, 2010; Rudnick et al., 2015a) forms the poleward Kuroshio and the equatorward Mindanao Current. The Kuroshio becomes a more coherent jet as it flows along the Taiwanese coast (e.g., Centurioni et al., 2004), into the East China Sea, and along the southern Japanese coast before separating from the continental margin near 35°N to form the Kuroshio Extension, an eastward, meandering jet in the open North Pacific. The Mindanao carries waters from the North Pacific southward to feed tropical circulation in both the Pacific and the Indian Oceans (Schönau et al., 2015). The Oyashio is the western boundary current of the North Pacific subpolar gyre and converges with the Kuroshio to the east of Japan. This convergence region has rich frontal structure as various water masses meet and are modified and is a key area for fisheries (Yasuda, 2003).

The Japan Meteorological Agency (JMA) has carried out repeat hydrographic survey 2-5 times annually at the PN line in the East China Sea since 1971 (Aoyama et al., 2008; Fig. 11) and at the TK line south of Kyushu since 1987 (Oka and Kawabe, 2003) to monitor physical and biogeochemical EOVs in the Kuroshio. JMA has also monitored the Ryukyu Current system (Ichikawa et al., 2004) flowing south of the Ryukyu Islands at the OK line southeast of Okinawa, which is connected to a zonal section along 24°N. Furthermore, the JMA has maintained physical and biogeochemical surveys along 137°E across the western North Pacific to monitor major currents of the subtropical and tropical gyres including the Kuroshio (Nakano et al. 2015; Oka et al., 2018). Monthly fisheries surveys and hydrographic stations along the A-line off Hokkaido have been occupied since 1987 (Kuroda et al., 2015) with collocated long-term moorings (Kono and Kawasaki, 1997). JAMSTEC

has sampled hydrographic stations K2 (47°N, 160°E) and KNOT (44°N, 155°E) in the subpolar north Pacific at least annually since 1997 (Wakita et al., 2010). The Kuroshio Extension Observatory (KEO; Cronin et al., 2015) is a surface mooring that has been located in the subtropical recirculation gyre south of the Kuroshio Extension at 32.3°N, 144.6°E (Fig. 11) since 2004. KEO monitors air-sea exchanges of heat, moisture, momentum, and CO_2; sea surface temperature, salinity, and ocean acidification; and upper ocean temperature, salinity, and currents below the surface buoy. Since 2014 a sediment trap mooring has been located at KEO (Honda et al., 2018). More recently, the CLIVAR Northwestern Pacific Ocean Circulation and Climate Experiment (NPOCE) has deployed an array of subsurface moorings, some with real time data transmission, across the western Pacific, South China Sea and Indonesian seas (Fig. 11) that cover the major currents in these regions (e.g., Hu et al., 2013, 2015; Zhang et al., 2014; Chen et al., 2015; Hu et al., 2016; Wang et al., 2017). Multiple XBT transects cross boundary currents within the region (see Goni et al., 2019). Gliders have been deployed for extended periods in the Kuroshio and Mindanao (Fig. 11), generally sampling obliquely across the boundary currents as they were advected downstream (e.g., Rainville et al., 2013; Schönau and Rudnick, 2017).

4.2.3 Southwestern Pacific

The East Australian Current is the subtropical western boundary of the South Pacific; it is a strong, meandering current with large poleward heat transport (Sloyan et al., 2016) that separates from the continental margin between 30°S and 32°S to join a dynamic eddy field (Cetina Heredia et al., 2014) in the Tasman Sea. The low-latitude WBC system of the South Pacific originates as the equatorward Gulf of Papua Current along the northeast coast of Australia, which then flows through the Solomon Sea as the New Guinea Coastal Undercurrent before feeding into the equatorial current system. This is a major contributor to the mass and heat budget of the tropical Pacific, acting as a conveyor belt for micro-nutrients from the western continental margins to the eastern Equatorial Pacific upwelling region. These low-latitude WBCs split into numerous branches around topographic obstacles and flow through narrow passages, presenting challenges for sustained observing.

The sustained observing system for the East Australian Current and its extension (Fig. 7) currently consists of high-density XBT transects (PX05, PX06, PX30, PX34; Goni et al., 2019); Argo floats; a deep moored array at approximately 27°S; HF radar sites near 32°S and 30°S; a regional array of shelf moorings (including biogeochemical and biological sensors) at 30°S, 34°S, and 36°S; and numerous glider deployments from northern Australia (11°S) to the Tasman Sea (42°S) (Roughan and Morris, 2011; Roughan et al., 2013, 2015). These observational platforms complement each other well, providing a distributed boundary current observational system for the East Australian Current that has been shown to constrain ocean models well (Kerry et al., 2018). Additional sustained measurements are needed to characterize the seasonal changes in the transports of mass, heat, and freshwater in the East Australian Current and its eddy field. Effective monitoring strategies would be to deploy moored arrays in key regions; to increase Argo float and drifter density in the WBC region; and to implement glider sampling along existing high-density XBT lines within the East Australian Current, its eddy field, and recirculation.

In the low-latitude WBC system, long-term, sustained observations of the heat and mass transport through the southern entrance of the Solomon Sea have been provided by gliders since 2007 (Davis et al., 2012) and an array of PIES since 2012 (Fig. 7). Concurrent, short-term process studies including mooring deployments have been conducted as part of the CLIVAR-SPICE program (Ganachaud et al., 2014). Future monitoring efforts should integrate measurements across platforms, with the existing measurements in the southern entrance complemented by observations at the

northern exits of the Solomon Sea (e.g., moorings, HF radars, and glider transects) to resolve the partitioning of the flow joining the equator (see Smith et al., 2019).

4.2.4 Agulhas Current

The Agulhas Current is the poleward WBC of the subtropical South Indian Ocean (Lutjeharms, 2006). It flows as a fast (>1.5 m s^{-1}), deep-reaching (>3000 m) jet along continental slope of southeast Africa (Beal and Bryden, 1999; Beal et al., 2015). Near 40°S, the Agulhas flows into the open ocean, where it retroflects under the influence of the large-scale wind stress curl to flow eastward into the Indian Ocean as the Agulhas Return Current (de Ruijter et al., 1999). Leakage of warm, salty Agulhas waters into the South Atlantic by rings, eddies and filaments (Boebel et al., 2003; Richardson, 2007) is thought to influence the AMOC on time scales from decades to millennia (Beal et al., 2011).

In 2010, the Agulhas Current Time-series experiment (ACT) established a moored array to measure the volume transport of the Agulhas Current along a satellite altimeter ground-track (#96) near 34°S (Fig. 8) for a period of three years. The array consisted of seven full-depth current meter moorings and four CPIES that captured the breadth and depth of the Agulhas jet, including during offshore meander events (Beal et al., 2015). Following ACT, a consortium of South African, U.S., and Dutch scientists deployed the Agulhas System Climate Array (ASCA) in 2016 for long-term monitoring of the Agulhas Current as part of GOOS. ASCA augmented the original ACT array design with conductivity-temperature recorders to measure the heat and freshwater fluxes. The long-term success of ASCA was dependent on an ambitious plan of capacity building and resource sharing among nations and, owing to a number of challenges, this plan was not fulfilled and the array was pulled out of the water in 2018, following a two-year deployment. In 2015, the Shelf Agulhas Glider Experiment (SAGE) demonstrated the feasibility of operating autonomous robotic platforms to sample the shelf regions of the Agulhas Current (Krug et al., 2017). Since SAGE, growing regional interest in monitoring with autonomous platforms led to formation of a South African multi-institutional scientific consortium named Gliders in the Agulhas (GINA). GINA conducted two additional glider missions in 2017 and 2018 and is working towards the development of a sustained glider observing system for the Agulhas Current coastal and shelf regions. The influence of the Agulhas leakage on the AMOC has been monitored since 2013 by an array of CPIES and tall moorings as part of the SAMBA line at 34.5°S (Fig. 8; Ansorge et al., 2014). Thus far, no sustained ecological or biogeochemical measurements have been made in the Agulhas, though the addition of oxygen sensors to SAMBA moorings is planned.

4.2.5 Southwestern Atlantic

In the South Atlantic, the WBC system consists of the poleward Brazil current and the equatorward North Brazil Undercurrent, both of which originate from the bifurcation of the South Equatorial Current between 10°S and 20°S (e.g., da Silveira et al., 1994; Rodrigues et al., 2007), and the equatorward Malvinas current in the subpolar gyre. The Brazil Current and Malvinas Current both separate from the South American continental margin between 35°S and 40°S to flow eastward at the Brazil-Malvinas confluence (Olson et al., 1988). The North Brazil Undercurrent constitutes a bottleneck for the interhemispheric mean flow of the upper limb of the AMOC as it transports warm waters of South Atlantic origin across the equator (e.g., Schott et al., 1998; Zhang et al., 2011; Rühs et al., 2015). The Deep Western Boundary Current carries much of the lower limb of the AMOC off the coast of South America (Schott et al., 2005; Meinen et al., 2013).

For more than a decade, high density XBT transects (Goni et al., 2019) have been occupied near 22°S and 34°S (AX97 and AX18) across South Atlantic WBCs (Fig. 12; Dong et al., 2015; Lima et al., 2016). Near 11°S, an array of four tall moorings and two PIES has measured transport of the North Brazil Current since 2013 (Fig. 12; Hummels et al., 2015). At 34.5°S (Fig. 12) an array of PIES, CPIES, and a bottom-mounted ADCP has monitored the Brazil Current and Deep Western Boundary Current (Meinen et al., 2013, 2017, 2018) in conjunction with periodic hydrographic surveys (Valla et al., 2018). A series of yearlong deployments of current meter arrays along 41°S since 1993 (Fig. 12; Vivier and Provost, 1999; Spadone and Provost, 2009; Paniagua et al., 2018), in conjunction with satellite altimetry, has allowed for production of a 24-year transport time series for the Malvinas Current (Artana et al., 2018a).

5 Future Outlook

We recommend establishing and maintaining a global network of boundary current observing systems. Each distinct observing system will need to be tailored to the unique aspects of that particular boundary current system, but also follow best-practices established by the international community. Such a network of regional boundary current observing systems is a crucial element of GOOS. To date, boundary current observing systems in different regions and countries have developed largely independently. Development and maintenance of a global network of boundary current observing systems that is fit for purpose would benefit from the standards outlined in the Framework for Ocean Observing (Lindstrom et al., 2012). In particular, application of the Framework across boundary current observing systems should foster communication and data sharing; contribute to capacity building, particularly in developing countries; encourage confidence and support from funding agencies; and promote international collaboration and scientific and technological innovation.

Boundary currents typically lie within the EEZs of coastal states, so development and maintenance of boundary current observing systems will require the cooperation and support of appropriate governing authorities. Considering the difficulty of obtaining international funding for observations in national waters, there is a need for a community of regional boundary observers. Moreover, many boundary currents span multiple countries, so that the observing system for a single boundary current system is likely to require collaboration and coordination between several countries. The advective nature of boundary currents may even require that mobile or drifting assets deployed within one country's EEZ be recovered within another EEZ. Sharing of measurements taken within EEZs, particularly those that have economic impacts such as some biogeochemical measurements, remains a challenge. By moving toward international collaboration in the design and implementation of boundary current systems as suggested by the Framework for Ocean Observing, there is hope for building the high-level governance structure needed to surmount the challenges posed by boundary currents falling within EEZs. The Large Marine Ecosystems effort has identified distinct boundary regions that cross international borders and has gained international traction through the Global Environment Facility and the International Union for Conservation of Nature; leveraging this effort to facilitate international cooperation and governance for sustained boundary current observations may be fruitful.

For any particular boundary current system, a complete observing system will require a combination of currently available observing platforms (Section 3), as well as future platforms, to optimally measure EOVs at necessary spatial and temporal resolutions to address relevant scientific and societal needs. Through the Framework process, specific observing platforms, sampling choices, and instruments would be matched to the relevant questions. Drifting and mobile assets that provide

spatially-resolved measurements at the expense of temporal resolution will need to be combined with moored assets that provide high-frequency measurements at key locations and land- or satellite-based remote sensing that provides spatially broad measurements of sea surface properties. Such integrated arrays, as are already in place in the California Current System, at the Ocean Observatories Initiative (OOI; Smith et al., 2018; Trowbridge et al., 2019) Endurance and Pioneer Arrays, and along the Australian coasts as part of the Integrated Marine Observing System, offer critical opportunities for intercalibration between instruments on fixed and mobile assets; such intercalibration is particularly important for biogeochemical sensors (e.g., Palevsky and Nicholson, 2018). Since similar needs arise in most boundary current systems, the Framework process should provide a means for determining the extent to which the same observing strategies should be applied to address similar needs in different systems. Additional studies that compare different sampling techniques in a given boundary current system could provide guidance on the strengths and limitations of each technique and how to better exploit their complementarity.

While the discussion of observing platforms in Section 3 focused on mature observing platforms with proven records of sustained operation in boundary currents, there is no doubt that recently developed observing platforms and sensing technology will become integral parts of future boundary current observing systems. For instance, more fast-moving autonomous underwater vehicles (AUVs) and autonomous surface vehicles (ASVs) will be deployed to conduct adaptive and targeted sampling in response to real time needs. Propeller-driven AUVs have thus far seen limited use in boundary currents. Though able to carry large instrument payloads and move much faster (1-2 m s^{-1}) than gliders, propeller-driven AUVs have been limited by battery endurance to missions typically lasting hours to days; improvements in battery technology and autonomous charging are expected to make propeller-driven vehicles capable of long-duration sampling in the near future. Fast-moving, long-endurance ASVs (e.g., Saildrones, Wavegliders) are poised to become key platforms for making measurements near the air-sea interface, including meteorological measurements, pCO_2, subsurface currents, and plankton biomass. Due to the use of renewable energy, these ASVs generally carry a larger number of sensors and have longer duration than other autonomous platforms (e.g., Zhang et al., 2017). Planned high-resolution, satellite-based altimetry measurements (e.g., SWOT), smaller and dramatically cheaper satellites (e.g., Cubesats), and, potentially, geostationary satellites positioned over boundary regions offer the prospect of dramatically increased spatial and temporal resolution of surface properties.

At some locations, boundary currents have been continuously observed for many years using various techniques. For instance, the CalCOFI program has maintained quarterly ship-based stations for more than 65 years (McClatchie, 2014), the WBTS has made cable- and ship-based measurements in the Florida Strait for more than 35 years (Section 4.2.1), and hydrographic sampling has occurred monthly along the inside edge of the East Australian Current since the 1940s (Lynch et al., 2014) and is now an integral part of the East Australian Current observing system (Roughan and Morris, 2011). Long-term measurements like these are invaluable for capturing decadal variability and secular trends. Sites at which decades-long measurements exist should be maintained and serve as anchors for comprehensive boundary current observing systems. These long-term measurement sites at the boundaries also serve as points at which the boundary current observing systems are linked to the basin-scale ocean observing system. Since 2004, the WBTS has been integrated with the UK-US RAPID-MOCHA program that measures meridional transport at 26.5°N in the North Atlantic, while several long-standing, cross-Pacific XBT transects intersect the U.S. West coast within the CalCOFI domain (Goni et al., 2019).

Existing boundary current observing systems are largely focused on measuring physical processes, with biogeochemical and ecosystem processes only beginning to gain traction, largely due to the advent of new sensors. The California Current System (Section 4.1.1) and Benguela (Section 4.1.4) are exceptions, having had sustained observations of EOVs relevant to physics, biogeochemistry, and biology and ecosystems for over 65 years and 30 years, respectively. However, these ship-intensive models are unlikely to be suited to all boundary current systems due to a wide range of factors (e.g., cost, proximity to the coast, existing infrastructure, available man-power). Although the methods for measuring many of the EOVs needed to monitor biogeochemical and, to a greater extent, ecosystem processes are time-intensive and require a platform for collecting water, new sensors are being developed to reliably measure a range of biogeochemical and biological EOVs. Many of these sensors have been successfully deployed on BGC-Argo floats as part of the SOCCOM project (Johnson et al., 2017). Increasing the measurements of biological and ecological EOVs should be prioritized if we are to understand, monitor, and predict the physical-biological connections and processes that support marine-based industries and activities and, importantly, seafood security.

Providing publicly available data in a timely manner is a key attribute of any ocean observing system. These observations should be provided in formats that are discoverable, accessible, and readily subset, following conventions agreed upon by the community (see Wilkinson et al. (2016) for a set of general principles for management of scientific data). Many platforms already provide observations in near real-time through a variety of services. Transmission of data through the Global Telecommunications System is particularly important if those observations are to be used in operational numerical modeling. Advances in real-time data collection from sub-surface moorings (e.g., Send et al., 2013) will be critical to providing boundary current observations in a timely manner for forecasting and prediction. Widespread dissemination of comprehensive boundary current observations can foster synergies with other disciplines, including the geophysics (tsunamis and earthquakes), physics, meteorological (e.g., tropical and extratropical cyclone forecasting; Domingues et al., 2019), and fisheries communities.

In addition to providing raw observations, there is a need for providing synthesized data products that are tailored to user needs. Integration of complementary data types can yield useful metrics. Further advances in data analysis techniques and statistical methods should aid in using multi-platform data to increase temporal and/or spatial resolution of metrics. The Southern California Temperature Index (Rudnick et al., 2017) is an example of such a data product.

Boundary current observations play a key role in constraining ocean models (e.g., Todd and Locke-Wynn, 2017), while models play a complementary role by filling gaps between sparse observations in a dynamically consistent manner (e.g., Todd et al., 2011b, 2012; Gopalakrishnan et al., 2013). Increased availability of boundary current observations, particularly in regions that are currently poorly sampled, should lead to continued improvements in regional models and predictive tools. At the same time, higher resolution climate models that can resolve boundary currents are becoming more plentiful and should begin to rely on high-resolution boundary current observations as constraints. One specific goal would be to reduce climate models' warm SST biases within EBCs; continuation and expansion of long-term measurements in EBCs as well as focused process studies to study upper ocean and atmospheric dynamics in EBCs would contribute to this goal. Observation impact studies derived from data assimilating models provide guidance on the value of a range of observation types in resolving boundary current transport, as well as for constraining the eddy field in ocean reanalyses (e.g., Kerry et al., 2016, 2018). It remains an open question how best to integrate models with interdisciplinary (e.g., biogeochemical) observations to study ecosystem dynamics, though advances are being made in the assimilation of biological parameters (e.g., Song et al., 2012).

Observing System Simulation Experiments tailored for boundary current systems can also provide insight to the type, spatial distribution, and frequency of observations required to improve numerical simulations of boundary current dynamics (Hoffman and Atlas, 2016). Targeted observations can reduce biases in the initialization of models used to forecast extreme weather events and support local decision making (Halliwell et al., 2017).

Downscaling coarse resolution climate model predictions through the application of higher resolution regional and coastal models is now common and has shown promise, but still faces research challenges. Furthermore, a significant amount of physical, biogeochemical and biological response on the continental shelf is due to episodic oceanic and atmospheric events at timescales of variability that are absent from coarse models and cannot be recovered locally. To be valid globally, the veracity of downscaled models needs to be appraised by supporting observations of shelf edge fluxes in a diversity of circulation regimes.

Funding sustained observing efforts is a significant challenge. Portions of the observing system that have proven their readiness for long-term deployment have been discontinued after one or more short-term funding cycles. For instance, it is currently not clear how ship-time and funding challenges will be met for a re-establishment of ASCA (Section 4.2.4) in the future. In the typical three-to-four-year cycles of scientific funding, early years (e.g., pilot phases) of observing efforts are readily fundable based on the promise of quick scientific results. Observing efforts that have endured for a decade or longer can leverage their long histories and clear relevance to decadal variability or secular trends to secure continued funding. The middle years, roughly years 4 through 10 as programs transition from pilot to mature components of the GOOS, are particularly difficult to fund.

The provision of robust three-dimensional and time-varying ocean circulation estimates in boundary current systems, resolving scales of a few kilometers, is seemingly within reach through advances in data-assimilative ocean models and rapid developments in observations platforms and sensors. However, the development of integrated observing systems that deliver the scope of observations required and the models capable of fully utilizing those observations is challenging. Success will require coordinated international collaborations, bringing together the expertise of the ocean modelling and observational communities. Establishment of an Ocean Boundary Task Team would provide a mechanism for the exchange of information regarding observing and model strategies, sensor developments, analysis techniques to combine data from the various observing platforms, and model development and application. The Task Team would also enable capacity building, encourage timely and appropriate transfer of knowledge, and provide a mechanism to instigate multinational observing systems with shared goals amongst participating nations. Endorsement of the Task Team by IOC/WMO or similar international organization is critical due to interests of multiple coastal state EEZs and the resulting complex governance needs.

6 Summary Recommendations

The following actions are recommended to promote development of a comprehensive global network of boundary current observing systems in the next decade:

1. Maintain existing long-term (i.e., multi-year) observational records;
2. Expand the use of mobile, autonomous platforms (e.g., gliders, AUVs, ASVs) to provide continuous, high-resolution, broad-scale monitoring of EOVs;
3. Deploy moored platforms at key locations to measure high-frequency variability;

4. Continue and expand the provisioning of real-time observations and encourage post-processed data to be made publicly available as quickly as possible; data should be provided in readily discoverable formats that can easily be subset;
5. Continue development and expand deployment of sensors for ecological and biogeochemical EOVs;
6. Establish an Ocean Boundary Task Team to foster international community development and end-user engagement and to guide evolution of observing systems as user requirements change;
7. Expand collaborations between observational efforts, modeling efforts, and societal users to meet stakeholder and end-user needs;
8. Increase focus on exchange between continental shelves and the deep ocean boundary currents to develop observing systems that span the continuum from the land to the deep ocean.

7 Conflict of Interest

The authors declare that the research was conducted in the absence of any commercial or financial relationships that could be construed as a potential conflict of interest.

8 Author Contributions

RET led the manuscript. Other lead authors (FPC, SC, SC, MG, MG, XL, JS, and NVZ) helped conceive the manuscript and participated in all stages of development. All other authors provided input and/or edited the text.

9 Funding

RET was supported by The Andrew W. Mellon Foundation Endowed Fund for Innovative Research at WHOI. FPC was supported by the David and Lucile Packard Foundation. MG was funded by NSF and NOAA/AOML. XL was funded by China's national key research and development projects (2016YFA0601803), the National Natural Science Foundation of China (41490641,41521091, and U1606402), and the Qingdao National Laboratory for Marine Science and Technology (2017ASKJ01). JS was supported by NOAA's Global Ocean Monitoring and Observing Program (Award NA15OAR4320071). We gratefully acknowledge the wide range of funding sources from many nations that have enabled the observations and analyses reviewed here.

10 Acknowledgments

We gratefully acknowledge the efforts of all parties involved in collecting, analyzing, and disseminating the wide ranging observations discussed here. We also thank the OCB Program, U.S. CLIVAR, MBARI, and OMIX for supporting the Ocean Carbon Hot Spots Workshop, which facilitated the discussion of carbon cycle research in Western Boundary Current systems. We gratefully acknowledge J. Hildebrandt (WHOI) for assistance in editing the final manuscript.

11 References

Adams, K., Barth, J.A., Shearman, R.K. (2016). Intraseasonal cross-shelf variability of hypoxia along the Newport, Oregon, hydrographic line. J. Phys. Oceanogr. 46, 2219-2238. doi: 10.1175/JPO-D-15-0119.1

1085 Alberty, M.S. (2018). Water Mass Transport and Transformation in the Tropics and Arctic. *UC San*
1086 *Diego*. ProQuest ID: Alberty_ucsd_0033D_18031. Merritt ID: ark:/13030/m58m27cn. Retrieved
1087 from https://escholarship.org/uc/item/9rf158pq

1088 Alberty, M., Sprintall, J., MacKinnon, J., Germineaud, C., Cravatte, S., Ganachaud, A. (2019). Data
1089 from: Moored Observations of Transport in the Solomon Sea. In Solomon Sea SPICE Mooring Data.
1090 UC San Diego Library Digital Collections. doi: 10.6075/J0639N12

1091 Alford, M.H., Sloyan, B.M., Simmons, H.L. (2017). Internal waves in the East Australian Current.
1092 Geophys. Res. Lett. 44, 12,280-12,288. doi: 10.1002/2017GL075246

1093 Alin, S.R., Feely, R.A., Dickson, A.G., Hernández-Ayón, J.M., Juranek, L.W., Ohman, M.D.,
1094 Goericke, R. (2012). Robust empirical relationships for estimating the carbonate system in the
1095 southern California Current System and application to CalCOFI hydrographic cruise data (2005–
1096 2011). J. Geophys. Res.: Oceans 117, C05033. doi: 10.1029/2011JC007511

1097 Álvarez-Salgado, X.A., Arístegui, J., Barton, E.D., Hansell, D.A. (2007). Contribution of upwelling
1098 filaments to offshore carbon export in the subtropical Northeast Atlantic Ocean. Limnol. Oceanogr.
1099 52(3), 1287-1292.

1100 Andersson, A.J., Krug, L.A., Bates, N.R., Doney, S.C. (2013). Sea-air CO_2 flux in the North Atlantic
1101 subtropical gyre: Role and influence of Sub-Tropical Mode Water formation. Deep-Sea Research
1102 Part II-Topical Studies in Oceanography 91, 57-70. 10.1016/j.dsr2.2013.02.022

1103 Andres, M. (2016), On the recent destabilization of the Gulf Stream path downstream of Cape
1104 Hatteras. Geophys. Res. Lett 43, 9836-9842. doi:10.1002/ 2016GL069966

1105 Andres, M., Jan, S., Sanford, T. B., Mensah, V., Centurioni, L. R., Book, J.W. (2015). Mean
1106 structure and variability of the Kuroshio from northeastern Taiwan to southwestern Japan.
1107 Oceanography 28, 84-95, doi: 10.5670/oceanog.2015.84

1108 Ansorge, I.J., Baringer, M.O., Campos, E.J.D., Dong, S., Fine, R.A., Garzoli, S.L, et al. (2014).
1109 Basin-wide oceanographic array bridges the South Atlantic. Eos 95, 53-54.

1110 Aoyama, M., Goto, H., Kamiya, H., Kaneko, I., Kawae, S., Kodama, H., et al. (2008). Marine
1111 biogeochemical response to a rapid warming in the main stream of the Kuroshio in the western North
1112 Pacific. Fish. Oceanogr. 17, 206-218. doi: 10.1111/j.1365-2419.2008.00473.x

1113 Archer, M.R., Keating, S.R., Roughan, M., Johns, W.E., Lumkpin, R., Beron-Vera, F., Shay, L.K.
1114 (2018). The kinematic similarity of two western boundary currents revealed by sustained high-
1115 resolution observations. Geophys. Res. Lett. 45, 6176-6185. doi: 10.1029/2018GL078429

1116 Archer, M.R., Roughan, M., Keating, S.R.,Schaeffer, A. (2017b). On the variability of the East
1117 Australian Current: Jet structure, meandering, and influence on shelf circulation. J. Geophys. Res.
1118 Oceans 122, 8464–8481. doi: 10.1002/2017JC013097

1119 Archer, M.R., Shay, L.K., Jaimes, B., Martinez-Pedraja, J. (2015). “Observing frontal instabilities of
1120 the Florida Current using high frequency radar,” in Coastal Ocean Observing Systems, eds. Y. Liu,
1121 H. Kerkering, R. H. Weisberg (Elsevier, Inc.), 179-208. doi: 10.1016/B978-0-12-802022-7.00011-0

1122 Archer, M.R., Shay, L.K., Johns, W.E. (2017a). The surface velocity structure of the Florida Current
1123 in a jet coordinate frame. J. Geophys. Res. Oceans 122, 9189–208. doi: 10.1002/2017JC013286

1124 Arístegui, J., Alvarez–Salgado, X.A., Barton, E.D., Figueiras, F.G., Hernández–León, S., Roy, C.,
1125 Santos, A.M.P. (2006). Oceanography and fisheries of the Canary Current/Iberian region of the
1126 eastern North Atlantic. In: The Sea, Vol. 14. Robinson, A. R. and Brink, K. H. eds. Harvard
1127 University Press, pp. 877–931.

1128 Arístegui, J., Barton, E.D., Alvarez Salgado, X.A., Santos, A.M.P., Figueiras, F.G., Kifani, S., et al.
1129 (2009). Sub-regional ecosystem variability in the Canary Current upwelling. Prog. Oceanogr. 83, 33-
1130 48.

1131 Arístegui, J., Sangrà, P., Hernández–León, S., Cantón, M., Hernández Guerra, A., Kerling, J.L.
1132 (1994). Island–induced eddies in the Canary Islands. Deep–Sea Res. I 41, 1509–1525.

1133 Arístegui, J., Tett, P., Hernández-Guerra, A., Basterretxea, G., Montero, M.F., Wild, K., et al. (1997).
1134 The influence of island-generated eddies on chlorophyll distribution: a study of mesoscale variation
1135 around Gran Canaria. Deep-Sea Res. 44, 71–96.

1136 Artana, C., Ferrari, R., Koenig, Z., Saraceno, M., Piola, A.R., Provost, C. (2016). Malvinas Current
1137 variability from Argo floats and satellite altimetry. J. Geophys. Res. Oceans 121(7). doi:
1138 10.1002/2016JC011889

1139 Artana, C., Ferrari, R., Koenig, Z., Sennechael, N., Saraceno, M., Piola, A.R., Provost, C. (2018a).
1140 Malvinas Current volume transport at 41°S: A 24 yearlong time series consistent with mooring data
1141 from 3 decades and satellite altimetry. J. Geophys. Res.: Oceans 123, 378–398. doi: 10.1002/
1142 2017JC013600

1143 Artana, C., Lellouche, J., Park, Y., Garric, G. , Koenig, Z., Sennéchael, N., Ferrari, R., Piola, A.R.,
1144 Saraceno, M., Provost, C. (2018b). Fronts of the Malvinas Current System: Surface and subsurface
1145 expressions revealed by satellite altimetry, Argo floats, and Mercator operational model outputs. J.
1146 Geophys. Res. Oceans 123, 5261-5285. doi: 10.1029/2018JC013887

1147 Auad, G., Roemmich D., and Gilson J. (2011). The California Current System in relation to the
1148 Northeast Pacific Ocean circulation. Progress in Oceanography 91, 576-592. doi:
1149 10.1016/j.pocean.2011.09.004

1150 Bacon, S. and Saunders, P.M. (2010). The deep western boundary current at Cape Farewell: Results
1151 from a moored current meter array. J. Phys. Oceanogr., 40, 815–829.

1152 Bakun, A., Black, B.A., Bograd, S.J., Garcia-Reyes, M., Miller, A.J., Rykaczewski, R.R., Sydeman,
1153 W.J. (2015). Anticipated effects of climate change on coastal upwelling ecosystems. Curr. Clim.
1154 Change Rep. 1(2), 85-93. doi: 10.1007/s40641-015-0008-4

1155 Bane, J.M., He, R., Muglia, M., Lowcher, C.F., Gong, Y., Haines, S.M. (2017). Marine hydrokinetic
1156 energy from western boundary currents. Ann. Rev. Mar. Sci. 9, 105-123. doi: 10.1146/annurev-
1157 marine-010816-060423

1158 Baringer, M.O. and Larsen, J. (2001). Sixteen years of Florida Current transport at 27N. Geophys.
1159 Res. Lett. 28(16), 3179-3182. doi: 10.1029/2001GL013246

1160 Barton, A.D., Dutkiewicz, S., Flierl, G., Bragg, J., Follows, M.J. (2010). Patterns of diversity in
1161 marine phytoplankton. Science 327(5972), 1509-1511. doi: 10.1126/science.1184961

1162 Barton, E.D, Arístegui, J., Tett, P., Cantón, M., García-Braun, J., Hernández-León, S., et al. (1998).
1163 The transition zone of the Canary Current upwelling region. Prog. Oceanogr. 41, 455–504.

1164 Barton, E.D. and Arístegui, J. (2004). The Canary Islands Transition – upwelling, eddies and
1165 filaments. Prog. Oceanogr. 62(2–4), 67–69.

1166 Bates, N., Pequignet, A.C., Johnson, R.J., Gruber, N. (2002). A variable sink for atmospheric CO_2 in
1167 Subtropical Mode Water of the North Atlantic Ocean. Nature 420, 489–493.

1168 Baumgartner M.F., and Fratantoni D.M., (2008). Diel periodicity in both sei whale vocalization rates
1169 and the vertical migration of their copepod prey observed from ocean gliders. Limnol. Oceanogr. 53,
1170 2197-2209. doi: 10.4319/lo.2008.53.5_part_2.2197.

1171 Beal, L.M., and Elipot, S. (2016). Broadening not strengthening of the Agulhas Current since the
1172 early 1990s. Nature 540(7634), 570-573. doi: 10.1038/nature19853

1173 Beal, L.M., Elipot, S., Houk, A., Leber, G.M. (2015). Capturing the transport variability of a western
1174 boundary jet: Results from the Agulhas Current Time-Series Experiment (ACT). J. Phys. Oceanogr.
1175 45(5), 1302-1324. doi: 10.1175/JPO-D-14-0119.1

1176 Beal, L.M., Hormann, V., Lumpkin, R., Foltz, G.R. (2013). The response of the surface circulation of
1177 the Arabian Sea to monsoonal forcing. J. Phys. Oceanogr. 43, 2008–2022. doi: 10.1175/JPO-D-13-
1178 033.1

1179 Beal, L.M., De Ruijter, W.P.M., Biastoch, A., Zahn, R., Cronin, M., Hermes, J., et al. (2011). On the
1180 role of the Agulhas system in ocean circulation and climate. Nature 472: 429-436, doi:
1181 10.1038/nature09983

1182 Beal, L.M., and H.L. Bryden (1999), The velocity and vorticity structure of the Agulhas Current at
1183 32°S, J. Geophys. Res., 104(C3), 5151–5176, doi: 10.1029/1998JC900056

1184 Bednaršek, N., Feely, R.A., Reum, J.C.P., Peterson, B., Menkel, J., Alin, S.R., Hales, B. (2014).
1185 *Limacina helicina* shell dissolution as an indicator of declining habitat suitability owing to ocean
1186 acidification in the California Current Ecosystem. Proc. Royal Soc. London B: Biological Sciences
1187 281. doi: 10.1098/rspb.2014.0123

1188 Bednaršek, N., Feely, R.A., Tolimieri, N., Hermann, A.J., Siedlecki, S.A., Waldbusser, G.G., et al.
1189 (2017). Exposure history determines pteropod vulnerability to ocean acidification along the US West
1190 Coast. Scientific Reports 7, 4526.

1191 Bednaršek, N., Feely, R.A., Beck, M.W., Glippa, O., Kanerva, M., Engström-Öst, J. (2018). El Niño-
1192 related thermal stress coupled with upwelling-related ocean acidification negatively impacts cellular
1193 to population-level responses in pteropods along the California Current System with implications for
1194 increased bioenergetic costs. Front. Mar. Sci. 4, 486. doi: 10.3389/fmars.2018.00486

1195 Benazzouz, A., Mordane, S., Orbi, A., Chagdali, M., Hilmi, K., Atillah, A., et al. (2014). An
1196 improved coastal upwelling index from sea surface temperature using satellite-based approach - The

1197 case of the Canary Current upwelling system. Cont. Shelf Res. 81, 38-54. doi:
1198 10.1016/j.csr.2014.03.012

1199 Bertrand, A., Chaigneau, A., Peraltilla, S., Ledesma, J., Graco, M., Monetti, F., Chavez. F.P. (2011).
1200 Oxygen: A fundamental property regulating pelagic ecosystem structure in the coastal southeastern
1201 tropical Pacific. PLOS ONE 6(12), e29558. doi:10.1371/journal.pone.0029558

1202 Bigorre, S.P., Weller, R.A., Edson, J.B., Ware, J.D. (2013). A surface mooring for air–sea interaction
1203 research in the Gulf Stream. Part II: Analysis of the observations and their accuracies. J. Atmos.
1204 Oceanic Technol., 30, 450–469, https://doi.org/10.1175/JTECH-D-12-00078.1

1205 Boebel, O., Lutjeharms, J., Schmid, C., Zenk, W., Rossby, T., Barron, C. (2003). The Cape
1206 Cauldron: a regime of turbulent inter-ocean exchange. Deep Sea Res. Part II 50(1), 57-86. doi:
1207 10.1016/S0967-0645(02)00379-X

1208 Boening, C., Willis, J.K., Landerer, F.W., Nerem, R.S., Fasullo, J. (2012), The 2011 La Niña: So
1209 strong, the oceans fell. Geophys. Res. Lett. 39, L19602. doi: 10.1029/2012GL053055

1210 Bond, N.A., Cronin, M.F., Sabine, C., Kawai, Y., Ichikawa, H., Freitag, P., Ronnholm, K. (2011).
1211 Upper ocean response to Typhoon Choi-Wan as measured by the Kuroshio Extension Observatory
1212 mooring. J. Geophys. Res.116. C02031. doi: 10.1029/2010JC006548

1213 Bowen, M., Markham, J., Sutton, P., Zhang, X., Wu, Q., Shears, N.T., Fernandez, D. (2017).
1214 Interannual variability of sea surface temperature in the Southwest Pacific and the role of ocean
1215 dynamics. J. Climate 30, 7481-7492. doi: 10.1175/JCLI-D-16-0852.1

1216 Bower, A.S., and Hunt, H.D. (2000a). Lagrangian observations of the Deep Western Boundary
1217 Current in the North Atlantic Ocean. Part I: Large-scale pathways and spreading rates. J. Phys.
1218 Oceanogr. 30(5), 764–783. doi: 10.1175/1520-0485(2000)030⟨0764:LOOTDW⟩2.0.CO;2

1219 Bower, A S., and Hunt, H.D. (2000b), Lagrangian observations of the Deep Western Boundary
1220 Current in the North Atlantic Ocean. Part II: The Gulf Stream–Deep Western Boundary Current
1221 crossover. J. Phys. Oceanogr. 30(5), 784–804. doi: 10.1175/1520-
1222 0485(2000)030⟨0784:LOOTDW⟩2.0.CO;2

1223 Brady, R.X., Lovenduski, N.S., Alexander, M.A., Jacox, M., N. Gruber (2018). On the role of
1224 climate modes in modulating the air-sea CO_2 fluxes in Eastern Boundary Upwelling Systems.
1225 Biogeosciences Discuss. doi: 10.5194/bg-2018-415

1226 Brandini, F.P., Boltovskoy, D., Piola, A., Kocmur, S., Röttgers, R., Abreu, P.C., Lopes, R.M. (2000).
1227 Multiannual trends in fronts and distribution of nutrients and chlorophyll in the southwestern Atlantic
1228 (30–62 S). Deep Sea Res. Part I: Oceanographic Research Papers 47(6), 1015-1033.

1229 Brassington, G.B. (2010). Estimating surface divergence of ocean eddies using observed trajectories
1230 from a surface drifting buoy. J. Atmos. Ocean. Tech., 27(4), 705–720

1231 Brassington, G.B., Summons, N., Lumpkin, R. (2011). Observed and simulated Lagrangian and eddy
1232 characteristics of the East Australian Current and the Tasman Sea. Deep Sea Res., 58, 559–573

1233 Bright, R.J., Xie, L., Pietrafesa, L.J. (2002). Evidence of the Gulf Stream's influence on tropical
1234 cyclone intensity. Geophys. Res. Lett. 29(16) doi:10.1029/2002GL014920

1235 Bushinsky, S.M. and Emerson, S.R. (2018), Biological and physical controls on the oxygen cycle in
1236 the Kuroshio Extension from an array of profiling floats. Deep Sea Res. I, in press doi:
1237 10.1016/j.dsr.2018.09.005

1238 Bushinsky, S.M., Emerson, S.R., Riser, S.C., Swift, D.D. (2016), Accurate oxygen measurements on
1239 modified Argo floats using in situ air calibrations, Limnol. Oceanogr. Methods 14, 491–505.
1240 doi:10.1002/lom3.10107

1241 Campagna, C., Piola, A.R., Marin, M.R., Lewis, M., Fernández, T. (2006). Southern elephant seal
1242 trajectories, ocean fronts and eddies in the Brazil/Malvinas Confluence. Deep-Sea Res. I 53, 1907-
1243 1924. doi: 10.1016/j.dsr.2006.08.015

1244 Capet, X., Estrade, P., Machu, É., Ndoye, S., Grelet, J., Lazar, A., Marie, L., Dausse, D., Brehmer, P.
1245 (2017). On the dynamics of the southern Senegal upwelling center: Observed variability from
1246 synoptic to superinertial scales. J. Phys. Oceanogr. 47(1), 155-180. doi: 10.1175/JPO-D-15-0247.1

1247 Carr, M-.E., Kearns, E.J. (2003). Production regimes in four Eastern Boundary Current systems. Deep-
1248 Sea Res. Pt. II 50, 3199-3221.

1249 Castelao, R., Glenn, S., Schofield, O. (2010). Temperature, salinity, and density variability in the
1250 central Middle Atlantic Bight. J. Geophys. Res. 115, C10005, doi:10.1029/2009JC006082

1251 Cavole, L.M., Demko, A.M., Diner, R.E., Giddings, A., Koester, I., Pagniello, C.M.L.S, et al. (2016).
1252 Biological impacts of the 2013–2015 warm-water anomaly in the Northeast Pacific: Winners, losers,
1253 and the future. Oceanography 29(2), 273–285. doi: 10.5670/oceanog.2016.32

1254 Cazenave, A., Dieng, H.-B., Meyssignac, B., von Schuckmann, K., Decharme, B., Berthier, E.
1255 (2014). The rate of sea-level rise. Nat. Clim. Change 4, 358–361. doi: 10.1038/nclimate2159

1256 Centurioni, L.R. (2018). "Drifter technology and impacts for sea surface temperature, sea-level
1257 pressure, and ocean circulation studies," in Observing the Oceans in Real Time, eds. R. Venkatesan,
1258 A. Tandon, E. D'Asaro, M. A. Atmanand, (Springer International Publishing), 37-57.

1259 Centurioni, L.R., Hormann, V., Talley, L.D., Arzeno., I., Beal, L., Caruso, M., et al. (2017), Northern
1260 Arabian sea circulation autonomous research (NASCar). A research initiative based on autonomous
1261 sensors. Oceanography 30(2), 74-87. doi: 10.5670/oceanog.2017.224

1262 Centurioni, L. R., and Niiler, P. P. (2003). On the surface currents of the Caribbean Sea. Geophys.
1263 Res. Lett. 30(6). doi: 10.1029/2002GL016231

1264 Centurioni, L.R., Niiler, P.P., Lee, D.-K. (2004) Observations of inflow of Philippine sea surface
1265 water into the South China Sea through the Luzon Strait. J. Phys. Oceanogr. 34, 113-121. doi:
1266 10.1175/1520-0485(2004)034<0113:OOIOPS>2.0.CO;2

1267 Centurioni, L. R., Niiler, P. N. and Lee, D.-K. (2009), Near-surface circulation in the South China
1268 Sea during the winter monsoon. Geophys. Res. Lett. 36, L06605, doi: 10.1029/2008GL037076

1269 Centurioni, L. R., Ohlmann, J. C., Niiler, P. P. (2008). Permanent meanders in the California Current
1270 System. J. Phys. Oceanogr. 38(8), 1690–1710. doi: 10.1175/2008JPO3746.1

1271 Cetina Heredia, P. Roughan, M., Van Sebille, E., Coleman, M.A. (2014). Long-term trends in the
1272 East Australian Current separation latitude and eddy driven transport. J. Geophys. Res.119.
1273 doi:10.1002/2014JC010071.

1274 Chan, H.Y., Xu, W.Z., Shin, P.K.S., Cheung, S.G. (2008). Prolonged exposure to low dissolved
1275 oxygen affects early development and swimming behaviour in the gastropod Nassarius festivus
1276 (Nassariidae). Marine Biology 153, 735–743.

1277 Chavez, F.P., Bertrand, A., Guevara, R., Soler, P., Csirke, J. (2008) The northern Humboldt Current
1278 System: brief history, present status and a view towards the future. Prog. Oceanogr. 79, 95-105. doi:
1279 10.1016/j.pocean.2008.10.012

1280 Chavez, F.P. and Messié, M. (2009). A comparison of eastern boundary upwelling ecosystems. Prog.
1281 Oceanogr. 83, 80-96, doi: 10.1016/j.pocean.2009.07.032

1282 Chavez, F.P., and Toggweiler, J.R. (1995). "Physical estimates of global new production: The
1283 upwelling contribution," in Upwelling in the Ocean: Modern Processes and Ancient Records,
1284 eds.C.P. Summerhayes et al. (John Wiley, Hoboken, N. J.), 313–320.

1285 Checkley, D. and Barth, J.A. (2009). Patterns and processes in the California Current System. Prog.
1286 Oceanogr. 83, 49-64. doi:10.1016/j.pocean.2009.07.028.

1287 Chen, K., Gawarkiewicz, G., Plueddemann, A. J. (2018). Atmospheric and offshore forcing of
1288 temperature variability at the shelf break: Observations from the OOI Pioneer Array. Oceanography
1289 31, 72-79. doi: 10.5670/oceanog.2018.112

1290 Chen, Z., Wu, L., Qiu, B., Li, L., Hu, D., Liu, C., et al. (2015). Strengthening Kuroshio observed at
1291 its origin during November 2010 to October 2012. Oceans 120, 2460-2470.
1292 doi:10.1002/2014JC010590.

1293 Claret, M., Galbraith, E.D., Palter, J.B., Bianchi, D., Fennel, K., Gilbert, D., et al. (2018). Rapid
1294 coastal deoxygenation due to ocean circulation shift in the northwest Atlantic. Nat. Clim. Change, 8,
1295 868-872. doi: 10.1038/s41558-018-0263-1

1296 Clayton, S., Dutkiewicz, S., Jahn, O., Follows, M. J. (2013). Dispersal, eddies, and the diversity of
1297 marine phytoplankton. Limnol. Oceanogr. *3*(1), 182-19. doi: 10.1215/21573689-2373515

1298 Clayton, S., Lin, Y.C., Follows, M.J., Worden, A. Z. (2017). Co-existence of distinct Ostreococcus
1299 ecotypes at an oceanic front. Limnol. Oceanogr. 62(1), 75-88. doi: 10.1002/lno.10373

1300 Clayton, S., Nagai, T., Follows, M. J. (2014). Fine scale phytoplankton community structure across
1301 the Kuroshio Front. J. Plankton Res. 36(4), 1017-1030. doi: 10.1093/plankt/fbu020

1302 Cockcroft, A. C., Schoeman, D.S., Pitcher, G.C., Bailey, G.W., van Zyl, D.L. (2000). A mass
1303 standing, or ''walkout,'' of west coast rock lobster Jasus lalandii in Elands Bay, South Africa:
1304 Causes, results and implications, in The Biodiversity Crisis and Crustacea, vol. 12, edited by J. C.
1305 von Kaupel Klein and F. R. Schram, pp. 673–688, A. A. Balkema, Rotterdam, Netherlands.

1306 Cockcroft, A. C., van Zyl, D., Hutchings, L. (2008). Large-scale changes in the spatial distribution of
1307 South African West Coast rock lobsters: An overview. Afr. J. Mar. Sci., 30(1), 149–159.

1308 Colas, F., Capet, X., McWilliams, J.C., Shchepetkin, A. (2008). 1997–1998 El Niño off Peru: A
1309 numerical study. Prog. Oceanogr. 79(2-4), 138-155.

1310 Colas, F., McWilliams, J.C., Capet, X., Kurian, J. (2012). Heat balance and eddies in the Peru-Chile
1311 current system. Clim. Dyn. 39, 509. doi: 10.1007/s00382-011-1170-6

1312 Conway, T.M., Palter, J.B., de Souza, G.F. (2018). Gulf Stream rings as a source of iron to the North
1313 Atlantic subtropical gyre. Nat. Geosci. 11, 594–598. doi: 10.1038/s41561-018-0162-0

1314 Cravatte, S., Ganachaud, A., Sprintall, J., Alberty, M., Germineaud, C., Brachet, C., et al. (2019).
1315 Solomon Sea SPICE Mooring Data. UC San Diego Library Digital Collections. doi:
1316 10.6075/J09W0CS2

1317 Cronin, M.F., Bond, N.A., Farrar, J.T., Ichikawa, H., Jayne, S.R., Kawai, Y., et al. (2013). Formation
1318 and erosion of the seasonal thermocline in the Kuroshio Extension recirculation gyre, Deep Sea Res.
1319 85, 62–74. doi:10.1016/j.dsr2.2012.07.018.

1320 Cronin, M.F., Pelland, N.A., Emerson, S.R., Crawford, W.R. (2015). Estimating diffusivity from the
1321 mixed layer heat and salt balances in the North Pacific. Oceans 120, 7346–7362.
1322 doi:10.1002/2015JC011010.

1323 Cronin, M.F., Gentemann, C.L., Edson, J., Ueki, I., Ando, K., Bourassa, M., et al. (2019). Air-sea
1324 fluxes with a focus on heat and momentum. Front. Mar. Sci., submitted.

1325 D'Adamo, N., Fandry, C., Bubarton S., Domingues, C. (2009). Northern sources of the Leeuwin
1326 Current and the" Holloway Current" on the North West Shelf. J. Roy. Soc. West. Aust., 92, 53-66.

1327 da Silveira, I. C. A., deMiranda, L.B., and Brown, W.S. (1994). On the origins of the North Brazil
1328 Current, J. Geophys. Res., 99(C11), 22501–22512, doi: 10.1029/94JC01776

1329 Davis, R. (2016). Data from: Solomon Sea ocean transport from gliders. Instrument Development
1330 Group, Scripps Institution of Oceanography. doi: 10.21238/s8SPRAY2718

1331 Davis, R.E., Kessler, W.S., Sherman, J.T. (2012). Gliders measure western boundary current
1332 transport from the South Pacific to the Equator. J. Phys. Oceanogr. 42, 2001–2013, doi:
1333 10.1175/JPO-D-12-022.1

1334 Dengler, M., Fischer, J., Schott, F.A., Zantopp, R. (2006). Deep Labrador Current and its variability
1335 in 1996-2005. Geophys. Res. Lett. 33, L21S06. doi: 10.1029/2006GL026702

1336 de Ruijter, W. P. M., Biastoch, A., Drijfhout, S. S., Lutjeharms, J. R. E., Matano, R. P., Pichevin, T.,
1337 et al. (1999). Indian-Atlantic interocean exchange: Dynamics, estimation and impact. J. Geophys.
1338 Res. 104(C9), 20885–20910. doi: 10.1029/1998JC900099

1339 Dever, M., Hebert, D., Greenan, B.J.W., Sheng, J., Smith, P.C. (2016) Hydrography and coastal
1340 circulation along the Halifax Line and the connections with the Gulf of St. Lawrence. Atmos. Ocean
1341 54:3, 199-217, doi:10.1080/07055900.2016.1189397

DeVries, T. (2014). The oceanic anthropogenic CO_2 sink: Storage, air-sea fluxes, and transports over the industrial era. Global Biogeochem. Cycles 28, 631–647. doi: 10.1002/2013GB004739

Dewitte, B., Vazquez-Cuervo, J., Goubanova, K., Illig, S., Takahashi, K., Cambon, G., et al. (2012). Change in El Niño flavours over 1958–2008: Implications for the long-term trend of the upwelling off Peru. Deep Sea Res. Part II: Topical Studies in Oceanography 77, 143-156.

deYoung, B., von Oppeln-Bronikowski, N., Matthews, J.B.R., Bachmayer, R. (2018). Glider operations in the Labrador Sea. J. Ocean Tech. 13(1), 108-120.

Diakhaté, M., de Coëtlogon, G., Lazar, A., Wade, M., Gaye, A.T. (2016). Intraseasonal varaibilty of tropical Atlantic sea-surface temperature: air-sea interaction over upwelling fronts. Q.J.R. Meteorol. Soc. 142, 372-386. doi: 10.1002/qj.2657

Di Lorenzo, E. and Mantua, N. (2016). Multi-year persistence of the 2014/15 North Pacific marine heatwave. Nat. Climate Change 6, 1042–1047. doi: 10.1038/nclimate3082

Domingues, C. M., Wijffels, S. E., Maltrud, M. E., Church, J. A., and Tomczak, M. (2006). Role of eddies in cooling the Leeuwin Current. Geophysical Research Letters, 33: L05603, doi: 10.1029/2005GL025216.

Domingues, C., Maltrud, M., Wijffels, S., Church, J., Tomczak, M. (2007) Simulated Lagrangian pathways between the Leeuwin Current System and the upper-ocean circulation of the southeast Indian Ocean. Deep-Sea Res. II 54, 797–817. doi: 10.1016/j.dsr2.2006.10.003.

Domingues, R., Baringer, M., Goni, G. (2016). Remote sources for year-to-year changes in the seasonality of the Florida Current transport. J. Geophys. Res. 121(10), 7547-7559. doi:10.1002/2016JC012070

Domingues, R., Goni, G., Baringer, M., Volkov, D.L. (2018). What caused the accelerated sea level changes along the United States East Coast during 2010-2015? Geophys. Res. Lett. 45, 13367-13376. doi: 10.1029/2018GL081183

Domingues, R., et al. (2019). Ocean observations in support of studies and forecasts of tropical and extratropical cyclones. Front. Mar. Sci., submitted.

Dong, S., Goni, G., Bringas, F. (2015). Temporal variability of the South Atlantic Meridional Overturning Circulation between 20°S and 35°S. Geophys. Res. Lett., 42, 7655–7662, doi: 10.1002/2015GL065603

Donohue, K.A., Watts, D.R., Tracey, K.L., Greene, A.D., Kennelly, M. (2010). Mapping circulation in the Kuroshio Extension with an array of Current and Pressure recording Inverted Echo Sounders. J. Atmos. Oceanic Technol., 27, 507-527. doi: 10.1175/2009JTECHO686.1

Douglass, E., Roemmich, D., Stammer, D. (2010). Interannual variability in North Pacific heat and freshwater budgets. Deep-Sea Res. Part II-Topical Studies in Oceanography 57, 1127-1140. doi: 10.1016/j.dsr2.2010.01.001

Duncombe Rae, C.M. (2005). A demonstration of the hydrographic partition of the Benguela upwelling ecosystem at 26'40°S. Afr. J. Mar. Sci. 27, 617–628.

1379 Elipot, S., and Beal, L.M. (2015). Characteristics, dnergetics, and origins of Agulhas Current
1380 meanders and their limited influence on ring shedding. J. Phys. Oceanogr. 45, 2294-2314. doi:
1381 10.1175/JPO-D-14-0254.1

1382 Elipot, S. and Beal, L.M. (2018). Observed Agulhas Current sensitivity to interannual and long-term
1383 trend atmospheric forcings. J. Climate 31, 3077–3098. doi: 10.1175/JCLI-D-17-0597.1

1384 Escribano, R., Morales, C.E. (2012). Spatial and temporal scales of variability in the coastal
1385 upwelling and coastal transition zone off central-southern Chile (35-40°S). Progr. Oceanogr. 92-95,
1386 1-7. doi: 10.1016/j.pocean.2011.07.019

1387 Espinoza, P., Lorrain, A., Ménard, F., Cherel, Y., Tremblay-Boyer, L., Argüelles, J., et al. (2017).
1388 Trophic structure in the northern Humboldt Current system: new perspectives from stable isotope
1389 analysis. Mar. Biol. 164:86. doi: 10.1007/s00227-017-3119-8

1390 Everett, J. D., Baird, M. E., Roughan, M., Suthers, I. M., Doblin, M. A. (2014). Relative impact of
1391 seasonal and oceanographic drivers on surface chlorophyll a along a Western Boundary Current.
1392 Prog. Oceanogr. 120, 340-351. doi: 10.1016/j.pocean.2013.10.016

1393 Ezer, T. (2015). Detecting changes in the transport of the Gulf Stream and the Atlantic overturning
1394 circulation from coastal sea level data: The extreme decline in 2009–2010 and estimated variations
1395 for 1935–2012, Global Planet. Change 129, 23-36. doi: 10.1016/j.gloplacha.2015.03.002

1396 Fassbender, A.J., Sabine, C.L., Feely, R.A., Langdon, C., Mordy, C.W. (2011). Inorganic carbon
1397 dynamics during northern California coastal upwelling. Cont. Shelf Res. 31(11):1180–1192.

1398 Fassbender, A.J., Sabine, C.L., Feifel, K.M. (2016). Consideration of coastal carbonate chemistry in
1399 understanding biological calcification. Geophys. Res. Lett. 43(9):4467–4476.

1400 Fassbender, A.J., Sabine, C.L., Cronin, M.F., Sutton, A.J. (2017a). Mixed-layer carbon cycling at the
1401 Kuroshio extension observatory, Global Biogeochem. Cycles 31, 272–288,
1402 doi:10.1002/2016GB005547

1403 Fassbender, A.J., Alin, S.R., Feely, R.A., Sutton, A.J., Newton, J.A., Byrne, R.H. (2017b) Estimating
1404 total alkalinity in the Washington State coastal zone: Complexities and surprising utility for ocean
1405 acidification research. Estuar. Coasts 40(2):404–418.

1406 Fassbender, A.J., Alin, S.R., Feely, R.A., Sutton, A.J., Newton, J.A., Krembs, C., et al. (2018).
1407 Seasonal carbonate chemistry variability in marine surface waters of the US Pacific Northwest. Earth
1408 Syst. Sci. Data, 10, 1367-1401, https://doi: 10.5194/essd-10-1367-2018

1409 Faye, S., Lazar, A., Sow, B.A., Gaye, A.T. (2015). A model study of the seasonality of sea surface
1410 temperature and circulation in the Atlantic North-eastern Tropical Upwelling System. Front. Phys. 3,
1411 76, doi: 10.3389/fphy.2015.00076

1412 Feely, R.A., Sabine, C.L., Hernandez-Ayon, J.M., Ianson, D., Hales, B. (2008). Evidence for
1413 upwelling of corrosive 'acidified' water onto the continental shelf. Science 320,1490-1492,
1414 doi:10.1126/science.1155676

1415 Feely, R.A., Alin, S., Carter, B., Bednaršek, N., Hales, B., Chan, F., et al. (2016). Chemical and
1416 biological impacts of ocean acidification along the west coast of North America. Estuar. Coast. Shelf
1417 Sci. 183(A), 260-270. doi: 10.1016/j.ecss.2016.08.043

1418 Feely, R.A., Okazaki, R.R., Cai, W.-J., Bednaršek, N., Alin, S.R., Byrne, R.H., Fassbender, A.
1419 (2018). The combined effects of acidification and hypoxia on pH and aragonite saturation in the
1420 coastal waters of the Californian Current Ecosystem and the northern Gulf of Mexico. Cont. Shelf
1421 Res. 152, 50–60. doi: 10.1016/j.csr.2017.11.002

1422 Feng, M., McPhaden, M.J., Xie, S.P., Hafner, J. (2013). La Niña forces unprecedented Leeuwin
1423 Current warming in 2011. Sci. Rep. *3*, 1277. doi:10.1038/srep01277

1424 Feng, M., Meyer, G., Pearce, A., Wijffels, S. (2003). Annual and interannual variations of the
1425 Leeuwin Current at 32S. J. Geophys. Res. 108(C11), 3355, doi:10.1029/2002JC001763

1426 Feng, M., Hendon, H.H., Xie, S.P., Marshall, A.G., Schiller, A., Kosaka, Y., et al. (2015). Decadal
1427 increase in Ningaloo Niño since the late 1990s. Geophys. Res. Lett., 42(1), 104-112. doi:
1428 10.1002/2014GL062509

1429 Fennel, K., Wilkin, J., Levin, J., Moisan, J., O'Reilly, J., Haidvogel, D. (2006). Nitrogen cycling in
1430 the Middle Atlantic Bight: Results from a three-dimensional model and implications for the North
1431 Atlantic nitrogen budget, Global Biogeochem. Cycles 20, GB3007. doi:10.1029/2005GB002456

1432 Fernandez, D., Bowen, M. and Sutton, P. (2018). Variability, coherence and forcing mechanisms in
1433 the New Zealand ocean boundary currents. Prog. Oceanogr. 165, 1680-188, doi:
1434 10.1016/j.pocean.2018.06.002

1435 Ferrari, R., Artana, C., Saraceno, M., Piola, A. R., Provost, C. (2017). Satellite altimetry and current-
1436 meter velocities in the Malvinas Current at 41°S: Comparisons and modes of variations. J. Geophys.
1437 Res. 122. doi: 10.1002/2017JC013340

1438 Fischer, J., Schott, F., Dengler, M. (2004). Boundary circulation at the exit of the Labrador Sea. J.
1439 Phys. Oceanogr. 34, 1548–1570.

1440 Fischer, J., Visbeck, M., Zantopp, R., Nunes, N. (2010). Interannual to decadal variability of outflow
1441 from the Labrador Sea. Geophys. Res. Lett. 37, L24610. doi:10.1029/2010GL045321

1442 Frajka-Williams, Ansorge, I.J., Baehr, J., Bryden, H.L., Chidichimo, M.P., Cunningham, S.A., et al.
1443 (2019). Atlantic Meridional Overturning Circulation: Observed transport and variability. Front. Mar.
1444 Sci., submitted.

1445 Fratantoni, P. S., and Pickart, R. S. (2007). The western North Atlantic shelfbreak current system in
1446 summer, J. Phys. Oceanogr. 37(10), 2509–2533. doi:10.1175/JPO3123

1447 Fratantoni, D.M. and Richardson, P.L. (2006) The evolution and demise of North Brazil Current
1448 rings. J. Phys. Oceanogr. 36, 1241–1264. doi: 10.1175/JPO2907.1

1449 Fréon, P., Coetzee, J. C., Van der Lingen, C. D., Connell, A. D., O'Donoghue, S. H., Roberts, M.J.,
1450 et al. (2010). A review and tests of hypotheses about causes of the KwaZulu-Natal sardine run. Afr. J.
1451 Mar Sci. *32*(2), 449-479. doi: 10.2989/1814232X.2010.519451

1452 Friederich, G.E., Walz, P.M., Burczynski, M.G., Chavez, F.P. (2002). Inorganic carbon in the central
1453 California upwelling system during the 1997-1999 El Niño-La Niña event. Prog. Oceanogr. 54:185-
1454 203. doi:10.1016/S0079-6611(02)00049-6

1455 Frölicher, T.L. and Laufkötter, C. (2018). Emerging risks from marine heat waves. Nat. Commun.
1456 9(650). doi: 10.1038/s41467-018-03163-6

1457 Fujioka, K., Fukuda, H., Furukawa, S., Tei, Y., Okamoto, S., Ohshimo, S. (2018). Habitat use and
1458 movement patterns of small (age-0) juvenile Pacific bluefin tuna (Thunnus orientalis) relative to the
1459 Kuroshio. Fish. Oceanogr. 27(3), 185-198. doi: 10.1111/fog.12244

1460 Furue, R., Guerreiro, K., Phillips, H.E., McCreary, J. P., Bindoff, N. (2017). On the Leeuwin Current
1461 System and its linkage to zonal flows in the South Indian Ocean as inferred from a gridded
1462 hydrography. J. Phys. Oceanogr. 47, 583-602. doi: 10.1175/JPO-D-16-0170.1

1463 Galarneau, T. J., Jr., Davis, C. A., Shapiro, M. A. (2013). Intensification of Hurricane Sandy (2012)
1464 through extratropical warm core seclusion. Mon. Weather Rev. 141, 4296–4231. doi: 10.1175/MWR-
1465 D-13-00181.1

1466 Ganachaud, A., Cravatte, S., Melet, A., Schiller, A, Holbrook, N.J., et al. (2014). The Southwest
1467 Pacific Ocean circulation and climate experiment (SPICE). J. Geophys. Res.: Oceans 119(11): 7660–
1468 7686. doi: 10.1002/2013JC00967

1469 Ganachaud, A., Cravatte, S., Sprintall, J., Germineaud, C., Alberty, M., Jeandel, C., et al. (2017), The
1470 Solomon Sea: its circulation, chemistry, geochemistry and biology explored during two
1471 oceanographic cruises, Elem. Sci. Anth. 5, 33. doi: 10.1525/elementa.221

1472 Garzoli, S.L., and Baringer, M.O. (2007). Meridional heat transport determined with expendable
1473 bathythermographs, Part II: South Atlantic transport. Deep Sea Res. Part I 54(8), 1402-1420.
1474 doi:10.1016/j.dsr.2007.04.013 2007

1475 Garzoli, S.L., Baringer, M.O., Dong, S., Perez, R.C., Yao, Q. (2012). South Atlantic meridional
1476 fluxes. Deep-Sea Res. Part I 71, 21-32. doi:10.1016/j.dsr.2012.09.003

1477 Gaube, P., Braun, C. D., Lawson, G. L., McGillicuddy, D. J., Della Penna, A., Skomal, G., et al.
1478 (2018). Mesoscale eddies influence the movements of mature female white sharks in the Gulf Stream
1479 and Sargasso Sea. Sci. Rep. 8(1), 7363. doi: 10.1038/s41598-018-25565-8

1480 Gawarkiewicz, G. G., and Linder, C.A. (2006). Lagrangian flow patterns north of Cape Hatteras
1481 using near-surface drifters. Prog. Oceanogr. 70, 181--195. doi: 10.1016/j.pocean.2006.03.020

1482 Gawarkiewicz, G., Todd, R.E., Zhang, W., Partida, J., Gangopadhyay, A., Monim, M.-U.-H. et al.
1483 (2018). The changing nature of shelf- break exchange revealed by the OOI Pioneer Array.
1484 Oceanography 31(1), 60–70. doi: 10.5670/oceanog.2018.110

1485 Gay, P. S., and Chereskin, T. K. (2009). Mean structure and seasonal variability of the poleward
1486 undercurrent off southern California. J. Geophys. Res. 114, C02007. doi: 10.1029/2008JC004886

1487 Guerrero R.A., Piola, A.R., Fenco, H., Matano, R.P., Combes, V., Chao, Y., et al. (2014). The
1488 salinity signature of the cross-shelf exchanges in the Southwestern Atlantic Ocean: Satellite
1489 observations, J. Geophys. Res. Oceans 119, 7794-7810. doi: 10.1002/2014JC010113

1490 Godfrey, J. S. and Weaver, A. J. (1991). Is the Leeuwin Current driven by Pacific heating and winds?
1491 Prog. Oceanogr. 27, 225–272. doi: 10.1016/0079-6611(91)90026-I

1492 Gómez-Letona, M., Ramos, A.G., Coca, J., Arístegui, J. (2017). Trends in primary production in the
1493 Canary Current Upwelling System—A regional perspective comparing remote sensing models.
1494 Front. Mar. Sci. 4, 370. doi: 10.3389/fmars.2017.00370

1495 Goni, G. J., et al. (2019), More than 50 years of continuous temperature section measurements by the
1496 Global Expendable Bathythermograph (XBT) Network, its integrability, societal benefits, and future.
1497 Fron. Mar. Sci., submitted.

1498 Goni, G.J., Bringas, F., Di Nezio, P.N. (2011). Observed low frequency variability of the Brazil
1499 Current Front. J. Geophys. Res. 116, C10037. doi:10.1029/2011JC007198

1500 Goni, G.J., Garzoli, S.L., Roubicek, A.J, Olson, D.B., and Brown, O.B. (1997). Agulhas ring
1501 dynamics from TOPEX/POSEIDON satellite altimeter data. J. Mar. Res. 55(5): 861-883. doi:
1502 10.1357/002224097322417

1503 Goni, G.J., Kamholz, S., Garzoli, S.L., Olson, D.B. (1996). Dynamics of the Brazil-Malvinas
1504 Confluence based on inverted echo sounders and altimetry. J. Geophys. Res. 101(C7):16,273-16,289.
1505 doi: 10.1029/96JC01146

1506 Goni, G.J., and Wainer, I. (2001). Investigation of the Brazil Current front variability from altimeter
1507 data. J. Geophys. Res. 106, 31117-31128. doi: 10.1029/2000JC000396

1508 Gopalakrishnan, G., Cornuelle, B. D., Hoteit, I., Rudnick, D. L., Owens, W. B. (2013). State
1509 estimates and forecasts of the loop current in the Gulf of Mexico using the MITgcm and its adjoint. J.
1510 Geophys. Res.118(7), 3292-3314. doi: 10.1002/jgrc.20239

1511 Gordon, A.L., Flament, P., Villanoy, C., Centurioni, L. (2014). The nascent Kuroshio of Lamon Bay.
1512 J. Geophys. Res. 119(7), 4251-4263. doi: 10.1002/2014JC009882

1513 Gorgues, T., Aumont, O., and Rodgers, K. B. (2010). A mechanistic account of increasing seasonal
1514 variations in the rate of ocean uptake of anthropogenic carbon, Biogeosciences, 7, 2581-2589,
1515 https://doi: 10.5194/bg-7-2581-2010.

1516 Graco, M., Purca, S., Dewitte, B., Castro, C., Morón, O., Ledesma, et al. (2017). The OMZ and
1517 nutrient features as a signature of interannual and low-frequency variability in the Peruvian upwelling
1518 system. Biogeosciences 14, 1–17, 2017. doi: 10.5194/bg-14-1-2017

1519 Grados, C., Chaigneau, A., Echevin, V., Dominguez, N. (2018). Upper ocean hydrology of the
1520 Northern Humboldt Current System at seasonal, interannual and interdecadal scales. Prog. Oceanogr.
1521 165. doi: 10.1016/j.pocean.2018.05.005

1522 Gruber, N., Keeling, C.D., Bates, N.R. (2002). Interannual variability in the North Atlantic Ocean
1523 carbon sink. Science 298 (5602), 2374-2378.

1524 Gula, J., Blacic, T.M., Todd, R.E. (2019). Submesoscale coherent vortices in the Gulf Stream.
1525 Geophys. Res. Lett., in press. doi: 10.1029/2019GL081919

1526 Guo, X., Zhu, X.H., Wu, Q.S., Huang, D. (2012). The Kuroshio nutrient stream and its temporal
1527 variation in the East China Sea. J. Geophys. Res.: Oceans, 117(C1). doi: 10.1029/2011JC007292

1528 Guo, X.Y., Zhu, X.H., Long, Y., Huang, D.J. (2013). Spatial variations in the Kuroshio nutrient
1529 transport from the East China Sea to south of Japan. Biogeosciences, 10(10), pp.6403-6417. doi:
1530 10.5194/bg-10-6403-2013

1531 Gutiérrez, D. (2016). Variabilidad climática, procesos oceanográficos y producción primaria frente al
1532 Perú.Boletín Técnico "Generación de información y monitoreo del Fenómeno El Niño." Instituto
1533 Geofísico del Perú, 3(6): 4-8.

1534 Haines, S., Seim, H., Muglia, M. (2017). Implementing quality control of high-frequency radar
1535 estimates and application to Gulf Stream surface currents. J. Atmos. Oceanic Technol. 34, 1207-
1536 1224. doi: 10.1175/JTECH-D-16-0203.1

1537 Hales, B., Takahashi, T., Bandstra, L. (2005). Atmospheric CO2 uptake by a coastal upwelling
1538 system, Global Biogeochem. Cycles 19, GB1009. doi: 10.1029/2004GB002295

1539 Halliwell, G. R., Mehari, M., Shay, L.K., Kourafalou, V.H., Kang, H., Kim J.-S., et al. (2017), OSSE
1540 quantitative assessment of rapid-response prestorm ocean surveys to improve coupled tropical
1541 cyclone prediction. J. Geophys. Res. Oceans 122, 5729–5748. doi: 10.1002/2017JC012760

1542 Hansen, D.V., and Poulain, P-M. (1996). Quality control and interpolation of WOCE/TOGA drifter
1543 data. J. Atmos. Oceanic Technol. 13, 900-909. doi:10.1175/1520-
1544 0426(1996)013<0900:QCAIOW>2.0.CO;2

1545 Harris, K.E., DeGrandpre, M.D., Hales, B. (2013). Aragonite saturation states in a coastal upwelling
1546 zone. Geophys. Res. Lett. 40, 2720-2725. doi: 10.1002/grl.50460.

1547 He, R., Chen, K., Moore, T., Li, M. (2010). Mesoscale variations of sea surface temperature and
1548 ocean color patterns at the Mid-Atlantic Bight shelfbreak. Geophys. Res. Lett. 37, L09607. doi:
1549 10.1029/2010GL042658

1550 Helly, J.J. and Levin. L.A. (2004).Global distribution of naturally occurring marine
1551 hypoxia on continental margins. Deep Sea Res. I 51, 1159-1168. doi:10.1016/j.dsr.2004.03.009

1552 Henderikx Freitas, F., Saldías, G.S., Goñi, M., Shearman, R.K., White, A.E. (2018). Temporal and
1553 spatial dynamics of physical and biological properties along the Endurance Array of the California
1554 Current ecosystem. Oceanography 31(1), 80–89, doi: 10.5670/oceanog.2018.113

1555 Henderikx Freitas, F., Siegel, D. A., Washburn, L., Halewood, S., Stassinos, E. (2016). Assessing
1556 controls on cross-shelf phytoplankton and suspended particle distributions using repeated bio-optical
1557 glider surveys. Oceans, 121, 7776–7794, doi: 10.1002/2016JC011781.

1558 Heslop, E.E., Ruiz, S., Allen, J., López-Jurado, J.L., Renault, L., Tintoré, J. (2012). Autonomous
1559 underwater gliders monitoring variability at "choke points" in our ocean system: a case study in the
1560 Western Mediterranean Sea. Geophys. Res. Lett. 39:L20604.

1561 Hill, K., Moltmann, T., Meyers, G. and Proctor, R. (2010). "The Australian integrated marine
1562 observing system (IMOS)," in Proceedings of OceanObs' 09: Sustained Ocean Observations and
1563 Information for Society, Eds. J. Hall, D.E. Harrison, and D. Stammer, (ESA Publication WPP-306).
1564 doi: 10.5270/OceanObs09

1565 Hill, K., Rintoul, S.R., Ridgway, K.R., Oke, P.R. (2011). Decadal changes in the South Pacific
1566 western boundary current system revealed in observations and ocean state estimates. J. Geophys.
1567 Res. 116, C01009. doi: 10.1029/2009JC005926

1568 Hobday, A.J., Alexander, L.V., Perkins, S.E., Smale, D.A., Straub, S.C., Oliver, E.C.J., et al. (2016).
1569 A hierarchical approach to defining marine heatwaves. Prog. Oceanogr. 141, 227-238. doi:
1570 10.1016/j.pocean.2015.12.014

1571 Hoffman, R.N. and Atlas, R, (2016). Future observing system simulation experiments. Bull. Amer.
1572 Meteor. Soc. 97, 1601–1616. doi: 10.1175/BAMS-D-15-00200.1

1573 Honda, M.C., Sasai, Y., Siswanto, E., Kuwano-Yoshida, A., Aiki, H., Cronin, M.F. (2018). Impact of
1574 cyclonic eddies and typhoons on biogeochemistry in the oligotrophic ocean based on
1575 biogeochemical/physical/meteorological time-series at station KEO. Prog. Earth Planet. Sci., 5, 42.
1576 doi: 10.1186/s40645-018-0196-3

1577 Houpert, L., Inall, M.E., Dumont, E., Gary, S., Johnson, C., Porter, M., et al. (2018). Structure and
1578 transport of the north atlantic current in the Eastern Subpolar Gyre from sustained glider
1579 observations. J. Geophys. Res.: Oceans 123, 6019–6038. doi: 10.1029/2018JC014162

1580 Howatt, T., Palter, J.B., Matthews, J. B., deYoung, B., Bachmayer, R., Claus, B. (2018). Ekman and
1581 eddy exchange of freshwater and oxygen across the Labrador Shelf Break, J. Phys. Oceanogr. 48(5),
1582 1015–1031. doi:10.1175/JPO-D-17-0148.1

1583 Hu, D., Hu, S., Wu, L., Li, L., Zhang, L., Diao, X., et al. (2013). Direct measurements of the Luzon
1584 undercurrent. J. Phys. Oceanogr. 43(7), 1417–1425. doi: 10.1175/JPO-D-12-0165.1

1585 Hu D., Wu, L., Cai, W., Sen Gupta, A., Ganachaud, A., Qiu, B. et al. (2015). Pacific western
1586 boundary currents and their roles in climate. Nature, 522, 299-308. doi: 10.1038/nature14504.

1587 Hu S., Hu, D., Guan, C., Wang, F., Zhang, L., Wang, F., et al. (2016). Interannual variability of the
1588 Mindanao Current/Undercurrent in direct observations and numerical simulations, J. Phys. Oceanogr.
1589 46, 483-499. doi: http://dx.doi: 10.1175/JPO-D-15-0092.1

1590 Hummels, R., Brandt, P., Dengler, M., Fischer, J., Araujo, M., Veleda, D., Durgadoo, J.V. (2015).
1591 Interannual to decadal changes in the western boundary circulation in the Atlantic at 11 degrees S.
1592 Geophys. Res. Lett. 42(18), 7615-7622.

1593 Hutchings, L., van der Lingen, C, .Shannon, L.J., Cawford, R.J.M., Verheye, H.M., Bartholomae, C.H.,
1594 et al. (2009a). The Benguela Current: an ecosystem of four components. Progr. Oceanogr., 83, 15-32.

1595 Hutchings L, Roberts MJ, Verheye HM. (2009b). Marine environmental monitoring programmes in
1596 South Africa: a review. S. Afr. J. Sci., 105, 94-102.

1597 Hutchings, L., Augustyn, C.J., Cockcroft, A., Van der Lingen, C., Coetzee, J., Leslie, R.W., et al.
1598 (2009c). Marine fisheries monitoring programmes in South Africa. S. Afr. J. Sci., 105(5-6), 182-192.

1599 Huyer, A., Wheeler, P. A., Strub, P. T., Smith, R. L. Letelier, R., Kosro, 2 P. M. (2007). The
1600 Newport line off Oregon – Studies in the North East Pacific. Prog. Oceanogr., 75, 126–160. doi:
1601 10.1016/j.pocean.2007.08.003

1602 Ichikawa, H., Nakamura, H., Nishina, A., Higashi, M. (2004). Variability of northeastward current
1603 southeast of Northern Ryukyu Islands. J. Oceanogr. 60:2, 351-363. doi:
1604 10.1023/B:JOCE.0000038341.27622.73

1605 Imawaki, S., H. Uchida, H. Ichikawa, M. Fuksawa, S. Umatani, the ASUKA group (2001). Satellite
1606 altimeter monitoring the Kuroshio Transport south of Japan. Geophys. Res. Lett., 28(1), 17-20. doi:
1607 10.1029/2000GL011796

1608 Imawaki, S., Bower, A., Beal, L., Qiu, B. (2013). "Western boundary currents," in Ocean circulation
1609 and climate: A 21st century perspective, eds. G. Siedler, S. M. Griffies, J. Gould, J. A. Church
1610 (Oxford, UK: Elsevier Academic Press), 305–338. doi: 10.1016/B978-0-12-391851-2.00013-1.

1611 Inoue, R., Honda, M., Fujiki, T., Matsumoto, K., Kouketsu, S., Suga, T. et al. (2016b). Western
1612 North Pacific Integrated Physical-Biogeochemical Ocean Observation Experiment (INBOX): Part 2.
1613 Biogeochemical responses to eddies and typhoons revealed from the S1 mooring and shipboard
1614 measurements. J. Mar. Res. 74, 71-99. doi:10.1357/002224016819257335

1615 Inoue, R., Suga, T., Kouketsu, S., Kita, T., Hosoda, S., Kobayashi, T., et al. (2016a). Western north
1616 Pacific integrated physical-biogeochemical ocean observation experiment (INBOX): Part 1.
1617 Specifications and chronology of the S1-INBOX floats. J. Mar. Res. 74, 43-69. doi:
1618 10.1357/002224016819257344

1619 Ito, T., and Follows, M.J. (2003) Upper ocean control on the solubility pump of CO2. J. Marine Res.,
1620 61, 465-489.

1621 Ito, S., Yoshie, N., Okunishi, T., Ono, T., Okazaki, Y., Kuwataet, A., et al. (2010). Application of an
1622 automatic approach to calibrate the NEMURO nutrient-phytoplankton-zooplankton food web model
1623 in the Oyashio region. Progr. Oceanogr. 87, 186-200. doi: 10.1016/j.pocean.2010.08.004

1624 Iudicone, D., Rodgers, K.B., Plancherel, Y., Aumont, O., Ito, T., Key, R.M., Madec, G., Ishii, M.
1625 (2016). The formation of the ocean's anthropogenic carbon reservoir. *Scientific reports*, *6*, p.35473.

1626 Jayne, S.R., Roemmich, D., Zilberman, N., Riser, S.C., Johnson, K.S., Johnson, G.C., et al. (2017).
1627 The Argo Program: Present and future. Oceanography 30(2):18–28. doi: 10.5670/oceanog.2017.213

1628 Johns, W.E., Baringer, M.O., Beal, L.M., Cunningham, S.A., Kanzow, T., Bryden, H.L., et al.
1629 (2011). Continuous array-based estimates of Atlantic Ocean heat transport at 26.5°N. J. Climate 24,
1630 2429-2449. doi:10.1175/2010JCLI3997.1

1631 Johns, W.E., Beal, L.M., Baringer, M.O., Molina, J.R., Cunningham, S.A., Kanzow, T., Rayner, D.
1632 (2008). Variability of shallow and deep western boundary currents off the Bahamas during 2004-
1633 2005: Results from the 26°N RAPID-MOC array. J. Phys. Oceanogr. 38, 605-623.
1634 doi:10.1175/2007JPO3791.1

1635 Johns, W.E., Kanzow, T., Zantopp, R. (2005), Estimating ocean transports with dynamic height
1636 moorings: An application in the Atlantic Deep Western Boundary Current at 26°N, Deep Sea Res.
1637 Part I 52, 1542-1567. doi: 10.1016/j.dsr.2005.02.002

1638 Johnson, C.R., Banks, S.C., Barrett, N.S., Cazassus, F., Dunstan, P.K., Edgar, et al. (2011). Climate
1639 change cascades: Shifts in oceanography, species' ranges and subtidal marine community dynamics
1640 in eastern Tasmania. J. Exp. Mar. Biol. Ecol. 400, 17-32. doi: 10.1016/j.jembe.2011.02.032

1641 Johnson, G.C. (2001) The Pacific Ocean subtropical cell surface limb. Geophys. Res. Lett. 28:1771–
1642 74

1643 Johnson, K. S., Plant, J.N., Coletti, L.J., Jannasch, H.W., Sakamoto, C.M., Riser, S.C., et al. (2017),
1644 Biogeochemical sensor performance in the SOCCOM profiling float array. J. Geophys. Res. 122,
1645 6416–6436. doi:10.1002/2017JC012838

1646 Johnston, T.M., Rudnick, D.L., Alford, M.H., Pickering, A., Simmons, H.L. (2013). Internal tidal
1647 energy fluxes in the South China Sea from density and velocity measurements by gliders. J. Geophys.
1648 Res.: Oceans 118(8), 3939-3949. doi: 10.1002/jgrc.20311

1649 Johnston, T.M.S., Rudnick, D.L. (2015). Mixing estimates in the California Current System from
1650 sustained observations by underwater gliders. Deep-Sea Res. II 112:61–78.

1651 Junker, T., Mohrholz, V., Schmidt, M., Siegfried, L., van der Plas, A. (2019). Coastal trapped wave
1652 propagation along the southwest African shelf as revealed by moored observations. J. Phys.
1653 Oceanogr., in press. doi: 10.1175/JPO-D-18-0046.1

1654 Junker, T., Mohrholz, V., Siegfried, L., van der Plas, A. (2017a). Seasonal to interannual variability
1655 of water mass characteristics and currents on the Namibian shelf. J. Mar. Sys. 165, 36–46.
1656 doi:10.1016/j.jmarsys.2016.09.003

1657 Junker, T., Mohrholz, V., Siegfried, L., van der Plas, A., Heene, T., Beier, S., (2017b). Daily means
1658 of bottom temperature and bottom oxygen measurements on the Namibian shelf at 18°S. Leibniz
1659 Institute for Baltic Sea Research, Warnemünde, PANGAEA. doi: 10.1594/PANGAEA.871251

1660 Junker, T., Mohrholz, V., Siegfried, L., van der Plas, A., Heene, T., Beier, S., (2017c). Daily means
1661 of horizontal currents measurements on the Namibian shelf at 18°S. Leibniz Institute for Baltic Sea
1662 Research, Warnemünde, PANGAEA. doi: 10.1594/PANGAEA.871253

1663 Junker, T., Mohrholz, V., Siegfried, L., van der Plas, A., Heene, T., Beier, S., (2017d). Daily means
1664 of horizontal currents measurements on the Namibian shelf at 20°S. Leibniz Institute for Baltic Sea
1665 Research, Warnemünde, PANGAEA. doi: 10.1594/PANGAEA.872098

1666 Junker, T., Mohrholz, V., Siegfried, L., van der Plas, A., Heene, T., Breier, S., (2017e): Daily means
1667 of bottom temperature and bottom oxygen measurements on the Namibian shelf at 20°S. Leibniz
1668 Institute for Baltic Sea Research, Warnemünde, PANGAEA. doi: 10.1594/PANGAEA.872099

1669 Juranek, L.W., Feely, R.A., Peterson, W.T., Alin, S.R., Hales, B., Lee, K., et al. (2009). A novel
1670 method for determination of aragonite saturation state on the continental shelf of central Oregon
1671 using multi-parameter relationships with hydrographic data. Geophys. Res. Lett. 36, L24601. doi:
1672 10.1029/2009GL040778

1673 Jury, M. R., Valentine, H. R., Lutjeharms, J. R. (1993). Influence of the Agulhas Current on summer
1674 rainfall along the southeast coast of South Africa. J. Appl Meteorol. 32, 1282-1287. doi:
1675 10.1175/1520-0450(1993)032<1282:IOTACO>2.0.CO;2

1676 Karstensen, J., Schütte, F., Pietri, A., Krahmann, G., Fiedler, B., Grundle, D., et al. (2017).
1677 Upwelling and isolation in oxygen-depleted anticyclonic modewater eddies and implications for
1678 nitrate cycling. Biogeosciences 14(8), 2167–2181. doi: 10.5194/bg-14-2167-2017

1679 Kelly, K.A., Small, R.J., Samelson, R.M., Qiu, B., Joyce, T.M. Kwon, Y., et al. (2010). Western
1680 boundary currents and frontal air–sea interaction: Gulf Stream and Kuroshio Extension. J. Climate
1681 23, 5644–5667. doi: 10.1175/2010JCLI3346.1

1682 Kerry, C., Powell, B., Roughan, M., Oke, P. (2016). Development and evaluation of a high-resolution
1683 reanalysis of the East Australian Current region using the Regional Ocean Modelling System (ROMS
1684 3.4) and Incremental Strong-Constraint 4-Dimensional Variational (IS4D-Var) data assimilation.
1685 Geosci. Model Dev. 9, 3779-3801. doi:10.5194/gmd-9-3779-2016

1686 Kerry, C., Roughan, M., Powell, B (2018). Observation impact in a regional reanalysis of the East
1687 Australian Current System, J. Geophys. Res.0. doi:10.1029/2017JC013685

1688 Kersalé, M, Lamont, T., Speich, S., Terre, T., Laxenaire, R., Roberts, M.J., et al. (2018). Moored
1689 observations of mesoscale features in the Cape Basin: characteristics and local impacts on water mass
1690 distributions. Ocean Sci. 14, 923-945. doi: 10.5194/os-14-923-2018

1691 Kim, S.Y., Terrill, E.J., Cornuelle, B.D., Jones, B., Washburn, L., Moline, M.A., et al. (2011).
1692 Mapping the U.S. West Coast surface circulation: A multiyear analysis of high-frequency radar
1693 observations. J. Geophys. Res.116, C03011. doi: 10.1029/2010JC006669

1694 Kim, S.Y. (2010). Observations of submesoscale eddies using high-frequency radar-derived
1695 kinematic and dynamic quantities. Cont. Shelf Res., 30(15), 1639-1655. doi:
1696 10.1016/j.csr.2010.06.011

1697 Kim, S.Y., and Kosro, P. M. (2013). Observations of near-inertial surface currents off Oregon:
1698 Decorrelation time and length scales. Oceans 118, 3723–3736. doi: 10.1002/jgrc.20235

1699 Klenz, T., Dengler, M., Brandt, P. (2018). Seasonal variability of the Mauritania Current and
1700 hydrography at 18°N. J. Geophys. Res. 123, 11, 8122-8137. doi: 10.1029/2018JC014264

1701 Kolodziejczyk, N., Testor, P., Lazar, A., Echevin, V., Krahmann, G., Chaigneau, A., et al. (2018).
1702 Subsurface fine-scale patterns in an anticyclonic eddy off Cap-Vert peninsula observed from glider
1703 measurements. J. Geophys. Res.: Oceans, 123, 6312–6329. doi: 10.1029/2018JC014135

1704 Kono, T. and Kawasaki, Y. (1997). Results of CTD and mooring observations southeast of
1705 Hokkaido. 1. Annual verocity and transport variations in the Oyashio. Bull. Hokkaido Natl. Fish.
1706 Res. Inst., 61, 65-81.

1707 Kopte, R., Brandt, P., Dengler, M., Tchipalanga, P.C.M., Macuéria, M., Ostrowski, M. (2017). The
1708 Angola Current: Flow and hydrographic characteristics as observed at 11°S. J. Geophys. Res. Oceans
1709 122. doi: 10.1002/2016JC012374

1710 Kopte, R., Brandt, P., Claus, M, Greatbatch, R.J., Dengler, M. (2018). Role of equatorial basin-mode
1711 resonance for the seasonal variability of the Angola Current at 11°S. J. Phys. Oceanogr. 48, 261-281.
1712 doi: 10.1175/JPO-D-17-0111.1

1713 Koszalka, I. and LaCasce, J.H. (2010). Lagrangian analysis by clustering. Ocean Dyn. 60, 957-972.
1714 doi: 10.1007/s10236-010-0306-2

1715 Krug, M., Swart, S., Gula, J.. (2017). Submesoscale cyclones in the Agulhas current. Geophys. Res.
1716 Lett. 44, 346-354. doi: 10.1002/2016GL071006

1717 Kuroda, H., Wagawa, T., Shimizu, Y., Ito, S., Kakehi, S., Okunishi, T., et al. (2015). Interdecadal
1718 decrease of the Oyashio transport on the continental slope off the southeastern coast of Hokkaido,
1719 Japan. J. Geophys. Res. Oceans, 120, 2504-2522. doi:10.1002/2014JC010402

1720 Kuroda, H., Wagawa, T., Kakehi, S., Shimizu, Y., Kusaka, A., Okunishi, T., et al. (2017). Long-term
1721 mean and seasonal variation of altimetry-derived Oyashio transport across the A-line off the
1722 southeastern coast of Hokkaido, Japan. Deep Sea Res. Part I: Oceanographic Research Papers 121,
1723 95-109, doi: 10.1016/j.dsr.2016.12.006

1724 LaCasce, J.H. (2008). Statistics from Lagrangian observations. Prog. Oceanogr. 77, 1-29.
1725 doi:10.1016/j.pocean.2008.02.002

1726 Landschützer, P., Gruber, N., Bakker, D.C.E., Schuster, U. (2014), Recent variability of the global
1727 ocean carbon sink, Global Biogeochem. Cycles, 28, 927-949, doi:10.1002/2014GB004853.

1728 Large, W.G. and Danabasoglu, G. (2006). Attribution and impacts of upper-ocean biases in CCSM3.
1729 J. Climate 19, 2325-2346. doi: 10.1175/JCLI3740.1

1730 Larsen, J.C and Sanford, T.B. (1985). Florida Current volume transports from voltage measurements.
1731 Science 227, 302-304. doi: 10.1126/science.227.4684.302

1732 Laurindo, L.C., Mariano, A., Lumpkin, R. (2017). An improved near-surface velocity climatology for
1733 the global ocean from drifter observations. Deep Sea Res.. I, 124, 73-92. doi:
1734 10.1016/j.dsr.2017.04.009

1735 Leber, G.M., Beal, L.M., Elipot, S. (2017). Wind and current forcing combine to drive strong
1736 upwelling in the Agulhas Current. J. Phys. Oceanogr. 47(1), 123-134. doi: 10.1175/JPO-D-16-0079.1

1737 Lee, E.A., and Kim, S.Y. (2018). Regional variability and turbulent characteristics of the satellite-
1738 sensed submesoscale surface chlorophyll concentrations. J. Geopyhs. Res. 123, 4250–4279. doi:
1739 10.1029/2017JC013732

1740 Lee, T. and Fukumori, I. (2003). Interannual-to-decadal variations of tropical-subtropical exchange in
1741 the Pacific Ocean: Boundary versus interior pycnocline transports. J. Climate 16, 4022-4042. doi:
1742 10.1175/1520-0442(2003)016<4022:IVOTEI>2.0.CO;2

1743 Lengaigne, M., Hausmann, U., Madec, G., Menkes, C.E., Vialard, J., Molines, J.M. (2012).
1744 Mechanisms controlling warm water volume interannual variations in the equatorial Pacific: diabatic
1745 versus adiabatic processes. Clim. Dyn. 38:1031–1046. doi: 10.1007/s00382-011-1051-z

1746 Lentini C., Goni, G.J., Olson, D. (2006). Investigation of Brazil Current rings in the confluence
1747 region. J. Geophys. Res. 111(C6), C06013. doi:10.1029/2005JC002988

1748 Levine, N. M., Doney, S. C., Lima, I., Wanninkhof, R., Bates, N. R., Feely, R. A. (2011). The impact
1749 of the North Atlantic Oscillation on the uptake and accumulation of anthropogenic CO2 by North
1750 Atlantic Ocean mode waters. Global Biogeochemical Cycles. 25. doi: 10.1029/2010GB003892

1751 Liang, X., Spall, M., Wunsch, C. (2017). Global ocean vertical velocity from a dynamically
1752 consistent ocean state estimate. J. Geophys. Res.122, 8208-8224. doi:10.1002/2017JC012985

1753 Lien, R.-C., Ma, B., Cheng, Y.-H., Ho, C.-R., Qiu, B., Lee, C.M., Chang, M.H. (2014). Modulation
1754 of Kuroshio transport by mesoscale eddies at the Luzon Strait entrance. J. Geophys. Res. Oceans 119,
1755 2129–2142. doi: 10.1002/2013JC009548

1756 Lien, R.-C., Ma, B., Lee, C.M., Sanford, T.B., Mensah, V., Centurioni, L.R., et al. (2015). The
1757 Kuroshio and Luzon Undercurrent east of Luzon Island. Oceanography 28(4), 54–63. doi:
1758 10.5670/oceanog.2015.81

1759 Lima, M.O., Cirano, M., Mata, M., Goes, M., Goni, G., Baringer, M.O. (2016). An assessment of the
1760 Brazil Current baroclinic structure and variability near 22°S in distinct ocean forecasting and analysis
1761 systems. Ocean Dyn. 66, 893 – 916. doi: 10.1007/s10236-016-0959-6

1762 Linder, C. A., and Gawarkiewicz, G. G. (1998). A climatology of the shelfbreak front in the Middle
1763 Atlantic Bight. J. Geophys. Res. 103(C9), 18,404–18,423. doi: 10.1029/98JC01438

1764 Lindstrom, E., Gunn, J., Fischer, A., McCurdy, A., Glover, L.K. (2012). A framework for Ocean
1765 Observing. By the Task Team for an Integrated Framework for Sustained Ocean Observing, Paris,
1766 France, UNESCO. http://dx.doi: 10.5270/OceanObs09-FOO

1767 Louw, D., van der Plas, A., Mohrholz, V., Wasmund, N., Junker, T., Eggert, A. (2016). Seasonal and
1768 interannual phytoplankton dynamics and forcing mechanisms in the northern Benguela upwelling
1769 system. J. Mar. Syst. 157, 124–134. http://dx.doi. org/10.1016/j.jmarsys.2016.01.009

1770 Lovechio, E., Gruber, N., Münnich, M. (2018). Mesoscale contribution to the long-range offshore
1771 transport of organic carbon from the Canary Upwelling System to the open North Atlantic.
1772 Biogeosciences 15, 5061-5091.

1773 Lowcher, C.F., Muglia, M., Bane, J.M., He, R., Gong, Y., Haines, S.M. (2017). Marine hydrokinetic
1774 energy in the Gulf Stream off North Carolina: An assessment using observations and ocean
1775 circulation models. In: Yang, Z. and Copping, A. (eds) Marine Renewable Energy. Springer, Cham.
1776 doi: 10.1007/978-3-319-53536-4_10

1777 Lumpkin, R. (2003). Decomposition of surface drifter observations in the Atlantic Ocean. Geophys.
1778 Res. Lett. 30(14), 1753. doi:10.1029/2003GL017519

1779 Lumpkin, R., and Garzoli. S.L. (2011). Interannual to decadal changes in the western South Atlantic's
1780 surface circulation. J. Geophys. Res.116, C01014. doi:10.1029/2010JC006285

1781 Lumpkin, R., and Johnson. G. (2013). Global ocean surface velocities from drifters: Mean, variance,
1782 El Niño-Southern Oscillation response, and seasonal cycle. .J. Geophys. Res.118(C6), 2992-3006.
1783 doi:10.1002/jgrc.20210

1784 Lumpkin R, Maximenko N, Pazos M. (2012) Evaluating where and why drifters die. J. Atmos.
1785 Ocean. Technol. 29:300–8

1786 Lumpkin, R., T. Özgökmen, L. Centurioni (2017) Advances in the application of surface drifters
1787 Annu. Rev. Mar. Sci., 9:1, 59-81

1788 Lumpkin, R., and Pazos, M.C. (2007). "Measuring surface currents with Surface Velocity Program
1789 drifters: The instrument, its data, and some recent results,".in Lagrangian Analysis and Prediction of
1790 Coastal and Ocean Dynamics, eds. A. Griffa, A.D. Kirwan, A.J. Mariano, T. Ozgokmen, and H.T.
1791 Rossby (Cambridge University Press),39-67.

1792 Lund, B., Haus, B.K., Horstmann, J., Graber, H.C., Carrasco, R., Laxague, N.J., et al. (2018). Near-
1793 surface current mapping by shipboard marine X-band radar: A validation. *J. Atmos. Oceanic*
1794 *Technol.,* **35**, 1077–1090, doi: 10.1175/JTECH-D-17-0154.1

1795 Lutjeharms, J. R. (2006). The Agulhas Current. Springer.

1796 Lynch, T.P., Morello, E.B., Evans, K., Richardson, A., Rochester, W., Steinberg, C. R., et al. (2014)
1797 IMOS National Reference Stations: A continental scale physical, chemical, biological coastal
1798 observing system. PLoS ONE 9(12), e113652. doi:10.1371/journal.pone.0113652

1799 Ma, X., Chang, P., Saravanan, R., Montuoro, R., Nakamura, H., Wu, D., et al. (2017). Importance of
1800 resolving Kuroshio front and eddy influence in simulating the North Pacific storm track. J. Climate
1801 30(5), 1861-1880. doi: 10.1175/JCLI-D-16-0154.1

1802 Machu, E., Capet, X., Estrade, P.A., Ndoye, S., Brajard, J., Baurand, F., et al. (2019). First evidence
1803 of anoxia and nitrogen loss in the southern Canary Upwelling System. Geophys. Res. Lett., in press.
1804 doi: 10.1029/2018GL079622

1805 Mackey, D. J., O'Sullivan, J. E., Watson, R. J. (2002). Iron in the western Pacific: A riverine or
1806 hydrothermal source for iron in the Equatorial Undercurrent. Deep Sea. Res. I 49, 877–893. doi:
1807 10.1016/S0967- 0637(01)00075-9

1808 Majumder, S., Goes, M., Polito, P.S., Lumpkin, R., Schmid, C., Lopez, H. (2019). Propagating
1809 modes of variability and their impact on the western boundary current in the South Atlantic. J.
1810 Geophys. Res.: Oceans 124, in press. doi: 10.1029/2018JC014812

1811 Majumder, S. and Schmid, C. (2018), A study of the variability in the Benguela Current volume
1812 transport, Ocean Sci., 14, 273-283, doi: 10.5194/os-14-273-2018

1813 Mansfield, K.L., Mendilaharsu, M.L., Putman, N.F., dei Marcovaldi, M.A., Sacco, A.E., Lopez, G.,
1814 et al. (2017). First satellite tracks of South Atlantic sea turtle 'lost years': seasonal variation in trans-
1815 equatorial movement. Proc. Biol. Sci, 284(1868), 20171730. doi: 10.1098/rspb.2017.1730

1816 Mantovanelli, A., Keating, S., Wyatt, L., Roughan, M., Schaeffer, A. (2017). Lagrangian and
1817 Eulerian characterization of two counter rotating submesoscale eddies in a western boundary current.
1818 J. Geophys. Res. Oceans, 122 (6), DOI: 10.1002/2016JC011968

1819 Marra, J., Houghton, R. W., Garside, C. (1990). Phytoplankton growth at the shelf-break front in the
1820 Middle Atlantic Bight. J. Mar. Res., 48, 851–868. doi: 10.1357/002224090784988665

1821 Marzeion, B., Cogley, J.G., Richter, K., Parkes, D. (2014). Attribution of global glacier mass loss to
1822 anthropogenic and natural causes. Science 345, 919-921. doi: 10.1126/science.1254702

1823 Mata M.M., Cirano, M., van Caspel, M.R., Fonteles, C.S., Goni, G., Baringer, M. (2012)
1824 Observations of Brazil Current baroclinic transport near 22°S: variability from the AX97 XBT
1825 transect. CLIVAR Exchanges 58(17), 5-10. doi: 10.1007/s10236-016-0959-6

1826 Matano, R.P. and Palma, E.D. (2008). On the upwelling of downwelling currents. J. Phys. Oceanogr.
1827 38(11), 2482-2500.

1828 Matano, R.P., Combes, V., Piola, A.R., Guerrero, R.A., Palma, E.D., Strub, P.T., et al. (2014). The
1829 salinity signature of the cross-shelf exchanges in the Southwestern Atlantic Ocean: Numerical
1830 simulations. J. Geophys. Res. Oceans 119, 7949–7968. doi: 10.1002/2014JC010116

1831 Maximenko, N., Niiler, P., Centurioni, L., Rio, M.-H. Melnichenko, O., Chambers, D., et al. (2009),
1832 Mean dynamic topography of the ocean derived from satellite and drifting buoy data using three
1833 different techniques. J. Atmos. Ocean. Tech., *26*(9), 1910-1919. doi: 10.1175/2009JTECHO672.1

1834 Mazzini, P.L.F., Barth, J.A., Shearman, R.K., Erofeev, A. (2014). Buoyancy-driven coastal currents
1835 off the Oregon coast during fall and winter. J. Phys. Oceanogr. 44, 2854-2876. doi: 10.1175/JPO-D-
1836 14-0012.1

1837 McClatchie, S. (2014). Regional Fisheries Oceanography of the California Current System: The
1838 CalCOFI program. Springer. doi: 10.1007/978-94-007-7223-6.

1839 McClatchie, S., Thompson, A. R., Alin, S. R., Siedlecki, S., Watson, W., Bograd, S. J (2016). The
1840 influence of Pacific Equatorial Water on fish diversity in the southern California Current System, J.
1841 Geophys. Res. Oceans 121. 6121-6136. doi:10.1002/2016JC011672.

1842 Meinen, C. S., Baringer, M. O., Garcia, R. F. (2010). Florida Current transport variability: An
1843 analysis of annual and longer-period signals. Deep Sea Res. I 57, 835-846.
1844 doi:10.1016/j.dsr.2010.04.001, 835-846

1845 Meinen, C.S., Garzoli, S.L., Perez, R.C., Campos, E., Piola, A.R., Chidichimo, M.P., et al. (2017).
1846 Characteristics and causes of Deep Western Boundary Current transport variability at 34.5° S during
1847 2009–2014. Ocean Science 13, 175-194. doi: 10.5194/os-13-175-2017

1848 Meinen, C.S., Johns, W.E., Garzoli, S.L., van Sebille, E., Rayner, D., Kanzow, T. et al. (2013).
1849 Variability of the deep Western Boundary Current at 26.5N during 2004-2009. Deep Sea Res. II 85,
1850 154-168. doi: 10.1016/j.dsr2.2012.07.036

1851 Meinen, C.S., Speich, S., Piola, A.R., Ansorge, I., Campos. E., Kersale, M., et al. (2018). Meridional
1852 Overturning Circulation transport variability at 34.5°S during 2009-2017: Baroclinic and barotropic

1853 flows and the dueling influence of the boundaries. Geophys. Res. Lett., 45(9):4810-4188, doi:
1854 10.1029/2018GL077408

1855 Meinen, C.S., and Watts, D.R. (2000). Vertical structure and transport on a transect across the North
1856 Atlantic Current near 42°N: Time series and mean. J. Geophys. Res. 105(C9), 21869–2189.
1857 doi:10.1029/2000JC900097

1858 Menna, M., Faye, S., Poulain, P.-M., Centurioni, L., Lazar, A., Gaye, A., et al. (2016). Upwelling
1859 features of the coast of north-western Africa in 2009-2013. Boll. Geofis. Teor. Appl. 57(1), 71-86.
1860 doi: 10.4430/bgta0164

1861 Messié, M., and Chavez, F.P. (2015). Seasonal regulation of primary production in eastern boundary
1862 upwelling systems. Prog. Oceanogr 134, 1-18. doi: 10.1016/j.pocean.2014.10.011

1863 Middleton, J.F. and Cirano, M. (2002). A Boundary Current along Australia's Southern Shelves: the
1864 Flinders Current. J. Geophys. Res. 107(C9), doi:10.1029/2000JC000701

1865 Middleton, J.F., Bye, J.T. (2007). A review of the shelf-slope circulation along Australia's southern
1866 shelves: Cape Leeuwin to Portland. Prog. Oceanogr. 75(1), 1-41.

1867 Mihanović, H., Pattiaratchi, C., Verspecht, F. (2016). Diurnal sea breezes force near-inertial waves
1868 along Rottnest continental shelf, southwestern Australia. J. Phys. Oceanogr. 46(11), 3487–3508. doi:
1869 10.1175/JPO-D-16-0022.1

1870 Mohrholz, V., Bartholomae, C.H., van der Plas, A.K., Lass, H.U. (2008). The seasonal variability of
1871 the northern Benguela undercurrent and its relation to the oxygen budget on the shelf. Continental Shelf
1872 Res., 28: 424-441

1873 Moloney, C.L., Van Der Lingen, C.D., Hutchings, L., Field, J.G. (2004). Contributions of the
1874 Benguela ecology programme to pelagic fisheries management in South Africa. African Journal of
1875 Marine Science, 26(1), 37-51.

1876 Monteiro P.M.S., van der Plas, A.K. (2006). Low oxygen water (LOW) variability in the Benguela
1877 system: Key processes and forcing scales relevant to forecasting. In: *Benguela: Predicting a Large*
1878 *Marine Ecosystem*. Shannon V et al. (eds). Elsevier, Amsterdam, Netherlands, pp. 71-90.

1879 Monteiro, P.M.S., van der Plas, A.K., Mélice, J.-L., Florenchie, P. (2008). Interannual hypoxia
1880 variability in a coastal upwelling system: Ocean–shelf exchange, climate and ecosystem-state
1881 implications. Deep Sea Res. I 55(4), 435-450. doi:10.1016/j.dsr.2007.12.010

1882 Mosquera-Vásquez, K., Dewitte, B., Illig, S, Takahashi, K., Garric, G. (2013). The 2002/2003 El
1883 Niño: Equatorial waves sequence and their impact on sea surface temperature. J. Geophys. Res.:
1884 Oceans 118(1), 346-357.

1885 Nagai, T., and Clayton, S. (2017). Nutrient interleaving below the mixed layer of the Kuroshio
1886 Extension Front. Ocean Dyn. 67(8), 1027-1046. doi: 10.1007/s10236-017-1070-3

1887 Nagano, A., Kizu, S., Hanawa, K., Roemmich, D. (2016). Heat transport variation due to change of
1888 North Pacific subtropical gyre interior flow during 1993–2012. Ocean Dynamics 66(12), 1637–1649.

1889 Nakamura, M., (2012). Impacts of SST anomalies in the Agulhas Current system on the regional
1890 climate variability. J. Climate 25(4),1213-1229. doi: 10.1175/JCLI-D-11-00088.1

1891 Nakano, H., Tsujino, H., Yasuda, M., Hirabara, T., Motoi, T., Ishii, M., Yamanaka, G. (2011).
1892 Uptake mechanisms of anthropogenic CO_2 in the Kuroshio Extension region in an ocean general
1893 circulation model. J. Oceanogr. 67, 765-783. doi:10.1007/s10872-011-0075-7

1894 Nakano, T., Kitamura, T., Sugimoto, S., Suga, T., Kamachi, M. (2015). Long-term variations of
1895 North Pacific Tropical Water along the 137°E repeat hydrographic section. J. Oceanography 71(3),
1896 229-238. doi: 10.1007/s10872-015-0279-3

1897 Nam, S., Kim, H.J., Send, U. (2011). Amplification of hypoxic and acidic events by La Nina
1898 conditions on the continental shelf off California. Geophys. Res. Lett. 38, L22602. doi:
1899 10.1029/2011gl049549

1900 Nguyen, L.T., and Molinari, J. (2012). Rapid intensification of a sheared, fast- moving hurricane over
1901 the Gulf Stream. Mon. Weather Rev., 140, 3361–3378. doi:10.1175/MWR-D-11-00293.1

1902 Niewiadomska, K., Claustre, H., Prieur, L., d'Ortenzio, F. (2008). Submesoscale physical-
1903 biogeochemical coupling across the Ligurian current (northwestern Mediterranean) using a bio-
1904 optical glider, Limnol. Oceanogr. 53, 2210-2225. doi: 10.4319/lo.2008.53.5_part_2.2210.

1905 Niiler, P.P. (2001). "The world ocean surface circulation," in Ocean Circulation and Climate, eds. G.
1906 Siedler, J. Church and J. Gould (Academic Press),193-204.

1907 Niiler, P.P., Maximenko, N.A., Panteleev, G.G., Yamagata, T., Olson, D.B. (2003), Near-surface
1908 dynamical structure of the Kuroshio Extension. J Geophys Res. 108(C6), 3193. doi:
1909 10.1029/2002JC001461

1910 Niiler, P.P., Sybrandy, A., Bi, K., Poulain, P. M., Bitterman, D. (1995). Measurements of the water-
1911 following capability of holey-sock and TRISTAR drifters. Deep Sea Res. I, 42, 1951-1964. doi:
1912 10.1016/0967-0637(95)00076-3

1913 Nkwinkwa Njouodo, A.S., Koseki, S., Keenlyside, N., Rouault, M. (2018). Atmospheric signature of
1914 the Agulhas Current. Geophys. Res. Lett. 45(10), 5185-5193. doi: 10.1029/2018GL077042

1915 Nowald, N., Iversen, M.H., Fischer, G., Ratmeyer, V., Wefer, G. (2015). Time series of in-situ
1916 particle properties and sediment trap fluxes in the coastal upwelling filament off Cape Blanc,
1917 Mauritania. Prog. Oceanogr. 137, 1-11.

1918 Nowald, N., Iversen, M.H., Fischer, G., Ratmeyer, V., Wefer, G. (2015). Time series of in-situ
1919 particle properties and sediment trap fluxes in the coastal upwelling filament off Cape Blanc,
1920 Mauritania. Progress in Oceanography. 137, 1-11.

1921 Oettli, P., Morioka, Y., Yamagata, T. (2016). A regional climate mode discovered in the North
1922 Atlantic: Dakar Niño/Niña. Sci. Rep. 6, 18782. doi: 10.1038/srep18782

1923 Ohman, M.D., Rudnick, D.L., Chekalyuk, A., Davis, R.E., Feely, R.A., Kahru, M., et al., (2013).
1924 Autonomous ocean measurements in the California Current Ecosystem. Oceanography 26, 18–25.

1925 Oka, E. and Kawabe, M. (2003). Dynamic Structure of the Kuroshio South of Kyushu in Relation to
1926 the Kuroshio Path Variations. J. Oceanogr. 59:5, 595-608. doi:
1927 10.1023/B:JOCE.0000009589.28241.93

1928 Oka, E., Ishii, M., Nakano, T., Suga, T., Kouketsu, S., Miyamoto, M., et al. (2018). Fifty years of the
1929 137E repeat hydrographic section in the western North Pacific Ocean. J. Oceanogr. 74, 115-145. doi:
1930 10.1007/s10872-017-0461-x

1931 Oka, E., Qiu, B., Takatani, Y., Enyo, K., Sasano, D., Kosugi, N., et al. (2015). Decadal variability of
1932 Subtropical Mode Water subduction and its impact on biogeochemistry. J. Oceanogr. 71, 389-400.
1933 doi: 10.1007/s10872-015-0300-x

1934 Oliveira L.R., Piola A.R., Mata, M.M., Soares, I.D. (2009). Brazil Current surface circulation and
1935 energetics observed from drifting buoys, J. Geophys. Res. 114, C10006. doi:10.1029/2008JC004900

1936 Oliver, E.C., Benthuysen, J.A., Bindoff, N.L., Hobday, A.J., Holbrook, N.J., Mundy, C.N., et al.
1937 (2017). The unprecedented 2015/16 Tasman Sea marine heatwave. Nat. Commun. 8, 16101. doi:
1938 10.1038/ncomms16101

1939 Oliver, E.C.J., O'Kane, T.J., Holbrook, N. J. (2015). Projected changes to Tasman Sea eddies in a
1940 future climate. Oceans 120, 7150–7165. doi: 10.1002/2015JC010993

1941 Olson, D., Podesta, G.P., Evans, R.H., Brown, O. (1988). Temporal variations in the separation of
1942 Brazil and Malvinas Currents. Deep Sea Res. 35, pp. 1971-1990. doi: 10.1016/0198-0149(88)90120-
1943 3

1944 O'Reilly, C. H. and Czaja, A. (2015). The response of the Pacific storm track and atmospheric
1945 circulation to Kuroshio Extension variability. Q.J.R. Meteorol. Soc. 141, 52-66. doi:10.1002/qj.2334

1946 O'Reilly, C.H., Minobe, S., Kuwano-Yoshida, A. (2016). The influence of the Gulf Stream on
1947 wintertime European blocking. Clim. Dynam. 47(5-6), 1545-1567. doi: 10.1007/s00382-015-2919-0

1948 Paduan, J. D., and Washburn, L. (2013). High-frequency radar observations of ocean surface
1949 currents. Annu. Rev. Mar. Sci. 5, 115–136, doi: 10.1146/annurev-marine-121211-172315

1950 Palacz, A.P., Pearlman, J., Simmons, S., Hill, K., Miloslavich, P., Telszewski, M., et al. (2017).
1951 Report of the workshop on the Implementation of Multi- disciplinary Sustained Ocean Observations
1952 (IMSOO). Global Ocean Observing System (GOOS) Report No. 223,
1953 http://www.goosocean.org/imsoo-report.

1954 Palevsky, H.I., and Nicholson, D.P. (2018). The North Atlantic biological pump: Insights from the
1955 Ocean Observatories Initiative Irminger Sea Array. Oceanography 31(1), 42-49.
1956 doi:10.5670/oceanog.2018.108

1957 Palevsky, H.I., and Quay, P.D. (2017). Influence of biological carbon export on ocean carbon uptake
1958 over the annual cycle across the North Pacific Ocean. Global Biogeochem. Cycles 31,1–15.
1959 doi:10.1002/2016GB005527

1960 Palevsky, H.I., Quay, P.D., Lockwood, D.E., Nicholson, D.P. (2016). The annual cycle of gross
1961 primary production, net community production, and export efficiency across the North Pacific Ocean.
1962 Global Biogeochem. Cycles 30(2), 361-380. doi:10.1002/2015GB005318

1963 Palter, J.B. and Lozier, M.S. (2008). On the source of Gulf Stream nutrients. J. Geophys. Res.
1964 113(C6), C06018. doi: 10.1029/2007jc004611

1965 Paniagua, G.F., Saraceno, M., Piola, A.R., Guerrero, R., Provost, C., Ferrari, R., et al. (2018).
1966 Malvinas Current at 40°S–41°S: First assessment of temperature and salinity temporal variability. J.
1967 Geophys. Res.: Oceans 123. doi: 10.1029/2017JC013666

1968 Park, J. and Sweet, W. (2015). Accelerated sea level rise and Florida Current transport, Ocean Sci.,
1969 11, 607-615, doi: 10.5194/os-11-607-2015

1970 Parks, A.B., Shay, L.K., Johns, W.E., Martinez-Pedraja, J., Gurgel, K.W. (2009). HF radar
1971 observations of small-scale surface current variability in the Straits of Florida. J. Geophys. Res. 114,
1972 C08002. doi: 10.1029/2008JC005025

1973 Parrilla, G., Neuer, S., Le Traon, P.-Y. (2002). Topical studies in oceanography: Canary Islands
1974 Azores Gibraltar Observations (CANIGO). Volume 1: Studies in the northern Canary Islands basin.
1975 Deep–Sea Res. II, 49, 3409-3413.

1976 Pattiaratchi, C., Hollings, B., Woo, M., Welhena, T. (2011). Dense shelf water formation along the
1977 south-west Australian inner shelf. Geophys. Res. Lett. 38, L10609. doi: 10.1029/2011GL046816

1978 Paulmier, A., Ruiz-Pino, D. (2009). Oxygen Minimum Zones (OMZs) in the Modern Ocean. Prog.
1979 Oceanogr., 80, p. 113-128, 2009

1980 Pearce A. and Feng, M. (2013). The rise and fall of the "marine heat wave" off Western Australia
1981 during the summer of 2010/11. J. Mar. Sys. 111-112, 139-156. doi: 10.1016/j.jmarsys.2012.10.009

1982 Pegliasco, C., Chaigneau, A., Morrow, R. (2015). Main eddy vertical structures observed in the four
1983 major Eastern Boundary Upwelling Systems. Oceans 120, 6008–6033. doi: 10.1002/2015JC010950.

1984 Pelegrí, J.L., and Csanady, G.T. (1991). Nutrient transport and mixing in the Gulf Stream. J.
1985 Geophys. Res. 96, 2577-2583. doi: 10.1029/90JC02535

1986 Pelegrí, J. L., Csanady, G. T., Martins, A. (1996), The North Atlantic nutrient stream, J.
1987 Oceanogr., 52, 275–299, doi: 10.1007/BF02235924.

1988 Pelland, N.A., Eriksen, C.C., Lee, C.M. (2013). Subthermocline eddies over the Washington
1989 continental slope as observed by Seagliders, 2003–09. J. Phys. Oceanogr. 43:2025–53.

1990 Perry, M.J., Sackmann, B.S., Eriksen, C.C., Lee, C.M. (2008). Seaglider observations of blooms and
1991 subsurface chlorophyll maxima off the Washington coast. Limnol. Oceanogr. 53, 2169-2179. doi:
1992 10.4319/lo.2008.53.5_part_2.2169

1993 Pickart, R.S., and Smethie, W.M. (1993), How does the Deep Western Boundary Current cross the
1994 Gulf Stream? J. Phys. Oceanogr. 23, 2602–2616. doi: 10.1175/1520-
1995 0485(1993)023<2602:HDTDWB>2.0.CO;2

1996 Pickart, R.S., and Watts, D.R. (1990), Deep Western Boundary Current variability at Cape Hatteras.
1997 J. Mar. Res. 48(4), 765–791. doi: 10.1357/002224090784988674

1998 Pietri, A., Echevin, V., Testor, P., Chaigneau, A., Mortier, L., Grados, C., et al. (2014). Impact of a
1999 coastal-trapped wave on the near-coastal circulation of the Peru upwelling system from glider data.
2000 Oceans 119, 2109–2120. doi: 10.1002/2013JC009270.

2001 Pietri, A., Testor, P., Echevin, V., Chaigneau, A., Mortier, L., Eldin, G., et al. (2013). Finescale
2002 vertical structure of the upwelling system off southern Peru as observed from glider data. J. Phys.
2003 Oceanogr. 43, 631–646. doi: 10.1175/JPO-D-12-035.1

2004 Pitcher, G.C., and Probyn, T.A. (2011). Anoxia in southern Benguela during the autumn of 2009 and
2005 its linkage to a bloom of the dinoflagellate *Ceratium balechii*. Harmful Algae 11, 23–32.

2006 Pitcher, G. C., Probyn, T.A., du Randt, A., Lucas, A.J., Bernard, S., Evers-King, H., et al. (2014).
2007 Dynamics of oxygen depletion in the nearshore of a coastal embayment of the southern Benguela
2008 upwelling system. J. Geophys. Res. Oceans 119, 2183–2200. doi: 10.1002/2013JC009443

2009 Pizarro, O., Ramírez, N., Castillo, M.I., Cifuentes, U., Rojas, W., Pizarro-Koch, M. (2016).
2010 Underwater glider observations in the oxygen minimum zone off central Chile. Bull. Amer. Meteor.
2011 Soc. 97, 1783–1789. doi: 10.1175/BAMS-D-14-00040.1

2012 Polo, I., Lazar, A., Rodriguez-Fonseca, B., Arnault, S. (2008). Oceanic Kelvin waves and tropical
2013 Atlantic intraseasonal variability: 1. Kelvin wave characterization. J. Geophys. Res. 113, C07009.
2014 doi: 10.1029/2007JC004495

2015 Pontes, G.M., Sen Gupta, A., Taschetto, A.S. (2016). Projected changes to South Atlantic boundary
2016 currents and confluence region in the CMIP5 models: the role of wind and deep ocean changes.
2017 Environ. Res. Lett. 11(9), 094013. doi: 10.1088/1748-9326/11/9/094013

2018 Poulain, P.M., and Niiler, P.P. (1989), Statistical-analysis of the surface circulation in the California
2019 Current System using satellite-tracked drifters. J. Phys. Oceanogr. 19(10), 1588-1603. doi:
2020 10.1175/1520-0485(1989)019<1588:SAOTSC>2.0.CO;2

2021 Probyn, T.A., Mitchellinnes, B.A., Brown, P.C., Hutchings, L., Carter, R.A. (1994). Review of
2022 primary production and related processes on the Agulhas-Bank. S. Afr. J. Sci. 90, 166-173.

2023 Qiu, B. and Chen, S. (2005). Variability of the Kuroshio Extension Jet, Recirculation Gyre, and
2024 Mesoscale Eddies on decadal time scales. J. Phys. Oceanogr., 35, 2090-2103. doi:
2025 10.1175/JPO2807.1

2026 Qiu, B., and Chen, S. (2010). Interannual-to-decadal variability in the bifurcation of the North
2027 Equatorial Current off the Philippines. J. Phys. Oceanogr. 40, 2525-2538. doi:
2028 10.1175/2010JPO4462.1

2029 Qiu, B., Chen, S., Schneider, N., Taguchi, B. (2014). A coupled decadal prediction of the dynamic
2030 state of the Kuroshio Extension System. J. Climate, 27, 1751-1764. doi: 10.1175/JCLI-D-13-00318.1

2031 Rainville, L., Lee, C.M., Rudnick, D.L., Yang, K.-C. (2013). Propagation of internal tides generated
2032 near Luzon Strait: Observations from autonomous gliders. J. Geophys. Res. 118(9), 4125-4138. doi:
2033 10.1002/jgrc.20293

2034 Reum, J. C. , Alin, S. R., Feely, R. A., Newton, J., Warner, M., McElhany, P. (2014). Seasonal
2035 carbonate chemistry covariation with temperature, oxygen, and salinity in a fjord estuary:
2036 implications for the design of ocean acidification experiments. PLoS ONE 9, e89619. doi:
2037 10.1371/journal.pone.0089619

2038 Reum, J.C.P., Alin, S.R., Harvey, C.J., Bednaršek, N., Evans, W., Feely, R.A., et al. (2016).
2039 Interpretation and design of ocean acidification experiments in upwelling systems in the context of
2040 carbonate chemistry co-variation with temperature and oxygen. ICES Journal of Marine Science
2041 73(3), 582-595. doi: 10.1093/icesjms/fsu231

2042 Révelard, A., Frankignoul, C., Sennéchael, N., Kwon, Y.O., Qiu, B. (2016). Influence of the decadal
2043 variability of the Kuroshio Extension on the atmospheric circulation in the cold season. J. Climate
2044 29(6), 2123-2144. doi: 10.1175/JCLI-D-15-0511.1

2045 Richardson, P.L. (2007). Agulhas leakage into the Atlantic estimated with subsurface floats and
2046 surface drifters. Deep Sea Res. I 54(8), 1361-1389. doi: 10.1016/j.dsr.2007.04.010

2047 Richter, I. (2015). Climate model biases in the eastern tropical oceans: causes, impacts and ways
2048 forward. WIREs Clim. Change, 6, 345-358.

2049 Ridgway, K.R. and Condie, S.A. (2004). The 5500-km-long boundary flow off western and southern
2050 Australia. J. Geophys. Res. 109(C4). doi: 10.1029/2003JC001921

2051 Ridgway, K.R. and Godfrey, J.S. (2015). The source of the Leeuwin Current seasonality. J. Geophys.
2052 Res. 120(10).6843-6864. doi: 10.1002/2015JC011049

2053 Rio, M.-H., Mulet, S., Picot, N. (2014). Beyond GOCE for the ocean circulation estimate: Synergetic
2054 use of altimetry, gravimetry, and in situ data provides new insight into geostrophic and Ekman
2055 currents. Geophys. Res. Lett. 41, 8918–8925. doi: 10.1002/2014GL061773

2056 Rio, M.H., and Santoleri, R. (2018). Improved global surface currents from the merging of altimetry
2057 and Sea Surface Temperature data. Remote Sens. Environ. 216, 770-785. doi:
2058 10.1016/j.rse.2018.06.003

2059 Riser, S.C., Freeland, H.J., Roemmich, D., Wijffels, S., Troisi, A., Belbéoch, M., et al. (2016).
2060 Fifteen years of ocean observations with the global Argo array. Nat. Clim. Change 6(2), 145–153.
2061 doi:10.1038/nclimate2872

2062 Rodgers, K.B., Sarmiento, J.L., Crevoisier, C., de Boyer Montegut,C. , Metzl, N., Aumont, O.
2063 (2008). A wintertime uptake window for anthropogenic CO_2 in the North Pacific. Global
2064 Biogeochem. Cycles 22, GB2020. doi: 10.1029/2006GB002920

2065 Rodrigues, R.R., Rothstein, L.M., Wimbush, M. (2007). Seasonal variability of the South Equatorial
2066 Current bifurcation in the Atlantic Ocean: A numerical study. J. Phys. Oceanogr. 37(1),16-30. doi:
2067 10.1175/JPO2983.1

2068 Roemmich, D., Boehme, L., Claustre, H., Freeland, H., Fukasawa, M., Goni, G., et al. (2010).
2069 "Integrating the Ocean Observing System: Mobile Platforms" in Proceedings of OceanObs'09:
2070 Sustained Ocean Observations and Information for Society (Vol. 1), Venice, Italy, 21-25 September
2071 2009, Hall, J., Harrison, D.E. & Stammer, D., Eds., ESA Publication WPP-306,
2072 doi:10.5270/OceanObs09.pp.33

2073 Roemmich, D., Alford, M., Claustre, H., Johnson, K., King, B., Moum, J., et al. (2019). On the future
2074 of Argo: An enhanced global array of physical and biogeochemical sensing floats. Front. Mar. Sci.,
2075 submitted.

2076 Rossby, H.T., Flagg, C.N., Donohue, K. (2010). On the variability of Gulf Stream transport from
2077 seasonal to decadal timescales, J. Mar. Res. 68(3–4), 503–522. doi:10.1357/002224010794657128

2078 Rossby, T., Flagg, C.N., Donohue, K., Sanchez-Franks, A., Lillibridge, J. (2014). On the long-term
2079 stability of Gulf Stream transport based on 20 years of direct measurements. Geophys. Res. Lett. 41,
2080 114–120. doi:10.1002/2013GL058636

2081 Rouault, M., Reason, C.J.C, Lutjeharms, J.R.E., Beljaars, A.C.M. (2003). Underestimation of latent
2082 and sensible heat fluxes above the Agulhas Current in NCEP and ECMWF analyses. J. Climate 16,
2083 776–782.

2084 Roughan, M. and Morris, B.D. (2011). Using high-resolution ocean timeseries data to give context to
2085 long term hydrographic sampling off Port Hacking, NSW, Australia. Proceedings Oceans'11
2086 MTS/IEEE Kona USA. doi**:** 10.23919/OCEANS.2011.6107032

2087 Roughan, M., Schaeffer, A., Kioroglou, S. (2013). Assessing the design of the NSW-IMOS Moored
2088 Observation Array from 2008-2013: Recommendations for the future. 2013 OCEANS - San Diego,
2089 San Diego, CA, 2013, pp. 1-7. doi: 10.23919/OCEANS.2013.6741092

2090 Roughan, M., Schaeffer, A., Suthers, I.M. (2015). Sustained Ocean Observing along the Coast of
2091 Southeastern Australia: NSW-IMOS 2007-2014, in Coastal Ocean Observing Systems, pp. 76 – 98.
2092 doi: 10.1016/B978-0-12-802022-7.00006-7

2093 Rudnick, D. (2016a). Data from: California Underwater Glider Network.Instrument Development
2094 Group, Scripps Institution of Oceanography. doi: 10.21238/s8SPRAY1618

2095 Rudnick, D. L. (2016b). Ocean research enabled by underwater gliders. Annu. Rev. Mar. Sci. 8, 519-
2096 541. doi: 10.1146/annurev-marine-122414-033913

2097 Rudnick, D. (2017). Data from: Spray underwater glider campaign in Gulf of Mexico.Instrument
2098 Development Group, Scripps Institution of Oceanography. doi: 10.21238/s8SPRAY0420

2099 Rudnick, D. L., and Cole, S.T. (2011). On sampling the ocean using underwater gliders. J. Geophys.
2100 Res. 116, C08010. doi: 10.1029/2010JC006849

2101 Rudnick, D.L., Gopalakrishnan, G., Cornuelle, B.D. (2015b). Cyclonic eddies in the Gulf of Mexico:
2102 observations by underwater gliders and simulations by numerical model. J. Phys. Oceanogr. 45(1),
2103 313-326. doi: 10.1175/JPO-D-14-0138.1

2104 Rudnick, D. L., Jan, S., Centurioni, L., Lee, C., Lien, R.-C., Wang, J., et al. (2011). Seasonal and
2105 mesoscale variability of the Kuroshio near its origin. Oceanography 24, 52-63. doi:
2106 10.5670/oceanog.2011.94

2107 Rudnick, D.L., Jan, S., Lee, C.M. (2015a). A new look at circulation in the western North Pacific.
2108 Oceanography 28, 16-23. doi: 10.5670/oceanog.2015.77

2109 Rudnick, D.L., Johnston, T.M., Sherman, J.T. (2013). High-frequency internal waves near the Luzon
2110 Strait observed by underwater gliders. J. Geophys. Res.: Oceans 118(2), 774-784. doi:
2111 10.1002/jgrc.20083

2112 Rudnick, D. L., Zaba, K.D., Todd, R.E., Davis, R.E. (2017). A climatology of the California Current
2113 System from a network of underwater gliders. Prog. Oceanogr. 154, 64-106.
2114 doi:10.1016/j.pocean.2017.03.002.

2115 Rühs, S., K. Getzlaff, J. V. Durgadoo, A. Biastoch, and C. W. Böning (2015). On the suitability of
2116 North Brazil Current transport estimates for monitoring basin-scale AMOC changes, Geophys. Res.
2117 Lett., 42, 8072–8080, doi: 10.1002/2015GL065695.

2118 Ryan, J.P., Ueki, I.., Chao, Y., Zhang, H., Polito, P.S., Chavez, F.P. (2006). Western Pacific
2119 modulation of large phytoplankton blooms in the central and eastern equatorial Pacific. J. Geophys.
2120 Res. 111, G02013. doi: 10.1029/2005JG000084.

2121 Rypina, I.I., Llopiz, J.K., Pratt, L.M., Lozier, M.S. (2014). Dispersal pathways of American eel
2122 larvae from the Sargasso Sea. Limnol. Oceanogr. 59(5), 1704-1714. doi: 10.4319/lo.2014.59.5.1704

2123 Saba, V.S., Griffies, S.M., Anderson, W.G., Winton, M., Alexander, M.A., Delworth, T.L., et al.
2124 (2016). Enhanced warming of the Northwest Atlantic Ocean under climate change. J. Geophys. Res.
2125 121(1), 118–132. doi: 10.1002/2015JC011346

2126 Sainz-Trapaga S., Goni, G., Sugimoto, T. (2001). Identification of the Kuroshio Extension, its
2127 bifurcations and northern branch from altimeter and hydrographic Data During October 1992 -
2128 August 1999: Spatial and temporal variability. Geophys. Res. Lett. 28(9), 1759-1762. doi:
2129 10.1029/2000GL012323

2130 Saraceno, M., Guerrero, R., Piola, A., Provost, C., Perault, F., Ferrari, R., et al. (2017). Malvinas
2131 Current 2014-2015: Mooring velocities. SEANOE. doi: 10.17882/51492

2132 Schaeffer, A., Gramoulle, A., Roughan, M., Mantovanelli, A. (2017). Characterizing frontal eddies
2133 along the East Australian Current from HF radar observations. J. Geophys. Res.122, 3964–3980. doi:
2134 10.1002/2016JC012171

2135 Schaeffer, A., Roughan, M., Morris, B. (2013). Cross-shelf dynamics in a Western Boundary
2136 Current. Implications for Upwelling. J. Phys. Oceanogr. 43, 1042-1059. doi: 10.1175/JPO-D-12-
2137 0177.1

2138 Schaeffer, A., Roughan, M. & Morris, B. 2014. CORRIGENDUM. J. Phys. Oceanogr. 44, 2812–
2139 2813. doi: 10.1175/JPO-D-14-0091.1

2140 Schaeffer, A., Roughan, M. (2015) Influence of a Western Boundary Current on shelf dynamics and
2141 upwelling from repeat glider deployments. Geophys. Res. Lett. 42, 121-128,
2142 doi:10.1002/2014GL062260.

2143 Schaeffer, A., Roughan, M., Jones, E.M., White, D. (2016a). Physical and biogeochemical spatial
2144 scales of variability in the East Australian Current separation from shelf glider measurements.
2145 Biogeosciences 13, 1967-1975. doi: 10.5194/bg-13-1967-2016

2146 Schaeffer, A. M. Roughan, T. Austin, J.D. Everett, D. Griffin, B. Hollings, E., et al. (2016b). Mean
2147 hydrography on the continental shelf from 26 repeat glider deployments along Southeastern
2148 Australia. Sci. Data 3, 160070 doi: 10.1038/sdata.2016.70

2149 Schaeffer, A., Roughan, M. (2017). Subsurface intensification of marine heatwaves off southeastern
2150 Australia: The role of stratification and local winds. Geophys. Res. Lett. 44, 5025-5033. doi:
2151 10.1002/2017GL073714

2152 Schmid, C. and Majumder S. (2018). Transport variability of the Brazil Current from observations
2153 and a data assimilation model. Ocean Sci. 14, 417-436. doi: 10.5194/os014-417-2018

2154 Schneider, W., Donoso, D., Garcés-Vargas, J., Escribano, R. (2016). Water-column cooling and sea
2155 surface salinity increase in the upwelling region off central-south Chile driven by a poleward
2156 displacement of the South Pacific. Prog. Oceanogr. 141, 38-58. doi: 10.1016/j.pocean.2016.11.004

2157 Schönau, M C., and Rudnick, D.L. (2017). Mindanao Current and Undercurrent: Thermohaline
2158 structure and transport from repeat glider observations. J. Phys. Oceanogr. 47(8), 2055-2075. doi:
2159 10.1175/JPO-D-16-0274.1

2160 Schönau, M.C., Rudnick, D.L., Cerovecki, I., Gopalakrishnan, G., Cornuelle, B.D. McClean, J.L. et
2161 al. (2015). The Mindanao Current: Mean structure and connectivity. Oceanography 28, 34–45. doi:
2162 10.5670/oceanog.2015.79

2163 Schott, F., Dengler, M., Zantopp, R.J., Stramma, L., Fischer, J., Brandt, P. (2005). The shallow and
2164 deep western boundary circulation of the South Atlantic at 5°-11°S. J. Phys. Oceanogr. 35, 2031-
2165 2053. doi: 10.1175/JPO2813.1

2166 Schott, F.A., Fischer, J., Stramma, L. (1998), Transports and pathways of the upper-layer circulation
2167 in the western tropical Atlantic. J. Phys. Oceanog., **28**(10), pp. 1904-1928.

2168 Schott, F., Xie, S.-P., McCreary, J.P. (2009). Indian Ocean circulation and climate variability. Rev.
2169 Geophys., 47, RG1002, doi:10.1029/2007RG000245

2170 Send, U. (2018). Data from: Spray glider data in support of mooring observations from the CORC
2171 project in the California Current starting 2007. Instrument Development Group, Scripps Institution of
2172 Oceanography. doi: 10.21238/s8SPRAY8857

2173 Send, U., Davis, R.E., Fischer, J., Imawaki, S., Kessler, W., Meinen, C., et al. (2010).” A global
2174 boundary current circulation observing network,” in Proceedings of OceanObs’09: Sustained Ocean
2175 Observations and Information for Society, vol. 2, eds. J. Hall, D. E. Harrison, D. Stammer (ESA
2176 Publication WPP-306, Venice, Italy). doi: 10.5270/OceanObs09.cwp.78

2177 Send, U., Regier, L., Jones, B. (2013). Use of underwater gliders for acoustic data retrieval from
2178 subsurface oceanographic instrumentation and bidirectional communication in the deep ocean. J.
2179 Atmos. Oceanic Technol. 30(5), 984-998. doi: 10.1175/JTECH-D-11-00169.1

2180 Sen Gupta, A., Ganachaud, A., McGregor, S., Brown, J.N., Muir, L. (2012). Drivers of the projected
2181 changes to the Pacific Ocean equatorial circulation. Geophys. Res. Lett. 39(9), L09605.
2182 doi:10.1029/2012GL051447

2183 Shannon, L.V., and Nelson, G. (1996). The Benguela: large-scale features and processes and system
2184 variability. In: Wefer G, Berger WH, Seidler G, Webb DJ (eds). *The South Atlantic: present and past*
2185 *circulation*. Berlin: Springer-Verlag pp. 163-210.

2186 Shinoda, A., Aoyama, J., Miller, M. J., Otake, T. Mochioka, N., Watanabe, S., et al. (2011)
2187 Evaluation of the larval distribution and migration of the Japanese eel in the western North Pacific.
2188 Rev. Fish. Biol. Fisher. 21(3), 591-611. doi: 10.1007/s11160-010-9195-1

2189 Siedlecki, S.A., Kaplan, I.C., Hermann, A.J., Nguyen, T.T., Bond, N.A., Newton, J.A., et al. (2016).
2190 Experiments with Seasonal Forecasts of ocean conditions for the Northern region of the California
2191 Current upwelling system. Scientific Reports 6, 27203.

2192 Silva, N., Rojas, N., Fedele, A. (2009). Water masses in the Humboldt Current System: Properties,
2193 distribution, and the nitrate deficit as a chemical water mass tracer for Equatorial Subsurface Water
2194 off Chile. Deep Sea Res. Part II: Topical Studies in Oceanography 56(16), 1004-1020. doi:
2195 10.1016/j.dsr2.2008.12.013

2196 Siqueira, L., and B. P. Kirtman (2016), Atlantic near-term climate variability and the role of a
2197 resolved Gulf Stream, Geophys. Res. Lett., 43, 3964–3972, doi: 10.1002/2016GL068694

2198 Slangen, A.B.A., Carson, M., Katsman, C.A. et al. (2014) Projecting twenty-first century regional
2199 sea-level changes Clim. Change 124: 317. doi: 10.1007/s10584-014-1080-9

2200 Sloyan, B.M. and O'Kane, T.J. (2015). Drivers of decadal variability in the Tasman Sea. J. Geophys.
2201 Res. 120, 3193-3210. doi:10.1002/2014JC010550

2202 Sloyan, B.M., Ridgway, K., Cowley, R. (2016). The East Australian Current and property transport at
2203 27^{o}S from 2012-2013. J. Phys. Oceanogr. 46, 993–1008. doi: 10.1175/JPO-D-15-0052.1

2204 Smeed, D.A., Josey, S.A., Beaulieu, C., Johns, W.E., Moat, B.I., Frajka-Williams, E. et al. (2018).
2205 The North Atlantic Ocean is in a state of reduced overturning. Geophys. Res. Lett., 45(3), 1527-1533.
2206 doi: 10.1002/2017GL076350

2207 Smith, L.M., Barth, J.A., Kelley, D.S., Plueddemann, A., Rodero, I., Ulses, G.A., et al. (2018). The
2208 Ocean Observatories Initiative, Oceanography 31(1), 16–35. doi: 10.5670/oceanog.2018.105.

2209 Smith, N., Kessler, W.S., Cravatte, S.E., Sprintall, J., Wijffels, S.E., Cronin, M.F., et al., Tropical
2210 Pacific Observing System, Front. Mar. Sci. 6:31. doi: 10.3389/fmars.2019.00031

2211 Soh, H.S., and Kim, S.Y. (2018). Diagnostic characteristics of submesoscale coastal surface currents.
2212 J. Geophys. Res. 123, 1838–1859. doi: 10.1002/2017JC013428

2213 Song H., Edwards, C.A., Moore, A.M., Fiechter, J. (2012). Incremental four-dimensional variational
2214 data assimilation of positive-definite oceanic variables using a logarithm transformation. Ocean
2215 Model. 54–55, 1-17. doi: 10.1016/j.ocemod.2012.06.001

2216 Spadone, A. and Provost C. (2009). Variations in the Malvinas Current volume transport since
2217 October 1992. J. Geophys. Res. 114, C02002. doi: 10.1029/2008JC004882

2218 St. Laurent, L., and Merrifield, S. (2017). Measurements of near-surface turbulence and mixing from
2219 autonomous ocean gliders. Oceanography 30(2):116–125. doi: 10.5670/oceanog.2017.231

2220 Steinfeldt, R., Sültenfuß, J., Dengler, M., Fischer, T., Rhein, M. (2015). Coastal upwelling off Peru
2221 and Mauritania inferred from helium isotope disequilibrium. Biogeosciences 12, 7519-7533.
2222 doi:10.5194/bg-12-7519-2015

2223 Strub, P.T., James, C., Combes, V., Matano, R., Piola, A., Palma, E., et al. (2015). Altimeter-derived
2224 seasonal circulation on the SW Atlantic Shelf: 27° – 43°S. J. Geophys. Res. Oceans 120, 3391–3418.
2225 doi:10.1002/2015JC010769

2226 Stuart-Smith, R.D., Brown, C.J., Ceccarelli, D.M., Edgar, G.J. (2018). Ecosystem restructuring along
2227 the Great Barrier Reef following mass coral bleaching. Nature 560, 92–96. doi: 10.1038/s41586-018-
2228 0359-9

2229 Subramanian, A.C., Balmaseda, M.A., Chattopadhyay, R., Centurioni, L., Cornuelle, B., DeMott, C.,
2230 et al. (2019). Ocean observations to improve our understanding, modeling, and forecasting of
2231 subseasonal-to-seasonal variability. Front. Mar. Sci., submitted.

2232 Sugimoto, S. and Hanawa, K. (2014). Influence of Kuroshio path variation south of Japan on
2233 formation of subtropical mode water. J. Phys. Oceanogr., 44(4), pp.1065-1077

2234 Sun, X., Vizy, E.K.; Cook, K.H. (2018). Land-atmosphere-ocean interactions in the southeastern
2235 Atlantic: interannual variability. Clim. Dynam. doi: 10.1007/s00382-018-4155-x

2236 Suthers, I.M, Young, J.W., Baird, M.E., Roughan, M., Everett, J.E., Brassington, G.B., et al. (2011).
2237 The strengthening East Australian Current, its eddies and biological effects — an introduction and
2238 overview. Deep Sea Res. 58(5), 538-546. doi: 10.1016/j.dsr2.2010.09.029

2239 Sutton, A.J., Sabine, C.L., Maenner-Jones, S., Lawrence-Slavas, N., Meinig, C., Feely, R.A., et al.
2240 (2014). A high-frequency atmospheric and seawater pCO_2 data set from 14 open-ocean sites using a
2241 moored autonomous system. Earth Syst. Sci. Data 6, 353-366. doi: 10.5194/essd-6-353-2014

2242 Sutton, A.J., Sabine, C.L., Feely, R.A., Cai, W.-J., Cronin, M.F., McPhaden, M.J et al. (2016). Using
2243 present-day observations to detect when anthropogenic change forces surface ocean carbonate
2244 chemistry outside preindustrial bounds. Biogeosciences 13(17), 5065-5083. doi:10.5194/bg-2016-
2245 104

2246 Sutton, A.J., Wanninkhof, R., Sabine, C.L., Feely, R.A., Cronin, M.F., R.A. Weller (2017).
2247 Variability and trends in surface seawater pCO2 and CO2 flux in the Pacific Ocean. Geophys. Res.
2248 Lett. 44(11), 5627–5636. doi: 10.1002/2017GL073814

2249 Swart, S., Speich, S., Ansorge, I.J., Goni, G.J., Gladyshev, S., Lutjeharms, J.R.E. (2008). Transport
2250 and variability of the Antarctic Circumpolar Current south of Africa. J. Geophys. Res. 113(C9),
2251 C09014. doi:10.1029/2007JC004223

2252 Takahashi, T., Sutherland, S..C., Wanninkhof, R., Sweeney, C., Feely, R.A., Chipman, D.W. et al..
2253 (2009), Climatological mean and decadal change in surface ocean pCO_2, and net sea-air CO_2 flux
2254 over the global oceans, Deep Sea Res. II, 56, 554-577.

2255 Talley, L.D., Feely, R.A., Sloyan, B.M., Wanninkhof, R., Baringer, M.O., Bulliser, J.L., et al. (2016).
2256 Changes in ocean heat, carbon content, and ventilation: A review of the first decade of GO-SHIP
2257 global repeat hydrography. Ann. Rev. Mar. Sci. 8, 185-215. doi: 10.1146/annurev-marine-052915-
2258 100829

2259 Tchipalanga, P., Dengler, M., Brandt, P., Kopte, R., Macuéria, M., Coelho, P., et al. (2018). Eastern
2260 boundary circulation and hydrography off Angola – building Angolan oceanographic capacities.
2261 Bull. Amer. Meteor. Soc. 99, 1589-1605. doi: 10.1175/BAMS-D-17-0197.1

2262 Testor et al. (2019). OceanGliders: a component of the integrated GOOS. Front. Mar. Sci., submitted.

2263 Thomsen, S., Karstensen, J., Kiko, R., Krahmann, G., Dengler, M., Engel, A. (2019). Remote and
2264 local drivers of oxygen and nitrate variability in the shallow oxygen minimum zone off Mauritania in
2265 June 2014. Biogeosciences 16, 979-998. doi:10.5194/bg-16-979-2019

2266 Thompson, J.D., and Schmitz, W.J. Jr. (1989). A limited-area model of the Gulf Stream: Design,
2267 initial experiments, and model-data intercomparison, J. Phys. Oceanogr. 19(6), 791–814. doi:
2268 10.1175/1520-0485(1989)019⟨0791:ALAMOT⟩2.0.CO;2

2269 Todd, R.E. (2017). High-frequency internal waves and thick bottom mixed layers observed by gliders
2270 in the Gulf Stream. Geophys. Res. Lett. 44(12), 6316-6325. doi:10.1002/2017GL072580

2271 Todd, R.E., Asher, T.G., Heiderich, J., Bane, J.M., Luettich, R.A. (2018b). Transient response of the
2272 Gulf Stream to multiple hurricanes in 2017. Geophys. Res. Lett., 45(19), 10,509-10,519. doi:
2273 10.1029/2018GL079180

2274 Todd, R.E., Gawarkiewicz, G.G., Owens, W.B. (2013). Horizontal scales of variability over the
2275 Middle Atlantic Bight shelf break and continental rise from finescale observations. J. Phys.
2276 Oceanogr. 43(1), 222-230. doi:10.1175/JPO-D-12-099.1

2277 Todd, R.E. and Locke-Wynn, L. (2017). Underwater glider observations and the representation of
2278 western boundary currents in numerical models. Oceanography, 30(2), 88-89.
2279 doi:10.5670/oceanog.2017.225

2280 Todd, R.E., and Owens, B. (2016). Data from: Gliders in the Gulf Stream. Instrument Development
2281 Group, Scripps Institution of Oceanography. doi: 10.21238/s8SPRAY2675

2282 Todd, R.E., Owens, W.B., Rudnick, D.L. (2016). Potential vorticity structure in the North Atlantic
2283 western boundary current from underwater glider observations. J. Phys. Oceanogr. 46(1):327-348.
2284 doi: 10.1175/JPO-D-15-0112.1

2285 Todd, R.E., Rudnick, D.L., Centurioni, L.R., Jayne, S.R., Lee, C.M. (2018a). "Boundary current
2286 observations with ALPS," in ALPS II—Autonomous and Lagrangian Platforms and Sensors. A
2287 Report of the ALPS II Workshop, eds. D. Rudnick, D. Costa, C. Lee, M.-L. Timmermans.

2288 Todd, R.E., Rudnick, D.L., Mazloff, M.R., Cornuelle, B.D., Davis, R.E. (2012). Thermohaline
2289 structure in the California Current System: observations and modeling of spice variance, J. Geophys.
2290 Res. 117, C02008. doi:10.1029/2011JC007589

2291 Todd, R.E., Rudnick, D.L., Davis, R.E., Ohman, M.D. (2011a). Underwater gliders reveal rapid
2292 arrival of El Niño effects off California's coast. Geophys. Res. Lett., 38, L03609. doi:
2293 10.1029/2010GL046376

2294 Todd, R.E., Rudnick, D.L., Mazloff, M.R., Davis, R.E., Cornuelle, B.D. (2011b). Poleward flows in
2295 the southern California Current System: Glider observations and numerical simulation. J. Geophys.
2296 Res. 116, C02026. doi:10.1029/2010JC006536

2297 Todd, R.E., Rudnick, D.L., Sherman, J.T., Owens, W.B., George, L. (2017). Absolute velocity
2298 estimates from autonomous underwater gliders equipped with Doppler current profilers. J. Atmos.
2299 Oceanic Technol. 34(2), 309-333. doi:10.1175/JTECH-D-16-0156.1

2300 Toole, J. M., Andres, M., Le Bras, I. A., Joyce, T. M., McCartney, M. S. (2017). Moored
2301 observations of the Deep Western Boundary Current in the NW Atlantic: 2004–2014. Oceans 122,
2302 7488–7505. doi: 10.1002/2017JC012984

2303 Trowbridge, J., Weller, R., Kelley, D., Dever, E., Plueddemann, A., Barth, J.A., Kawka, O. (2019).
2304 The Ocean Observatories Inititiative. Front. Mar. Sci. 6:74. doi: 10.3389/fmars.2019.00074

2305 Valdivieso, M., Haines, K., Balmaseda, M., Chang, Y.-S., Drevillon, M., Ferry, N., et al. (2017). An
2306 assessment of air–sea heat fluxes from ocean and coupled reanalyses, Clim 49, 983. doi:
2307 10.1007/s00382-015-2843-3

2308 Valla, D., and Piola, A.R. (2015). Evidence of upwelling events at the northern Patagonian shelf
2309 break. J. Geophys. Res.: Oceans 120(11), 7635-7656.

2310 Valla, D., Piola, A.R., Meinen, C.S., Campos, E. (2018). Strong mixing and recirculation in the
2311 northwestern Argentine Basin. J. Geophys. Res.: Oceans 123, 4624–4648. doi:
2312 10.1029/2018JC013907

2313 Van der Lingen, C. D., P. Fréon, L. Hutchings, C. Roy, G. W. Bailey, C. Bartholomae, A. C., et al.
2314 (2006), Forecasting shelf processes of relevance to living marine resources in the BCLME, in
2315 Benguela: Predicting a Large Marine Ecosystem, Large Mar. Ecosyst. Ser., vol. 14, edited by V.
2316 Shannon et al., pp. 309–347, Elsevier, Amsterdam, Netherlands.

2317 van Sebille, E., Beal, L.M., Biastoch, A. (2010), Sea surface slope as a proxy for Agulhas Current
2318 strength, Geophys. Res. Lett., 37, ISSN: 0094-8276

2319 van Sebille, E., Baringer, M.O., Johns, W.E.,. Meinen, C.S., Beal, L.M., de Jong, M.F., et al. (2011).
2320 Propagation pathways of classical Labrador Sea water from its source region to 26°N. J. Geophys.
2321 Res.,116, C12027. doi:10.1029/2011JC007171

van Sebille, E., Wilcox, C., Lebreton, L., Maximenko, N., Hardesty, B.D., Van Franekar, J.A., et al. (2015) A global inventory of small floating plastic debris. Environ. Res. Lett. 10:1088/1748-9326/10/12/124006

Van Uffelen, L.J., Roth, E.H., Howe, B.M., Oleson, E.M., Barkley, Y. (2017). A Seaglider-integrated digital monitor for bioacoustic sensing. IEEE J. Oceanic Eng. 42, 800-807. doi: 10.1109/JOE.2016.2637199

Vélez-Belchí, P., Centurioni, L.R., Lee, D.-K., Jan, S., Niiler, P.P (2013). Eddy induced Kuroshio intrusions onto the continental shelf of the East China Sea. J. Mar. Res. 71(1-2), 83-107. doi: 10.1357/002224013807343470

Vivier, F., and Provost, C. (1999). Direct velocity measurements in the Malvinas Current. J. Geophys. Res. 104(C9), 21083–21103. doi: 10.1029/1999JC900163

Volkov, D.L., Baringer, M., Smeed, D., Johns, W., Landerer, F. (2019). Teleconnection between the Atlantic Meridional Overturning Circulation and sea level in the Mediterranean Sea. J. Climate 32, 935-955. doi: 10.1175/JCLI-D-18-0474.1

Wada, A., Cronin, M.F., Sutton, A.J., Kawai, Y., Ishii, M. (2013) Numerical simulations of oceanic pCO_2 variations and interactions between Typhoon Choi-wan (0914) and the ocean. J. Geophys. Res.: Oceans 118, 2667-2684. doi: 10.1002/jgrc.20203

Wagawa T., Tamate, T., Kuroda, H., Ito, S., Kakehi, S., Yamanome, T., Kodama, T. (2016). Relationship between coastal water properties and adult return of chum salmon (Oncorhynchus keta) along the Sanriku coast, Japan. Fish. Oceangr., 25, 598-609. doi:10.1111/fog.12175

Wakita, M., Watanabe, S., Murata, A., Tsurushima, N., Honda, M. (2010). Decadal change of dissolved inorganic carbon in the subarctic western North Pacific Ocean. Tellus B 62:5, 608-620. doi: 10.1111/j.1600-0889.2010.00476.x

Wang, D., Flagg, C.N., Donohue, K., Rossby, H.T. (2010) Wavenumber spectrum in the Gulf Stream from shipboard ADCP observations and comparison with altimetry measurements. J. Phys. Oceanogr. 40, 840–844. doi: 10.1175/2009JPO4330.1

Wang F., Zhang, L., Hu, D., Wang, Q., Zhai, F., Hu, S. (2017). The vertical structure and variability of the western boundary currents east of the Philippines from direct observations. J. Oceanogr. 73, 743–758. doi: 10.1007/s10872-017-0429-x

Weeks, S. J., Barlow, R., Roy, C., Shillington, F.A. (2006). Remotely sensed variability of temperature and chlorophyll in the southern Benguela: upwelling frequency and phytoplankton response. African J. Mar. Sci. 28(3-4), 493-509. doi: 10.2989/18142320609504201

Weller, R.A., Bigorre, S.P., Lord, J., Ware, J.D., Edson, J.B. (2012). A surface mooring for air–sea interaction research in the Gulf Stream. Part I: Mooring design and instrumentation. J. Atmos. Oceanic Technol. 29, 1363–1376. doi: 10.1175/JTECH-D-12-00060.1

Wijffels, S. E., Meyers, G., Godfrey, J.S. (2008), A 20-yr average of the Indonesian Throughflow: Regional currents and the interbasin exchange. J. Phys. Oceanogr., 38, 1965–1978, doi:10.1175/2008JPO3987.1

2360 Wilkinson, M.D., Dumontier, M., Aalbersberg, I.J., Appleton, G., Axton, M., Baak, A., et al., (2016).
2361 The FAIR guiding principles for scientific data management and stewardship. Sci. Data, 3, 160018.
2362 doi: 10.1038/sdata.2016.18

2363 Williams, R.G., McDonagh, E.L., Roussenov, V.M., Torres-Valdes, S., King, B., Sanders, R.,
2364 Hansell, D.A. (2011). Nutrient streams in the North Atlantic: Advective pathways of inorganic and
2365 organic nutrients. Global Biogeochem. Cycles, 25(GB4008). doi: 10.1029/2010GB003853

2366 Williams, R.G., Roussenov, V., Follows, M. J. (2006). Nutrient streams and their induction into the
2367 mixed layer. Global Biogeochem. Cycles, 20(1), GB1016. doi: 10.1029/2005gb002586

2368 Woo, L.M., and Pattiaratchi, C.B. (2008). Hydrography and water masses off the western Australian
2369 coast. Deep-Sea Res. I 55, 1090–1104. doi:10.1016/j.dsr.2008.05.005

2370 Wu, C-R., Chang, Y-L., Oey, L-Y., Chang, C-W. J., Hsin, Y-C. (2008). Air-sea interaction between
2371 tropical cyclone Nari and Kuroshio, Geophys. Res. Lett. 35(L12605). doi:10.1029/2008GL033942

2372 Wu, L., Cai, W., Zhang, L., Nakamura, H., Timmermann, A., Joyce, T., et al. (2012). Enhanced
2373 warming over the global subtropical western boundary currents. Nat. Clim. Change, 2(3), 161–166.
2374 doi: 10.1038/nclimate1353

2375 Wyatt, L.R. Mantovanelli, A., Heron, M.L., Roughan M., Steinberg, C.R. (2018). Assessment of
2376 surface currents measured with high-frequency phased-array radars in two regions of complex
2377 circulation IEEE, J. Oceanic Engineering. V43 (2) pp 484-505, doi: https://doi:
2378 10.1109/JOE.2017.2704165

2379 Yamamoto, A., Palter, J.B., Dufour, C O., Griffies, S.M., Bianchi, D., Claret, M., Galbraith, E.D.
2380 (2018). Roles of the ocean mesoscale in the horizontal supply of mass, heat, carbon and nutrients to
2381 the Northern Hemisphere subtropical gyres. J. Geophys. Res. doi: 10.1029/2018JC013969

2382 Yang, Y.J., Jan, S., Chang, M.-H., Wang, J., Mensah, V., Kuo, T.-H., et al. (2015). Mean structure
2383 and fluctuations of the Kuroshio east of Taiwan from in situ and remote observations. Oceanography
2384 28(4),74–83. doi: 10.5670/oceanog.2015.83

2385 Yang, H., Lohmann, G., Wei, W., Dima, M., Ionita, M., Liu, J. (2016). Intensification and poleward
2386 shift of subtropical western boundary currents in a warming climate. Oceans 121, 4928–4945. doi:
2387 10.1002/2015JC011513

2388 Yasuda, I. (2003). Hydrographic structure and variability in the Kuroshio-Oyashio transition area. J.
2389 Oceanogr. 59, 389–402. doi: 10.1023/A:1025580313836

2390 Yasunaka, S., Nojiri, Y., Nakaoka, S., Ono, T., Mukai, H., Usui, N. (2013). Monthly maps of sea
2391 surface dissolved inorganic carbon in the North Pacific: Basin-wide distribution and seasonal
2392 variation, J. Geophys. Res. Oceans 118, 3843– 3850. doi: 10.1002/jgrc.20279

2393 Yasunaka, S., Nojiri, Y., Nakaoka, S.-i., Ono, T., Whitney, F.A., Telszewski, M. (2014). Mapping of
2394 sea surface nutrients in the North Pacific: Basin-wide distribution and seasonal to interannual
2395 variability. J. Geophys. Res.: Oceans 119, 7756-7771. doi: 0.1002/2014JC010318

2396 Zaba, K.D., and Rudnick, D.L. (2016). The 2014–2015 warming anomaly in the Southern California
2397 Current System observed by underwater gliders. Geophys. Res. Lett. 43(3), 1241–1248. doi:
2398 10.1002/2015GL067550

2399 Zantopp, R., Fischer, J., Visbeck, M., Karstensen, J. (2017). From interannual to decadal: 17 years of
2400 boundary current transports at the exit of the Labrador Sea. J. Geophys. Res. Oceans 122, 1724–
2401 1748. doi: 10.1002/2016JC012271

2402 Zhang, D., Cronin, M.F., Lin, X., Inoue, R., Fassbender, A.J., Bishop, S.P., Sutton, A. (2017).
2403 Observing air-sea interaction in western boundary currents and their extension regions:
2404 Considerations for OceanObs'19, CLIVAR Variations 15(4), 23-30. doi: 10.5065/D6SJ1JB2

2405 Zhang, D., Msadek, R., McPhaden, M.J., Delworth, T. (2011). Multidecadal variability of the North
2406 Brazil Current and its connection to the Atlantic meridional overturning circulation. J. Geophys. Res.
2407 116(C4). doi: 10.1029/2010JC006812

2408 Zhang, J., Gilbert, D., Gooday, A.J., Levin, L., Naqvi, S.W.A., Middelburg, J.J., et al. (2010).
2409 Natural and human-induced hypoxia and consequences for coastal areas: synthesis and future
2410 development. Biogeosciences 7:1443-1467. doi:10.5194/bg-7-1443-2010

2411 Zhang L., Hu, D., Hu, S., Wang, F., Wang, F., Yuan, D. (2014). Mindanao Current/Undercurrent
2412 measured by a subsurface mooring, J. Geophys. Res. 119, 3617–3628. doi: 10.1002/2013JC009693

2413 Zhang, S., Curchitser, E.N., Kang, D., Stock, C.A., Dussin, R. (2018). Impacts of mesoscale eddies
2414 on the vertical nitrate flux in the Gulf stream region. J. Geophys. Res. 123, 497–513. doi:
2415 10.1002/2017JC013402

2416 Zhang, W.G. and Gawarkiewicz, G.G. (2015). Dynamics of the direct intrusion of Gulf Stream ring
2417 water onto the Mid-Atlantic Bight shelf. Geophys. Res. Lett. 42, 7687–7695.
2418 doi:10.1002/2015GL065530

2419 Zhang, W. G., and Partida, J. (2018). Frontal subduction of the Mid-Atlantic Bight shelf water at the
2420 onshore edge of a warm-core ring. J. Geophys. Res., in press doi: 10.1029/2018JC013794

2421 Zhang, Z., Zhao, W., Tian, J., Yang, Q., Qu, T. (2015). Spatial structure and temporal variability of
2422 the zonal flow in the Luzon Strait. J. Geophys. Res. 120, 759–776. doi: 10.1002/2014JC010308

2423 Zhou, C., Zhao, W., Tian, J., Yang, Q., Qu, T. (2014). Variability of the Deep-Water Overflow in the
2424 Luzon Strait. J. Phys. Oceanogr. 44, 2972–2986. doi: 10.1175/JPO-D-14-0113.1

2425 Zilberman, N.V., Roemmich, D., Gille, S. (2013). The Mean and the Time Variability of the Shallow
2426 Meridional Overturning Circulation in the Tropical South Pacific Ocean. J. Climate 26, 4069-4087.
2427 doi: 10.1175/JCLI-D-12-00120.1

2428 Zilberman, N.V., Roemmich, D., Gille S. (2014). Meridional volume transport in the South Pacific:
2429 Mean and SAM-related variability. J. Geophys. Res. Oceans 119, 2658-2678. doi:
2430 10.1002/2013JC009688

Zilberman, N.V., Roemmich, D.H., Gille, S.T., Gilson, J. (2018). Estimating the velocity and transport of western boundary current systems: A case study of the East Australian Current near Brisbane. J. Atmos. Oceanic Technol. 35, 1313-1329. 10.1175/JTECH-D-17-0153.1

Zuidema, P., Chang, P., Medeiros, B., Kirtman, B.P., Mechoso, R., Schneider, E.K., et al. (2016). Challenges and prospects for reducing coupled climate model SST biases in the eastern tropical Atlantic and Pacific Oceans: The U.S. CLIVAR Eastern Tropical Oceans Synthesis Working Group. Bull. Amer. Meteor. Soc. 97, 2305–2328. doi: 10.1175/BAMS-D-15-00274.1

12 Data Availability Statement

Many of the observations reviewed here can be obtained from the sources listed in Table 2.

2440 ***Table 1:*** *List of Essential Ocean Variables from www.goosocean.org/eov with indications of which*
2441 *observing platforms are able to sample each variable.*

		Autonomous Underwater Gliders	Drifters	Moorings	Profiling Floats	Satellite Remote Sensing	High-Frequency Radar	Ships of Opportunity	Research Ships	Expendable Bathythermographs	Inverted Echo Sounders	Submarine Cables
Physics	**Sea state**		X	X		X		X	X			
	Ocean surface stress			X		X			X			
	Sea ice			X		X			X			
	Sea surface height					X						
	Sea surface temperature	X	X	X	X	X		X	X	X		
	Subsurface temperature	X		X	X				X	X	X	
	Surface currents	X	X	X	X	X	X	X	X			
	Subsurface currents	X		X	X			X	X		X	X
	Sea surface salinity	X		X	X	X		X	X			
	Subsurface salinity	X		X	X				X			
	Ocean surface heat flux			X		X			X			
Biogeochemistry	**Oxygen**	X		X	X			X	X			
	Nutrients	X		X				X	X			
	Inorganic Carbon			X				X	X			
	Transient tracers			X					X			
	Particulate matter	X		X				X	X			
	Nitrous oxide			X					X			
	Stable carbon isotopes							X	X			
	Dissolved organic carbon								X			
	Ocean color					X						
Biology and Ecosystems	**Phytoplankton biomass and diversity**	X	X	X	X	X		X	X			
	Zooplankton biomass and diversity	X		X					X			
	Fish abundance and distribution	X		X					X			
	Marine turtles, birds, mammals abundance and distribution			X					X			
	Hard coral cover and composition								X			
	Seagrass cover								X			
	Macroalgal canopy cover								X			
	Mangrove cover								X			
	Ocean sound	X		X					X			
	Microbe biomass and diversity (*emerging)								X			
	Benthic invertebrate abundance and distribution (*emerging)								X			

2442

2443 ***Table 2:*** *Examples of sustained boundary current observing efforts since 2009. Included are in situ*
2444 *and land-based observing efforts extending longer than one year in the period 2009-2018. Key*
2445 *references since 2009 and sources for publicly available data are included.*

Region	Platform	References	Data Source
Agulhas	Gliders	Krug et al., 2017	
Agulhas	Moorings	Beal et al., 2015; Elipot and Beal, 2015, 2018; Beal and Elipot, 2016; Kersalé et al. 2018	http://www.aoml.noaa.gov/phod/research/moc/samoc/sam/;
Agulhas	XBT		http://www.aoml.noaa.gov/phod/hdenxbt/index.php; http://www-hrx.ucsd.edu
Angola Current	Moorings	Kopte et al., 2017; 2018; Tchipalanga et al., 2018	https://doi.org/10.1594/PANGAEA.868684; https://doi.org/10.1594/PANGAEA.886492
Benguela Current	Argo	Pegliasco et al., 2015; Majumder and Schmid, 2018	http://www.argodatamgt.org
Benguela Current	Research Vessels		http://www.mfmr.gov.na/; http://data.ocean.gov.za/pub/DATA/;
Benguela Current	Moorings	Junker et al., 2017a, 2019	https://doi.org/10.1594/PANGAEA.871251 (Junker et al., 2017b); https://doi.org/10.1594/PANGAEA.871253 (Junker et al., 2017c); https://doi.org/10.1594/PANGAEA.872098 (Junker et al., 2017d); https://doi.org/10.1594/PANGAEA.872099 (Junker et al., 2017e); https://www.ocims.gov.za
Brazil Current	Drifters	Oliveira et al., 2009	http://www.aoml.noaa.gov/phod/gdp/index.php
Brazil Current	Moorings	Meinen et al., 2017, 2018	http://www.aoml.noaa.gov/phod/SAMOC_international/samoc_data.php
Brazil Current	Research Vessels	Valla et al., 2018	
Brazil Current	XBT	Garzoli et al., 2012; Mata et al., 2012; Lima et al., 2016; Majumder et al., 2019	http://www.aoml.noaa.gov/phod/hdenxbt/index.php
Brazil Current	Argo	Schmid and Majumder, 2018	http://argodatamgt.org

North Brazil Undercurrent	Moorings	Hummels et al., 2015	https://doi.org/10.1594/PANGAEA.886415; https://doi.org/10.1594/PANGAEA.886420; https://doi.org/10.1594/PANGAEA.886426; https://doi.org/10.1594/PANGAEA.886428
California Current System	Drifters		http://www.aoml.noaa.gov/phod/gdp/index.php
California Current System	Gliders	Todd et al., 2011a,b, 2012; Pelland et al., 2013; Mazzini et al., 2014; Johnston and Rudnick, 2015; Adams et al., 2016; Zaba and Rudnick, 2016; Rudnick et al., 2017; Henderikx Freitas et al., 2018	https://spraydata.ucsd.edu/projects/CUGN (Rudnick, 2016a); https://spraydata.ucsd.edu/projects/CORC (Send, 2018); http://www.oceanobservatories.org/
California Current System	High-Frequency Radar	Kim, 2010; Kim et al., 2011; Kim and Kosro, 2013;	
California Current System	Moorings	Nam et al., 2011; Harris et al., 2013; Ohman et al., 2013; Siedlecki et al., 2016; Sutton et al., 2014, 2016; Fassbender et al., 2016, 2017b, 2018	http://www.oceanobservatories.org/; https://www.nodc.noaa.gov/ocads/oceans/Coastal/north_america_west.html; ftp://data.ndbc.noaa.gov/data/oceansites/
California Current System	Research Vessels	Juranek et al., 2009; Fassbender et al., 2011, 2017b, 2018; Alin et al., 2012; Bednaršek et al., 2014, 2017, 2018; Reum et al., 2014, 2016; Feely et al., 2016, 2018; McClatchie, 2014; McClatchie et al., 2016;	http://www.calcofi.org; https://www.nodc.noaa.gov/ocads/oceans/Coastal/north_america_west.html
California Current System	Ship of Opportunity	Fassbender et al., 2018	
California Current System	XBT	Douglass et al., 2010; Auad et al., 2011	http://www-hrx.ucsd.edu
California Current System	Argo	Pegliasco et al., 2015	http://www.argodatamgt.org
East Auckland Current	XBT	Bowen et al., 2017; Fernandez et al., 2018	http://www-hrx.ucsd.edu
East Australian Current	Argo	Zilberman et al., 2014, 2018	https://portal.aodn.org.au; http://www.argodatamgt.org

East Australian Current	Drifters	Brassington, 2010; Brassington et al., 2011	http://www.aoml.noaa.gov/phod/gdp/index.php
East Australian Current	Gliders	Roughan et al., 2015; Schaeffer and Roughan, 2015; Schaeffer et al., 2016a, 2016b	https://portal.aodn.org.au; http://imos.org.au/facilities/aodn/
East Australian Current	High-Frequency Radar	Roughan et al., 2015; Archer et al., 2017b, 2018; Mantovanelli et al., 2017; Schaeffer et al., 2017; Wyatt et al., 2018	www.oceanography.unsw.edu.au/radar.html https://portal.aodn.org.au
East Australian Current	Moorings	Roughan et al., 2013, 2015; Schaeffer et al., 2013, 2014; Lynch et al., 2014; Schaeffer and Roughan, 2017; Sloyan et al., 2016; Alford et al., 2017	https://portal.aodn.org.au
East Australian Current	XBT	Hill et al., 2011; Suthers et al., 2011; Sloyan and O'Kane 2015; Zilberman et al., 2018;	https://portal.aodn.org.au; http://www-hrx.ucsd.edu
Gulf Stream	Gliders	Todd et al., 2016, 2018b; Todd, 2017; Todd and Locke-Wynn, 2017; Gula et al., 2019	https://spraydata.ucsd.edu/projects/GS (Todd and Owens, 2016)
Gulf Stream	High-Frequency Radar	Parks et al., 2009; Archer et al., 2015, 2017a; Haines et al., 2017	http://cordc.ucsd.edu/projects/mapping/maps/
Gulf Stream	Moorings	Weller et al., 2012; Bigorre et al. 2013; Bane et al., 2017; Lowcher et al., 2017	http://www.whoi.edu/science/PO/linew/
Gulf Stream	Research Vessels	Meinen et al., 2010	http://www.aoml.noaa.gov/phod/floridacurrent/; http://www.whoi.edu/science/PO/linew/
Gulf Stream	Ship of Opportunity	Rossby et al., 2010; Wang et al., 2010	http://oleander.bios.edu/
Gulf Stream	XBT	Domingues et al., 2018	http://www.aoml.noaa.gov/phod/hdenxbt/index.php
Gulf Stream	Submarine Cable	Meinen, et al., 2010	http://www.aoml.noaa.gov/phod/floridacurrent/
Kuroshio	Argo	Sugimoto and Hanawa, 2014; Oka et al., 2015; Bushinsky et al., 2016; Inoue et al., 2016a,b; Fassbender et al., 2017a;	http://www.argodatamgt.org

		Bushinsky and Emerson, 2018	
Kuroshio	HF Radar	Yang et al., 2015	
Kuroshio	Drifters	Velez-Belchi et al., 2013; Gordon et al., 2014; Andres et al., 2015	http://www.aoml.noaa.gov/phod/gdp/index.php
Kuroshio	Gliders	Rudnick et al., 2011; Rudnick et al., 2013; Johnston et al., 2013; Rainville et al., 2013; Lien et al., 2014; Lien et al., 2015	
Kuroshio	Moorings	Bond et al., 2011; Cronin et al., 2013, 2015; Hu et al., 2013; Wada et al., 2013; Lien et al. 2014, 2015; Sutton et al., 2014, 2016, 2017; Zhou et al., 2014; Chen et al., 2015; Yange et al., 2015; Zhang et al., 2015; Fassbender et al., 2017a; Honda et al., 2018	https://www.nodc.noaa.gov/ocads/oceans/Moorings/Pacific.html; ftp://data.ndbc.noaa.gov/data/oceansites
Kuroshio	Research Vessels	Yasunaka et al., 2013, 2014; Sugimoto and Hanawa, 2014; Yang et al., 2015; Nakano et al., 2015; Oka et al., 2018	
Kuroshio	Ship of Opportunity	Palevsky et al., 2016; Palevsky and Quay 2017	
Kuroshio	XBT	Nagano et al., 2016	http://www-hrx.ucsd.edu
Labrador Current	Gliders	deYoung et al., 2018; Howatt et al., 2018	
Labrador Current	Moorings	deYoung et al., 2018	
Leeuwin Current	Gliders	Pattiaratchi et al., 2011	
Leeuwin Current	Argo	Furue et al., 2017	http://www.argodatamgt.org
Leeuwin Current	High-Frequency Radar	Mihanović et al., 2016	
Leeuwin Current	Moorings	Lynch et al., 2014;	
Loop Current (Gulf	Gliders	Gopalakrishnan et al., 2013; Rudnick et al., 2015b; Todd et al.,	https://spraydata.ucsd.edu/projects/GoM (Rudnick,

of Mexico)		2016	2017)
Malvinas Current	Argo	Artana et al., 2016, 2018b;	http://www.argodatamgt.org
Malvinas Current	Moorings	Valla and Piola, 2015; Ferrari et al., 2017; Artana et al., 2018a; Paniagua et al., 2018	https://doi.org/10.17882/51492 (Saraceno et al., 2017); https://www.seanoe.org/data/00403/51479/; https://www.seanoe.org/data/00403/51492/
Mediterranean	Gliders	Heslop et al., 2012	
Middle Atlantic Bight	Gliders	Castelao, et al., 2010; Todd et al., 2013; Zhang and Gawarkiewicz, 2015; Dever et al., 2016; Gawarkiewicz et al., 2018	http://www.oceanobservatories.org/
Middle Atlantic Bight	Moorings	Chen et al., 2018; Gawarkiewicz et al., 2018; Zhang and Partida, 2018	http://www.oceanobservatories.org/
Mindanao	Gliders	Schönau et al., 2015; Schönau and Rudnick, 2017	
Mindanao	Moorings	Zhang et al., 2014; Hu et al., 2016; Wang et al., 2017	
NE Atlantic (Subpolar)	Gliders	Houpert et al., 2018	
Canary Current System	Drifters	Menna et al., 2016	
Canary Current System	Gliders	Karstensen et al. 2017; Kolodziejczyk et al., 2018	
Canary Current System	Mooring	Nowald et al., 2015	http://www.fixo3.eu
Canary Current System	Research Vessels	Steinfeldt 2015; Capet et al., 2017; Klenz et al., 2018; Machu et al., 2019; Thomsen et al., 2019	
Canary Current System	Argo	Pegliasco et al., 2015	http://www.argodatamgt.org
NW Atlantic Deep Western Boundary Current	Moorings	Fischer et al., 2004, 2010; Dengler et al., 2006; Bacon and Saunders, 2010; Johns et al., 2008, 2011; Toole et al., 2017; Zantopp et al.,	http://www.whoi.edu/science/PO/linew/; www.oceansites.org

		2017	
NW Atlantic Deep Western Boundary Current	Research Vessels	van Sebille et al., 2011	http://www.whoi.edu/science/PO/linew/
Oyashio	Research Vessels	Kuroda et al., 2015, 2017	http://tnfri.fra.affrc.go.jp/seika/a-line/a-line_index2.html
Peru-Chile Current System	Gliders	Pietri et al., 2013, 2014; Pizarro et al., 2016	
Peru-Chile Current System	Argo	Pegliasco et al., 2015	http://www.argodatamgt.org
Peru-Chile Current System	Research Vessels	Espinoza et al., 2017; Graco et al., 2017; Grados et al., 2018	
Peru-Chile Current System	Research Vessels	Escribano and Morales, 2012; Schneider et al., 2016	http://www.antares.ws
Solomon Sea	Argo	Zilberman et al., 2013	http://www.argodatamgt.org
Solomon Sea	Gliders	Davis et al., 2012	https://spraydata.ucsd.edu/projects/Solomon (Davis, 2016)
Solomon Sea	Moorings	Ganachaud et al., 2014, 2017; Alberty, 2018	http://www.solomonseaoceanography.org/; 10.6075/J09W0CS2 (Cravatte et al., 2019); 10.6075/J0639N12 (Alberty et al., 2019)
Solomon Sea	XBT	Zilberman et al., 2013	http://www-hrx.ucsd.edu
Somali Current	Drifters	Beal et al., 2013; Centurioni et al., 2017	http://www.aoml.noaa.gov/phod/gdp/index.php
South China Sea	Drifters	Centurioni et al., 2009	http://www.aoml.noaa.gov/phod/gdp/index.php

2446

2447

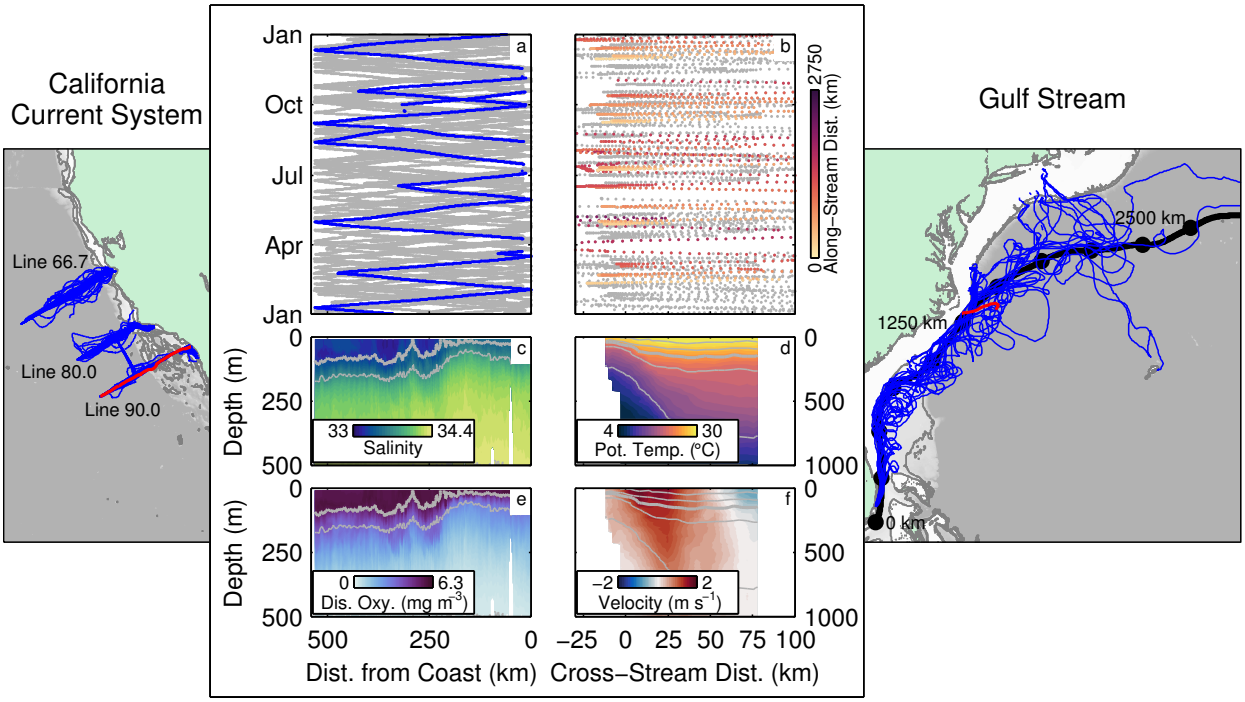

Figure 1: *Examples of multi-year, glider-based sampling in (left) an eastern boundary current system and (right) a western boundary current. Trajectories of all Spray gliders surveying the California Current System along CalCOFI lines 66.7, 80.0, and 90.0 (Rudnick et al., 2017 and references therein) and the Gulf Stream along the US East Coast (Todd 2017; Todd and Locke-Wynn 2017; Todd et al., 2018) are shown on the background map. (a,b) Glider sampling as a function of month and cross-shore or cross-stream distance with sampling in all years in grey and calendar year 2017 in color; Gulf Stream sampling in 2017 is colored by along-stream distance from 25°N following the mean 40-cm SSH contour (black trajectory on map with dots every 250 km). (c-f) Example transects of salinity and dissolved oxygen along CalCOFI line 90.0 off Southern California in May 2017 and of potential temperature and velocity toward 50° across the Gulf Stream near Cape Hatteras in August 2017 (red transects on map).*

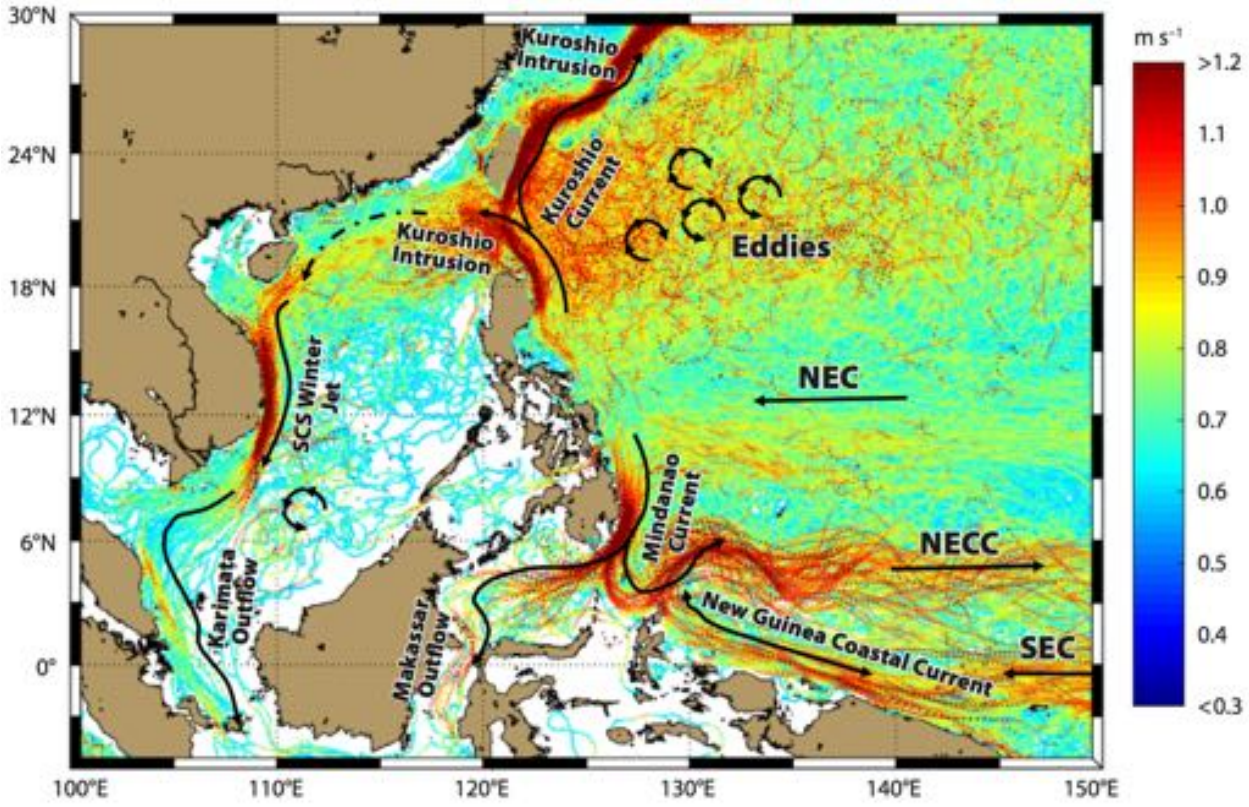

Figure 2: *Trajectories and near-surface velocity estimates from Global Drifter Program drifters in the western Pacific and marginal seas. Over 1.2 million discrete measurements from 1982 to 2014 are included. Paths of various boundary currents are clearly visible, as is the rich eddy field in the region of the Subtropical Countercurrent around 18-24°N. NEC = North Equatorial Current, NECC = North Equatorial Counter Current, SEC = South Equatorial Current, SCS = South China Sea. (Figure from Todd et al., 2018a.)*

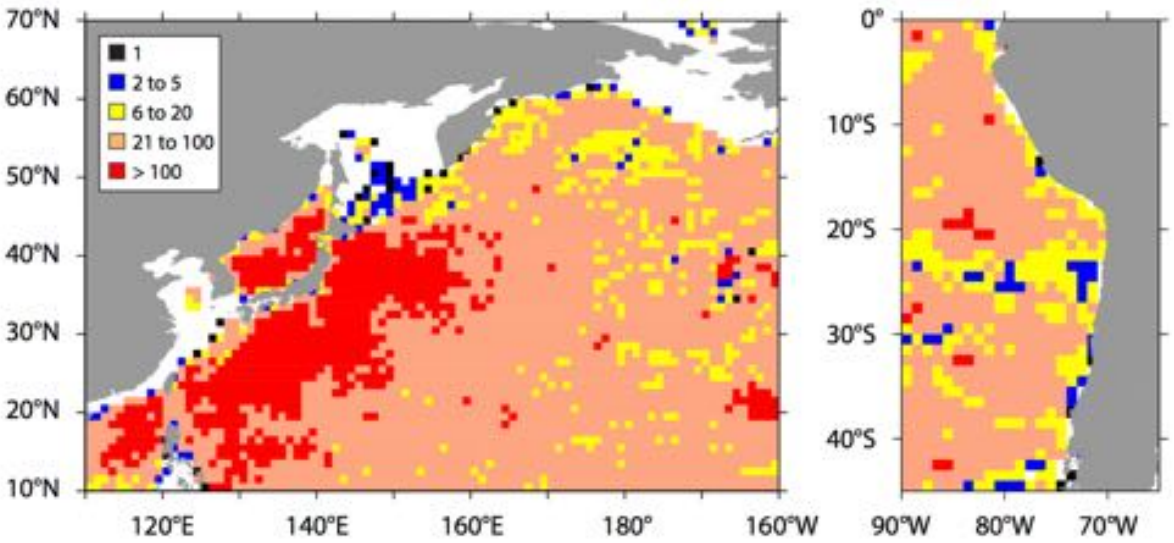

2469

2470 ***Figure 3:*** *Sampling density of Argo float (including Core Argo and BGC Argo) profiles per 1°*
2471 *latitude x 1° longitude bin, collected between January 2009 and September 2018, in the Kuroshio*
2472 *region (left panel), and the Peru-Chile Current region (right panel).*

2473

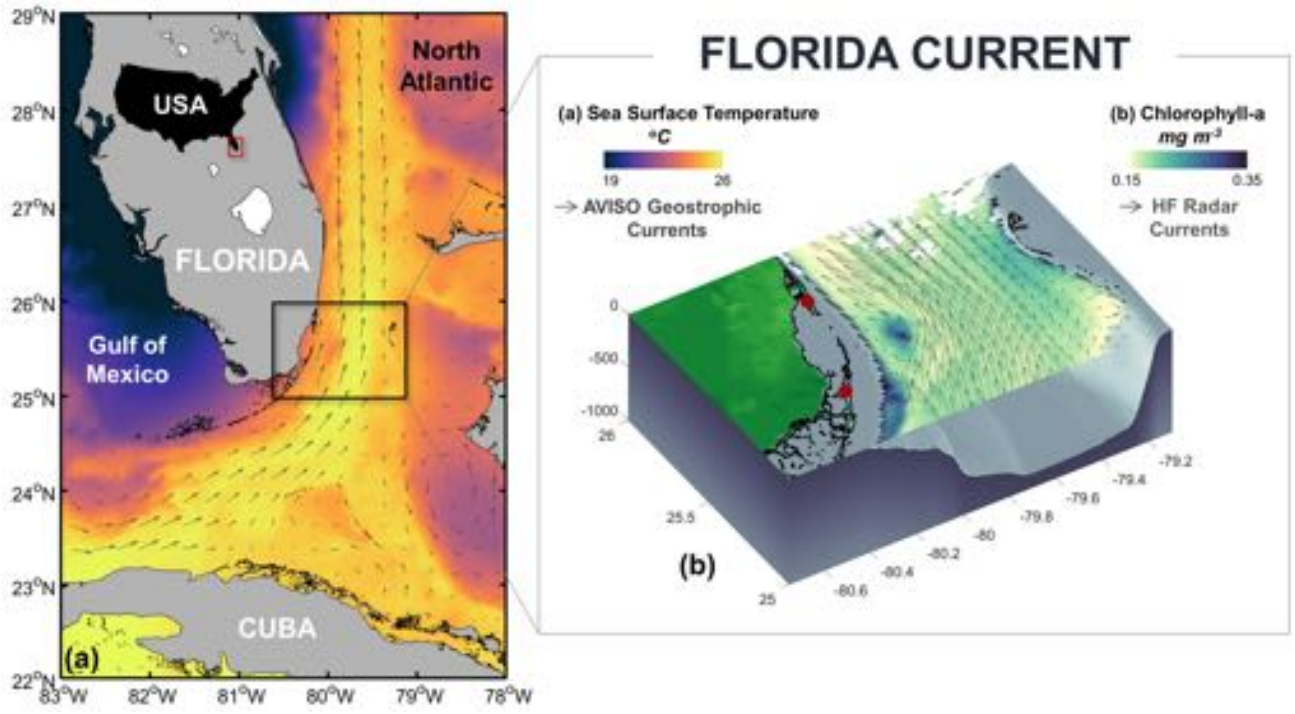

Figure 4: *Example of combined satellite- and land-based remote sensing of the Florida Current. (a) SST from GHRSST and surface geostrophic currents from AVISO. (b) Chlorophyll from MODIS AQUA and surface currents from HF radars (HF radar data from Archer et al., 2017a).*

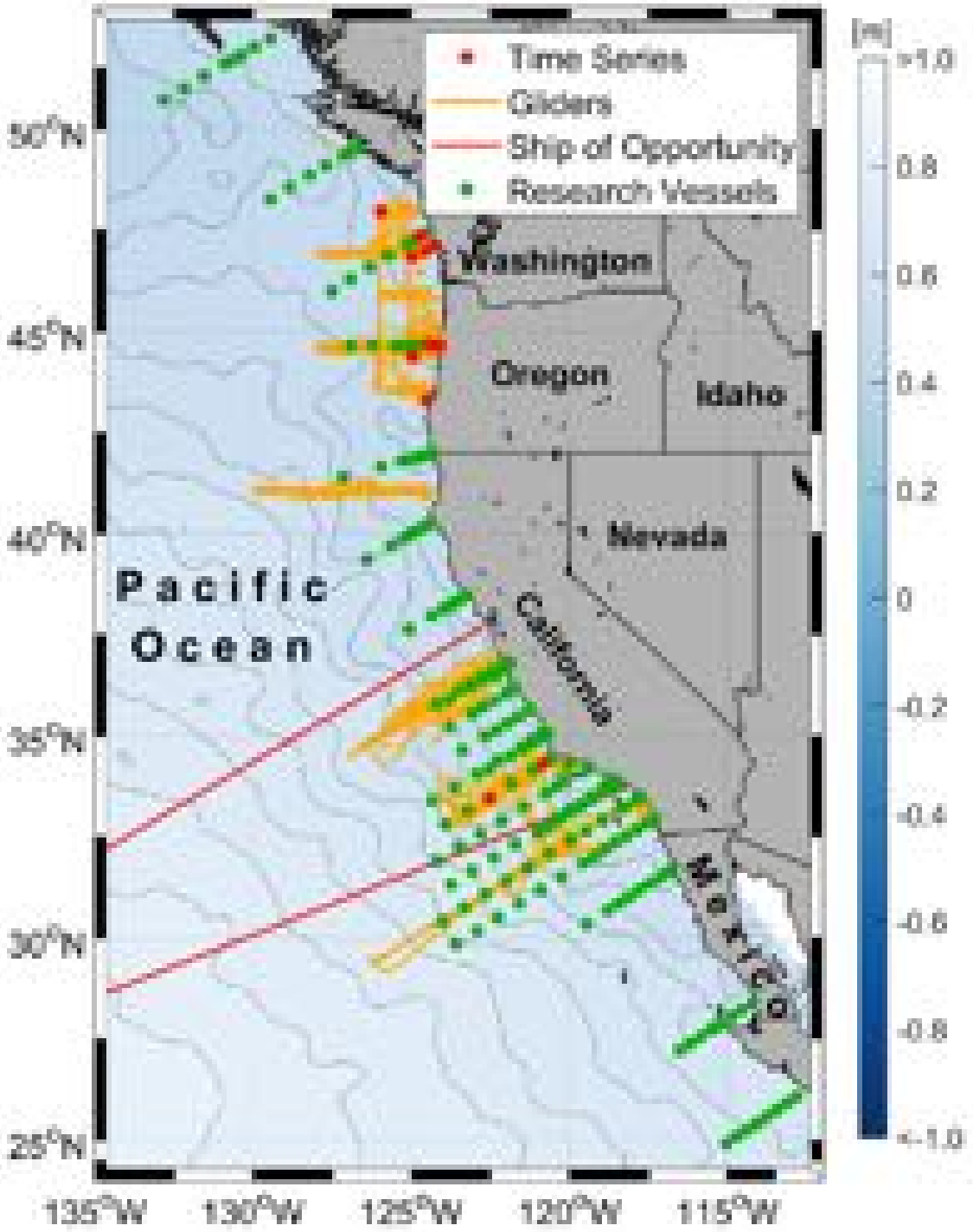

Figure 5: *Map of observing efforts extending more than one year during the past decade for the California Current System (Section 4.1.1). Glider trajectories are shown in orange, SOOP/XBT lines are red, moorings are red dots, and stations routinely occupied by research vessels are green. Contours are mean sea surface height over the period 2009-2017 from AVISO.*

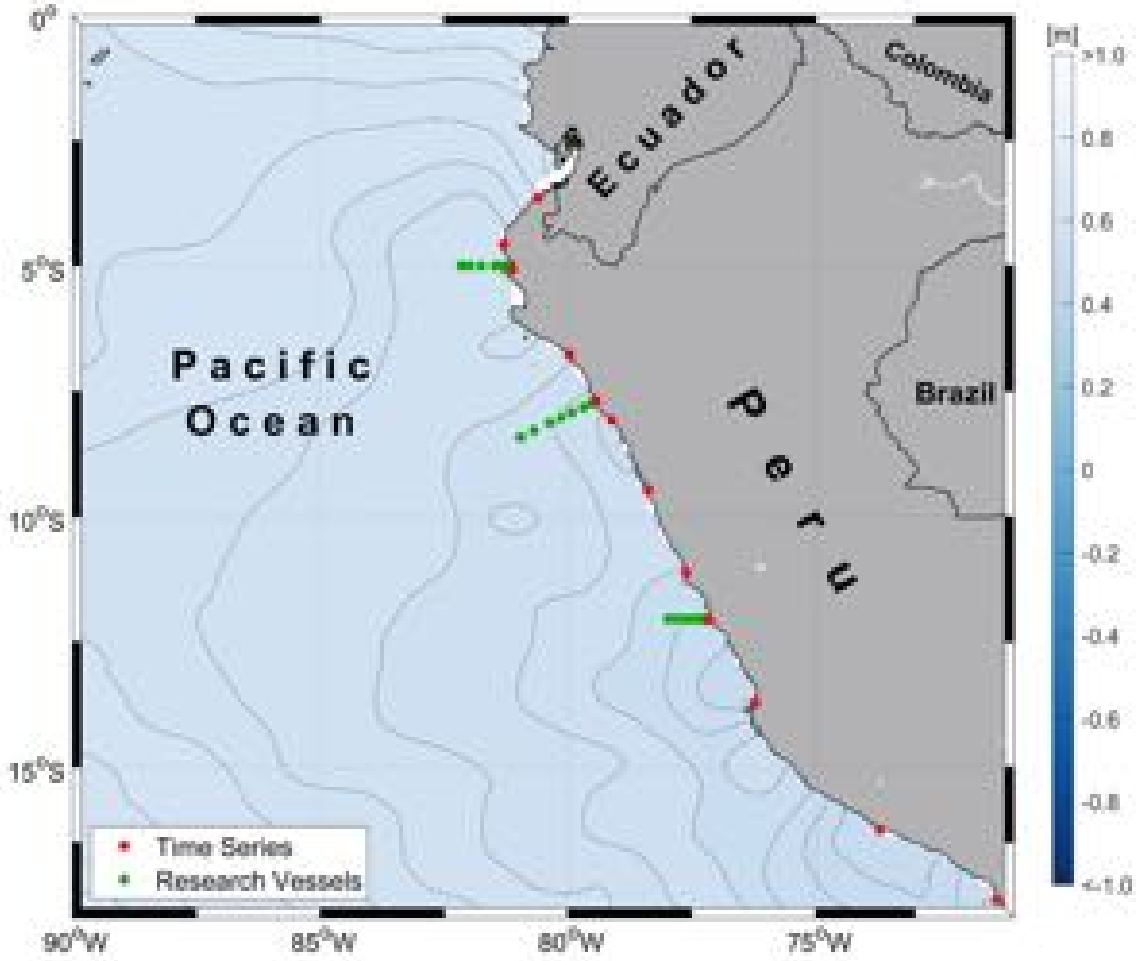

2484

2485 ***Figure 6:*** *Map of the boundary current observing effort for the Peru-Chile Current System (Section*
2486 *4.1.2) with details as in Fig. 5.*

2487

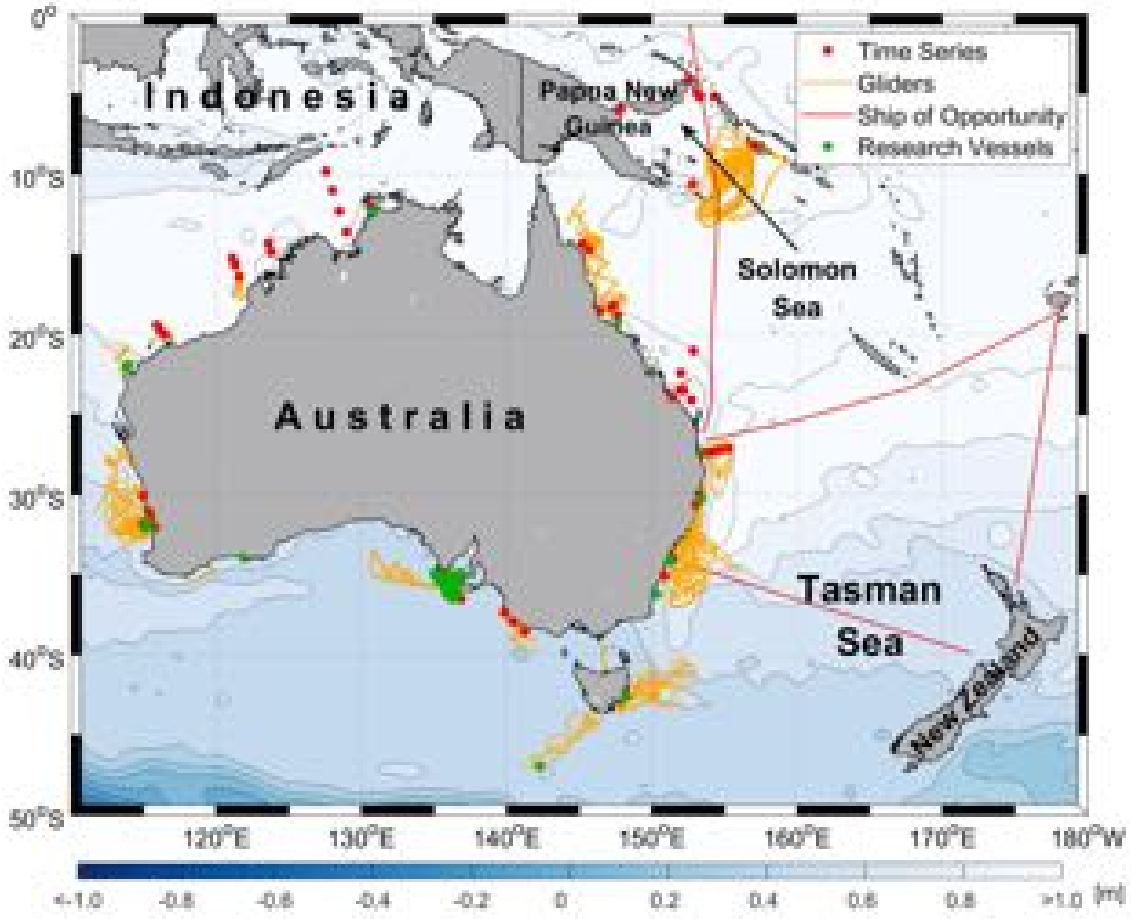

Figure 7: *Map of the boundary current observing efforts for the Leeuwin and South Australian Current Systems (Section 4.1.3) and the Southwestern Pacific (Section 4.2.3) with details as in Fig. 5.*

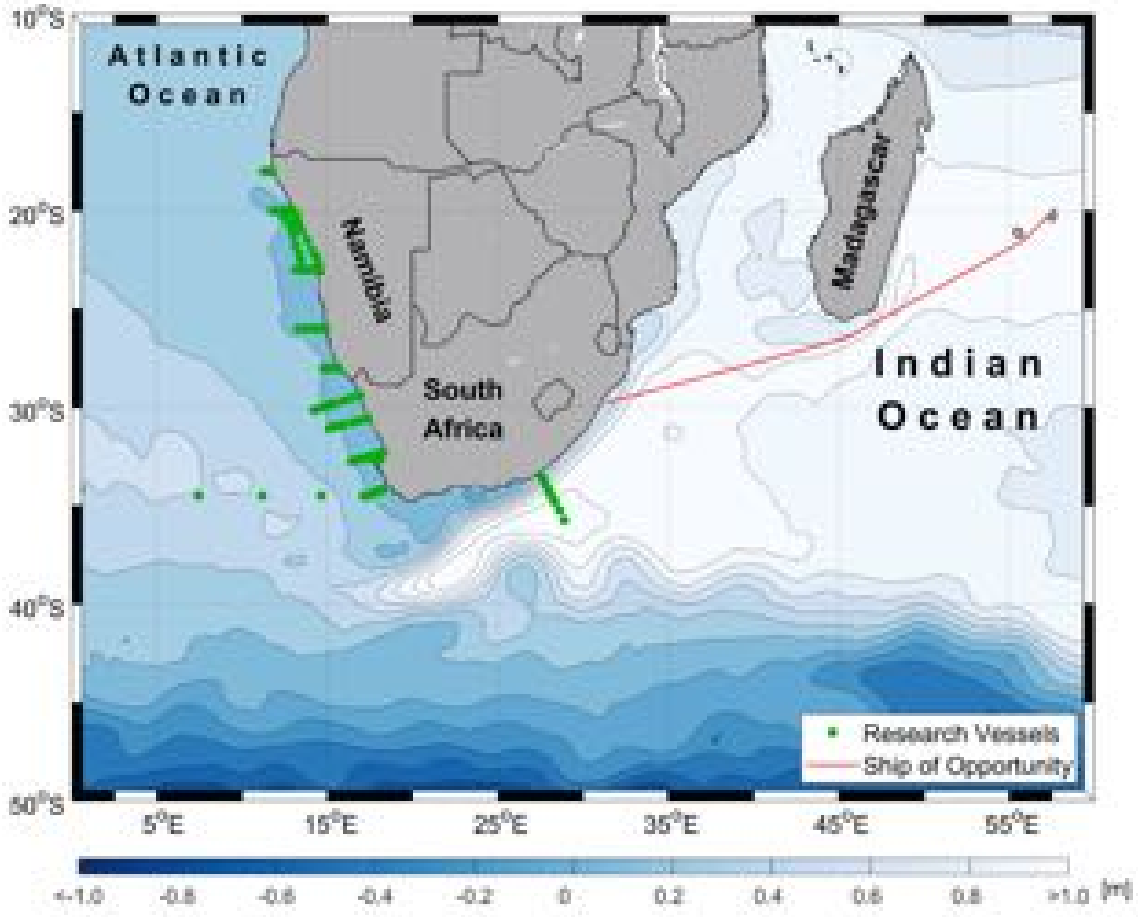

2492

2493 ***Figure 8:*** *Map of the boundary current observing effort for the Bengula Current System (Section*
2494 *4.1.4) and the Agulhas Current (Section 4.2.4) with details as in Fig. 5.*

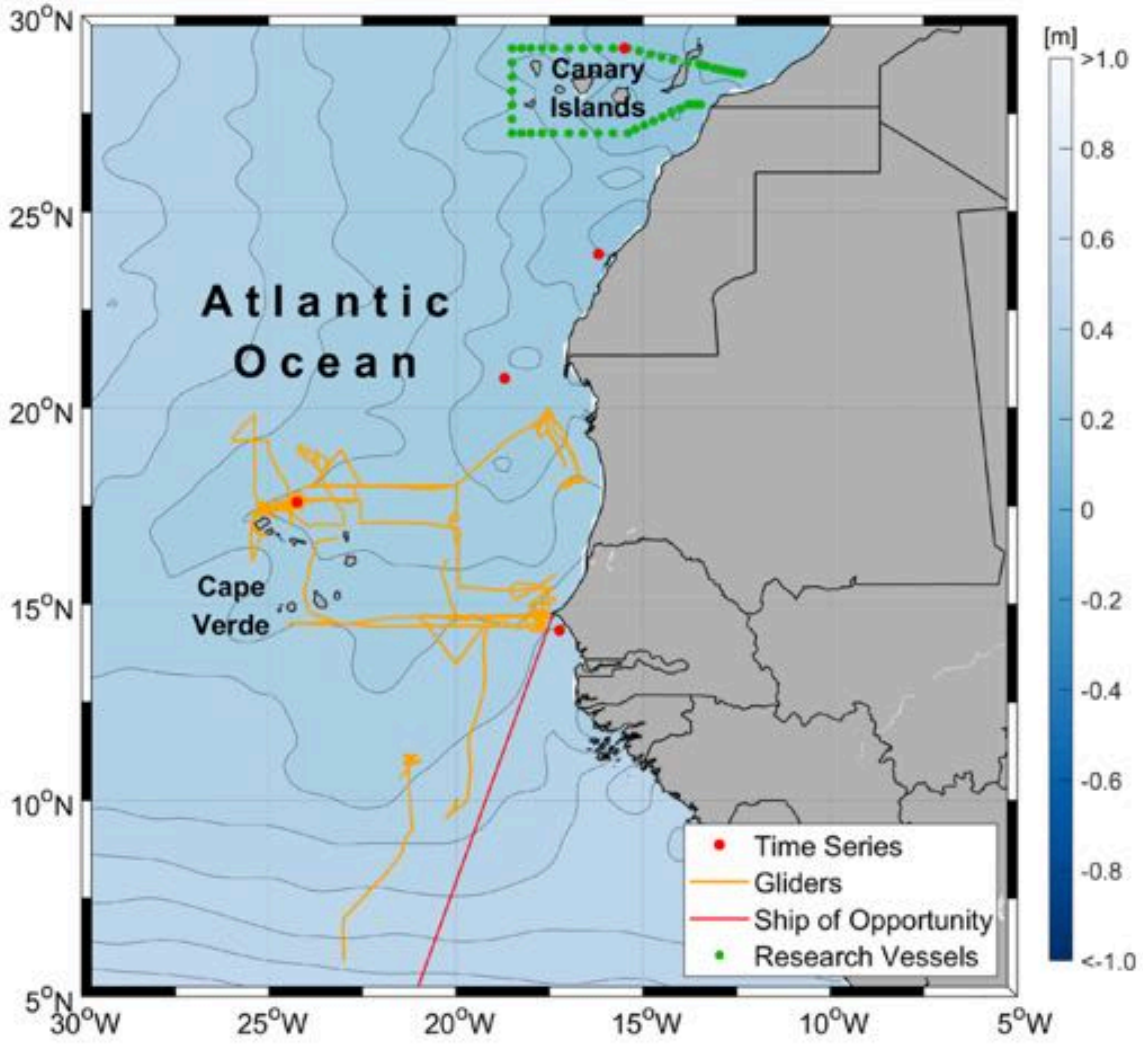

Figure 9: *Map of the boundary current observing effort for the Canary Curret System (Section 4.1.5) with details as in Fig. 5.*

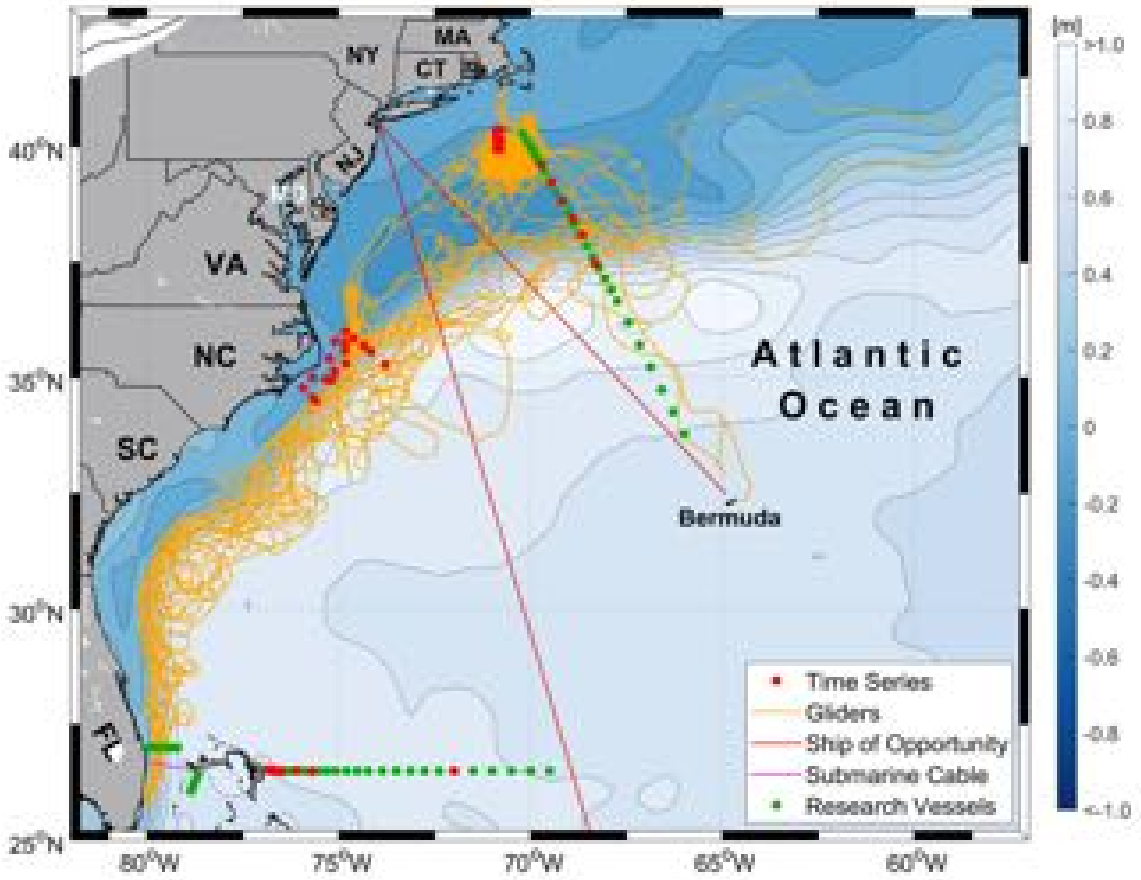

2498

2499 ***Figure 10:*** *Map of the boundary current observing efforts for the Northwestern Atlantic (Section*
2500 *4.2.1) with details as in Fig. 5 and the addition of the submarine cable location in the Florida Strait.*

2501

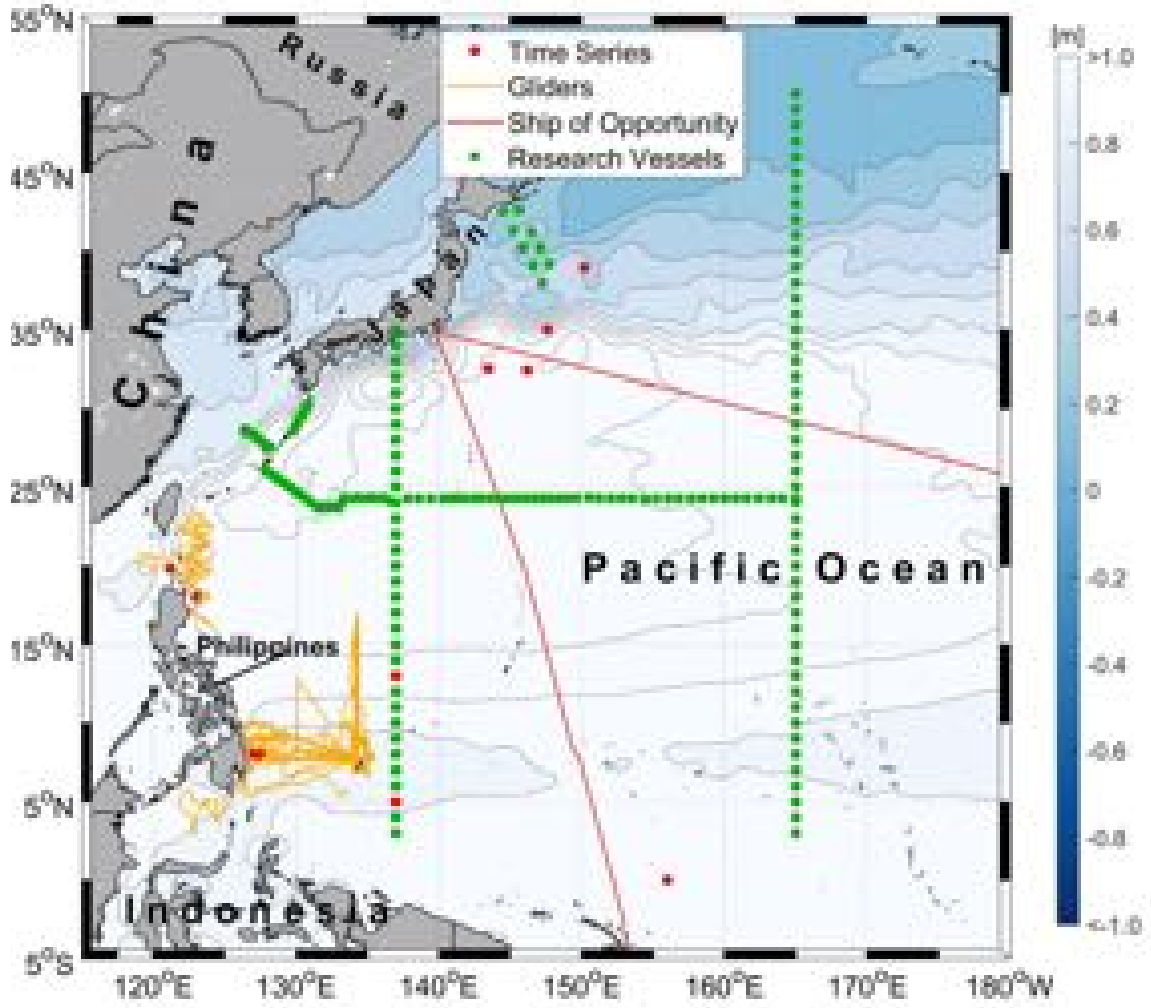

Figure 11: *Map of the boundary current observing effort for the Northwestern Pacific (Section 4.2.2) with details as in Fig. 5.*

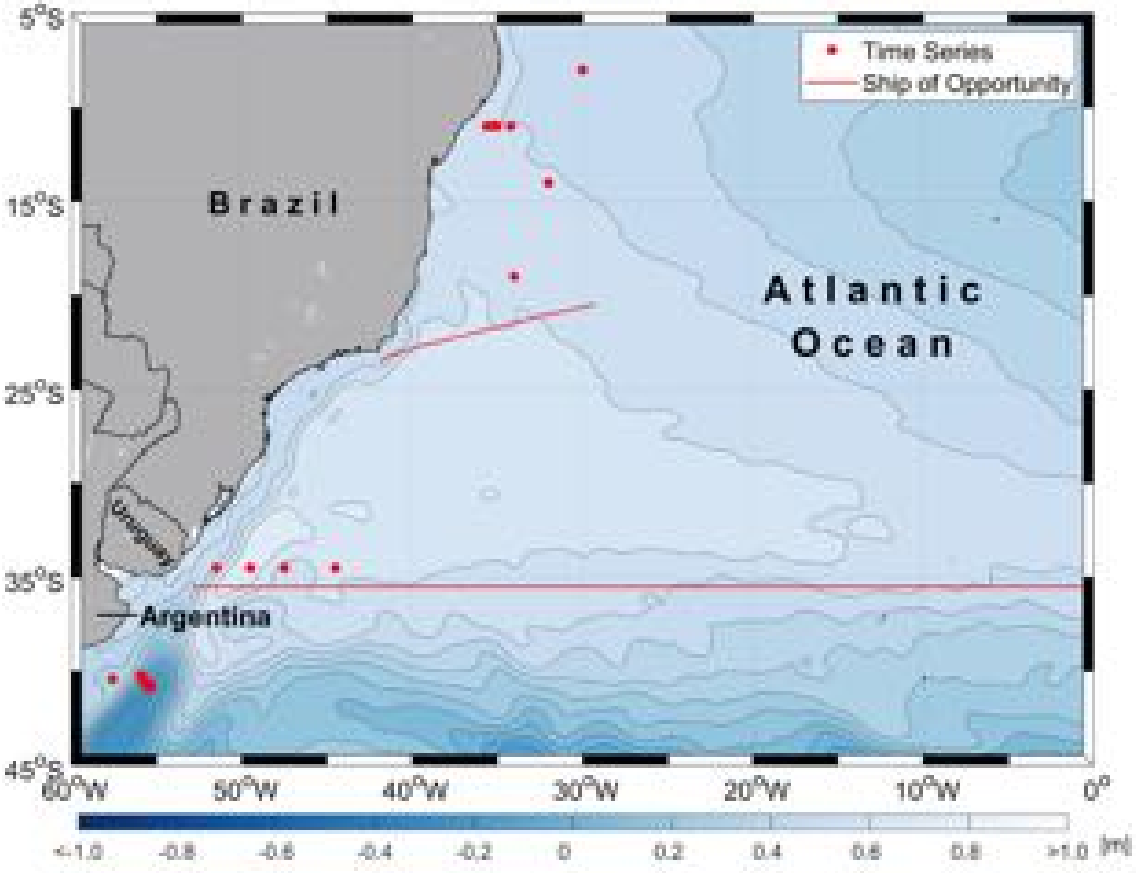

Figure 12: *Map of the boundary current observing system for the Southwestern Atlantic (Section 4.2.5) with details as in Fig. 5.*